2012

Design and Performance Analyses of Condensing Heat Exchangers for Recovering Water and Waste Heat from Flue Gas

Nipun Goel
Lehigh University

Design and Performance Analyses of Condensing Heat Exchangers for Recovering Water and Waste Heat from Flue Gas

by

Nipun Goel

A Thesis

Presented to the Graduate and Research Committee

Of

Lehigh University

in Candidacy for the Degree of

Master of Science

in

Mechanical Engineering

Lehigh University

May 2012

Approval Sheet

Thesis is accepted and approved in partial fulfillment of the requirements for the Master of Science in Mechanical Engineering.

Design and Performance Analyses of Condensing Heat Exchangers for Recovering Water and Waste Heat from Flue Gas

Nipun Goel

_____

Date Approved

_____

Dr. Edward K. Levy

Thesis Advisor

_____

Dr. Gary Harlow

Department Chair Person

Acknowledgments

I would like to express my deepest gratitude to Dr. Edward Levy and the Energy Research Center for all the support and encouragement during my graduate studies. Dr. Levy has been forever inspiring and I look forward to future opportunities of working with him.

I would like to thank Dr. Harun Bilirgen, Mr. Zheng Yao and Mr Joshua Charles of the Energy Research Center for all their help and guidance. I would like the thank Michael Kessen, Daniel Hazell and Gordon Jonas for their unlimited help and support in my research. I would like to extend my thanks to Jodie Johnson and Ursla Levy of the Energy Research Center for their commitment to make the experience of working at Energy Research Center last for a lifetime.

I would also like to thank Namrata Maski, my family and my friends for believing in me and their unconditional support throughout the course of my study at Lehigh University.

Table of Contents

Approval Sheet III

Acknowledgments IV

Table of Contents V

List of Figures VI

List of Tables IX

Abstract 1

Nomenclature 2

1. Introduction 5

2. Theory 7

2.1. Condensing Flue Gas Heat exchanger 7

2.2. Water-to-Water Heat Exchanger 15

2.3. Estimation of Cost 21

2.3.1. Capital Cost 21

2.3.2. Operating Cost 22

3. Effects of Operating Conditions 24

4. Effect of Tube Diameter on Performance and Cost 27

5. Heat Exchanger Arrangements 34

5.1. Heat Exchanger placed Upstream of Wet FGD, Flue gas at 303°F 34

5.2. Heat Exchanger placed Downstream of Wet FGD, Flue Gas at 135°F 45

5.3. Precooled Flue Gas using Water Spray, Flue Gas at 155°F 48

5.4. Coupled Heat Exchanger, Flue gas at 135°F 52

5.5. Cascaded Heat Exchanger, Flue Gas at 300°F -135°F 62

6. Discussion of Results & Conclusion 84

7. Assumptions 87

References 89

Appendix A 91

Vita 96

List of Figures

Figure 1 - Typical temperature distributions inside a heat exchanger 8

Figure 2 - Thermal resistances between flue gas and cooling water in the absence of condensation 10

Figure 3 - Water-to-Water Heat Exchanger Model 15

Figure 4 - Shell Side Leakage Streams and Eddy Formation due to Baffles 20

Figure 5 - Change in Gross Unit Power output with Boiler Feed Water Temperature at exit of Heat Exchanger (14) 25

Figure 6 - Change in Cycle Heat Rate with Boiler Feed Water Temperature at exit of Heat Exchanger (14) 25

Figure 7 - Change in Boiler Feed Water Flow Rate with Boiler Feed Water Temperature at exit of Heat Exchanger 26

Figure 8 - Impact of Tube Diameter on Total Heat Transfer 29

Figure 9 - Impact of Tube Diameter on Rate of Condensation 29

Figure 10 - Impact of Tube Diameter on Cooling Water Temperature at exit of Heat Exchanger. 30

Figure 11 - Impact of Tube Diameter on Total Annual Cost of Heat Exchanger 30

Figure 12 - Impact of Diameter on Power Requirements for 20ft long Heat Exchanger 32

Figure 13 - Impact of Diameter on Total Annual cost for 20ft long Heat Exchanger 33

Figure 14 - Impact of using high temperature BFW on Condensation Efficiency of Heat Exchanger placed Upstream of Wet FGD 37

Figure 15 - Impact of high temperature BFW on temperature of BFW at the exit of Heat Exchanger, placed Upstream of Wet FGD 37

Figure 16 - Impact of high Temperature BFW on Total Annual Cost of Heat Exchanger Placed Upstream of Wet FGD 38

Figure 17 - Temperature Profiles for subcases with variable BFW inlet temperatures for heat exchanger upstream of wet FGD 40

Figure 18 - Temperature Profiles for Subcases 1-4, Model 1, System without FGD 43

Figure 19 - Cost Benefit Analysis of Heat Exchanger placed before Wet FGD and Boiler Feedwater extracted before FWH1 (14) 44
Figure 20 - Change in Net Power for Heat Exchanger placed before Wet FGD and Boiler Feedwater extracted before FWH1 (14) 44
Figure 21 - Impact of Transverse Pitch on Condensation Efficiency of Heat Exchanger placed Downstream of Wet FGD 46
Figure 22 - Impact of Transverse Pitch on Temperature of Cooling Water at the Exit of Heat Exchanger placed Downstream of Wet FGD 47
Figure 23 - Impact of Transverse Pitch on Total Annual cost of Heat Exchanger placed Downstream of Wet FGD 47
Figure 24 - Condensation Efficiency for Heat Exchanger with Precooled Flue Gas compared to UHX and DHX 50
Figure 25 - Boiler Feedwater Exit Temperature for Heat Exchanger with Precooled Flue Gas compared to UHX and DHX 51
Figure 26 - Total Annual Cost for Heat Exchanger with Precooled Flue Gas compared to UHX and DHX 51
Figure 27 - Flow diagram for Coupled Heat Exchanger Arrangement 53
Figure 28 - Trend for Temperature of Feedwater at the exit of Coupled Heat Exchanger assembly compared to system using only Boiler Feedwater or only Cooling Water for various Cooling Water to Flue Gas Mass Flow Rate Ratios 57
Figure 29 - Condensation Efficiency for Coupled Heat Exchanger assembly compared to system using only Boiler Feedwater or only Cooling Water for various Cooling Water to Flue Gas Mass Flow Rate Ratios 58
Figure 30 - Total power required for Coupled Heat Exchanger assembly compared to system using only Boiler Feedwater or only Cooling Water for various Cooling Water to Flue Gas Mass Flow Rate Ratios 58
Figure 31 - Impact of cooling water to flue gas mass flow rate ratio on effectiveness of HX2 of Coupled Heat Exchanger Assembly 59

Figure 32 - Impact of Cooling Water to Flue Gas Mass Flow Rate Ratio on Temperature of Cooling Water at the inlet of HX1 of Coupled Heat Exchanger Assembly 60
Figure 33 - Process Flow Diagram for Coupled Heat Exchanger with Cooling Water to Flue Gas Mass Flow Rate Ratio of 1.0 61
Figure 34 - Process Flow Diagram for Coupled Heat Exchanger with Cooling Water to Flue Gas Mass Flow Rate Ratio of 1.5 61
Figure 35 - Flow Diagram for Cascaded Heat Exchanger Arrangement 62
Figure 36 - Trend for Temperature of Boiler Feedwater at the Exit of DHX for various Target Feedwater Temperatures at the Exit of UHX-DHX Assembly. 64
Figure 37 - Trend for Rate of Condensation in DHX for various Target Boiler Feedwater Temperatures at the Exit of UHX-DHX Assembly. 65
Figure 38 - Total Capital Cost associated with DHX for various Target Boiler Feedwater Temperatures at the Exit of UHX-DHX Assembly. 66
Figure 39 - Annual Operating Cost associated with DHX for various Target Boiler Feedwater Temperatures at the Exit of UHX-DHX Assembly 66
Figure 40 - Trend for Total Annual Cost associated with DHX for various Target Boiler Feedwater Temperatures at the Exit of UHX-DHX Assembly 67
Figure 41 - Temperature Profiles in UHX of UHX-DHX assembly for various target Temperatures of Boiler Feedwater at the Exit of UHX 74
Figure 42 - Condensation Efficiency and Total Annual Cost for UHX of UHX-DHX Assembly for various target boiler feedwater temperatures at the exit of UHX 75
Figure 43 - Rate of Condensation for UHX-DHX assembly compared to UHX only and DHX only cases for different Target Boiler Feedwater Temperatures 79
Figure 44 - Total Annual Cost for UHX-DHX assembly compared to UHX only and DHX only cases for different Target Boiler Feedwater Temperatures 79
Figure 45 - Change in Turbine Power with Target Boiler Feedwater Exit Temperature 82
Figure 46 - Net Profit from using UHX-DHX assembly compared to system with Only UHX and Only DHX 82

List of Tables

Table 1 - Coefficients, c_i, for calculating Euler's constant for in-line square banks (11). 19

Table 2 - Fixed Process Conditions for studying the impact of Tube Diameter..... 28

Table 3 - Fixed Heat Exchanger Geometry for studying the impact of Tube Diameter..... 28

Table 4 - Variable Parameters for studying the impact of Tube Diameter..... 28

Table 5 - Impact of Tube Diameter on Pressure Drop for 20ft Heat Exchanger Length 31

Table 6 - Impact of Tube Diameter on Total Annual Cost for 20ft Heat Exchanger Length..... 32

Table 7 - Fixed Process Conditions for Heat Exchanger Placed Upstream of Wet FGD..... 35

Table 8 - Fixed Heat Exchanger Geometry for Heat Exchanger Placed Upstream of Wet FGD .. 36

Table 9 - Various Process Conditions for Heat Exchanger Placed Upstream of Wet FGD 36

Table 10 - Simulation results for the sub-cases A-F for Heat Exchanger placed upstream of the Wet FGD Unit..... 41

Table 11 - Simulation results for the sub-cases 1 – 4 for Heat Exchanger placed upstream of the Wet FGD Unit..... 42

Table 12 - Fixed Process Conditions for Heat Exchanger placed Downstream of Wet FGD..... 45

Table 13 - Fixed Heat Exchanger Geometry for Heat Exchanger placed Downstream of Wet FGD 46

Table 14 - Variable Parameter for Heat Exchanger placed Downstream of Wet FGD 46

Table 15 - Fixed Process Conditions for Precooled Flue Gas using Water Spray..... 49

Table 16 - Fixed Heat Exchanger Geometry for Precooled Flue Gas using Water Spray 49

Table 17 - Variable Parameter for Heat Exchanger for Precooled Flue Gas using Water Spray.. 49

Table 18 - Fixed Process Conditions for UHX without using Water Spray for Precooling Flue Gas 49

Table 19 - Fixed Process Conditions for DHX without using Water Spray for Precooling Flue Gas 50

Table 20 - Fixed Process Conditions for system using Boiler Feedwater for comparison with Coupled Heat Exchanger..... 55

Table 21 - Fixed Heat Exchanger Geometry for system using Boiler Feedwater for comparison with Coupled Heat Exchanger 55
Table 22 - Fixed Process Conditions for system using Cooling Water for comparison with Coupled Heat Exchanger 55
Table 23 - Fixed Heat Exchanger Geometry for system using Cooling Water for comparison with Coupled Heat Exchanger 55
Table 24 - Fixed Process Conditions for Coupled Heat Exchanger Assembly 56
Table 25 - Fixed Geometry for HX1 of Coupled Heat Exchanger Assembly 56
Table 26 - Fixed Geometry for HX2 of Coupled Heat Exchanger Assembly 56
Table 27 - Variable Process Condition for system using Cooling Water and Coupled Heat Exchanger 57
Table 28 - Fixed Process Conditions for DHX of Cascaded Heat Exchangers Assembly 63
Table 29 - Fixed Heat Exchanger Geometry for DHX of Cascaded Heat Exchangers Assembly. 63
Table 30 - Variable mass flow rate of boiler feedwater for DHX and UHX of Cascaded Heat Exchangers Assembly (14) 64
Table 31 - Simulation results for DHX of Duct Length 12ft and various Boiler Feedwater Target Temperatures at the Exit of Cascaded Heat Exchanger Assembly 69
Table 32 - Fixed Process Conditions for UHX of Cascaded Heat Exchanger Assembly 70
Table 33 - Fixed Heat Exchanger Geometry for UHX of Cascaded Heat Exchangers Assembly. 70
Table 34 - Simulation results for UHX of UHX-DHX Assembly for various Boiler Feedwater Target Temperatures at the Exit of Cascaded Heat Exchanger Assembly 71
Table 35 - Results from Simulations for various Boiler Feedwater Target Temperatures at the Exit of UHX-DHX Assembly 77
Table 36 - Results from Simulations for various Boiler Feedwater Target Temperatures at the Exit of System with Only UHX 78
Table 37 - Results of Cost Benefit Analysis for system with Only DHX 81
Table 38 - Results of Cost Benefit Analysis for system with Only UHX 81
Table 39 - Results of Cost Benefit Analysis for system with UHX-DHX Assembly 81

Abstract

There has been an increasing interest in new technologies to improve the efficiency of coal based thermal power plants and to reduce the consumption of cooling water for cooling towers. This report discusses the opportunities of recovering heat and water from flue gas using condensing heat exchangers.

Simluations were performed to develop heat exchanger designs for one or more heat exchangers used upstream and/or downstream of the wet FGD. The impact on water condensation efficiency, total heat transfer and total annual cost were analyzed for five different arrangements. The impact of heat exchanger design parameters such as heat exchanger tube diameter and tube transverse pitch was analyzed. Additionally, the prospects of precooling the flue gas using water spray and its impact on performance of heat exchanger was also studied.

Nomenclature

Symbol	*Meaning*	*Units*
A_{eff}	Tube effective surface area	ft^2
A_i	Tube inner surface area	ft^2
A_{ic}	Tube inner surface area for one cell	ft^2
A_o	Tube outer surface area	ft^2
A_{oc}	Tube outer surface area for one cell	ft^2
C	Empirical coefficient depending on tube arrangement	-
C_{bfw}	Heat capacity rate of boiler feedwater	BTU/hr·°F
c_i	Tube geometry constant for calculation of Euler's constant	-
C_{max}	Maximum heat capacity rate of cooling water	BTU/hr·°F
C_{min}	Minimum heat capacity rate of cooling water	BTU/hr·°F
$C_{p,cw}$	Specific heat of cooling water	BTU/lbm·°F
$C_{p,fg}$	Specific heat of flue gas	BTU/lbm·°F
d_i	Tube inner diameter	in
d_o	Tube outer diameter	in
Eu	Euler's constant	-
f	Friction factor	-
h_{bfw}	Convective heat transfer coefficient for boiler feedwater	BTU/hr·ft^2·°F
h_{cw}	Convective heat transfer coefficient for cooling water	BTU/hr·ft^2·°F
h_f	Convective heat transfer coefficient for condensate film	BTU/hr·ft^2·°F
h_{fg}	Convective heat transfer coefficient for wet flue gas	BTU/hr·ft^2·°F
h_l	Latent heat of water vapor	BTU/lb
k	Specific heat ratio	-
k_{bfw}	Thermal conductivity of boiler feedwater	BTU/hr·°F·ft
k_{cw}	Thermal conductivity of cooling water	BTU/hr·°F·ft
k_{fg}	Thermal conductivity of flue gas	BTU/hr·°F·ft
K_L	Pressure loss coefficient	-
k_m	Mass transfer coefficient	lb/mol·hr·ft^2
k_w	Thermal conductivity of tube material	BTU/hr·°F·ft
L	Length of tube	ft
m	Empirical coefficient depending on tube arrangement	-
$\dot{m}_{cw}$	Mass flow rate of cooling water	lb/hr

$\dot{m}_{fg}$	Mass flow rate of flue gas	lb/hr
N	Total number of tubes in Heat Exchanger	-
N_b	Number of baffle plates	-
N_L	Total number of tube rows	-
N_{tu}	Number of transfer units	-
Nu_{bfw}	Nusselt number for boiler feedwater	-
Nu_{cw}	Nusselt number for cooling water	-
Nu_{fg}	Nusselt number for flue gas	-
P_{atm}	Atmospheric Pressure	psi
p_{bfw}	Pressure of boiler feedwater	psi
p_{cw}	Pressure of cooling water	psi
p_{fg}	Pressure of flue gas	psi
P_{in}	Pressure of flue gas at the exit of exchanger	psi
P_{out}	Pressure of flue gas at the inlet of exchanger	psi
Pr	Prandtl number	-
Pr_s	Surface Prandtl number	-
P_{tot}	Total pressure of flue gas	psi
q	Rate of heat transfer	BTU/hr
Q	Total volume flow rate of cooling water	ft^3/s
$R_{boiler\ feedwater}$	Thermal resistance of boiler feedwater	hr·°F/BTU
$R_{cooling\ water}$	Thermal resistance of cooling water	hr·°F/BTU
Re_{bfw}	Reynolds number of boiler feedwater	-
Re_{cw}	Reynolds number of cooling water	-
$Re_{cw,max}$	Maximum Reynolds number of cooling water	-
$Re_{fg,max}$	Maximum Reynolds number of flue gas	-
R_{fl}	Thermal resistance due to fouling on tube inner wall	hr·°F/BTU
$R_{flue\ gas}$	Thermal resistance of flue gas	hr·°F/BTU
r_i	Tube inner radius	in
r_o	Tube outer radius	in
R_{total}	Total thermal resistance of control volume	hr·°F/BTU
R_{wall}	Thermal resistance of tube wall	hr·°F/BTU
S_l	Longitudinal Pitch	in
S_t	Transverse pitch	in

T_{bfw}	Temperature of boiler feedwater	°F
T_{cw}	Bulk mean temperature of cooling water	°F
T_{fg}	Bulk mean temperature of flue gas	°F
T_i	Gas-condensate film interfacial temperature	°F
T_{ow}	Tube outer wall temperature	°F
U_0	Overall heat transfer coefficient	BTU/hr·ft2·°F
V_{avg}	Aaverage velocity of cooling water	ft/s
V_{cw}	Velocity of cooling water	ft/s
$V_{cw,max}$	Maximum velocity of cooling water	ft/s
$V_{bfw,avg}$	Average velocity of boiler feedwater	ft/s
V_{max}	Maximum velocity of flue gas	ft/s
W_{pump}	Pump power	hp
y_{H2O}	Mole fraction of water vapor in the flue gas	vol%wet
y_i	Mole fraction of water vapor at the wall interface	vol%wet

Greek Symbols:

Δ	Difference or change	-
η	Efficiency	-
ε	Heat exchanger effectiveness	-
ρ	Density	lb/ft3
χ	Pressure drop correction factor	-

1. Introduction

Power plants are a larger consumer of water than any other industry. Water is used for generating steam, cooling and other process requirements. The demand for electricity is ever-growing and thus the demand of water for power generation. As a result, water availability issues are becoming more and more important. A lot of emphasis is laid on recovering and re-using as much water as possible. This study will concentrate on recovering water from flue gas.

A coal based power plant burning lignite coal releases roughly 16% moisture by volume (wet basis) in the flue gas as lignite coal contains 40% moisture by mass. Employing a wet scrubber after the ESP further increases the moisture content in flue gas. For example, consider a 600 MW power plant unit using PRB coal. The flue gas flow rate is of the order of 6.33 million lb/hr. Of this nearly 12% by volume (0.76 million lb/hr) is moisture. If the unit has a wet FGD to remove SO_2 from flue gas stream, the flue gas coming out of the FGD will be saturated with water. Furthermore, typical evaporation rate of cooling tower for 600MW unit is 1.6 million lb/hr. All this water in flue gas and the cooling tower is simply lost to the atmosphere.

Recovering water from the flue gas using condensing flue gas heat exchangers can help reduce the water intake requirements and also recover waste heat from the flue gas which can be used for other processes like supplying sensible heat to feed water or pre-drying the coal. Besides this, with moisture taken out from the flue gas, the load on the Induced Draft fan is also reduced thus reducing the unit auxiliary power.

In this study, five different heat exchanger arrangements were investigated.

1. Heat exchanger placed upstream of the FGD unit, also referred to as UHX in the study.
2. Heat exchanger placed downstream of the FGD unit, also referred to as DHX in the study.
3. Heat exchanger with pre-cooled flue gas using water spray.
4. DHX coupled with a water-to-water shell and tube heat exchanger to obtain space flexibility.
5. Combined use of UHX and DHX (cascaded arrangement).

All the heat exchangers are counter cross flow type with bare tube banks in inline arrangement. Hot flue gas flows outside the heat exchanger tubes and cooling water flows inside the tubes. The flue gas will be cooled down as it travels through the heat exchangers and the cooling water will absorb this heat. When the tube wall temperature goes below the water vapor dew point temperature, water vapor in the flue gas will start condensing out.

The total cost associated with the use of the heat exchanger can be divided into two parts: 1) manufacturing and installation cost, & 2) operating cost. The manufacturing cost comprises primarily the cost of tube material and the labor cost. The operating cost will be from the additional fan power required due to the pressure drop in flue gas across the tube bank and the pump power required due to the pressure drop in the cooling water as in passes through heat exchanger tubes. The effects of changing the tube diameter, keeping the tube thickness at schedule 40, on the cost and performance of the heat exchanger were investigated.

Lastly the advantages and disadvantages associated with different heat exchanger models were evaluated.

2. Theory

In this study, we have used heat exchangers for two different purposes. The first heat exchanger (at times referred to as HX1) is also called a condensing flue gas heat exchanger having flue gas and water as the two fluid streams. The other exchanger is a water-to-water shell and tube heat exchanger and is at times referred to as HX2 in this report. As the name indicates, HX2 has water flowing inside as well as outside the heat exchanger tubes. Both HX1 and HX2 are counter-cross flow heat exchangers with inline tube arrangement.

For the condensing flue gas heat exchanger, a MATLAB code was developed by Jeong (1) to simulate the heat and mass transfer processes occurring inside the exchanger. The results from the code were verified with data obtained from a lab scale model of the exchanger. The results are available in Jeong's Ph.D. dissertation report. The code was modified by Lavigne (2) and then further by Hazell (3) to calculate the pressure drop in flue gas and cooling water streams as they pass through the heat exchanger.

A separate MATLAB code was developed for the water-to-water heat exchanger. This code **only approximately** determines the heat transfer between the fluids and the pressure drop for both the fluid streams as they pass through the exchanger.

The governing equations for both the condensing heat exchanger and the water-to-water heat exchanger are described in the following sections.

2.1.Condensing Flue Gas Heat Exchanger

Flue gas can be described as a mixture of water vapor and non-condensable gases. Typically for a counter flow heat exchanger, the temperature profile of flue gas and the cooling water along the length of the heat exchanger will be as indicated in the Figure (1). Further, the temperature of the tube wall in contact with the flue gas will also decrease along the length as indicated. When the tube wall temperature goes below the dew point temperature of water vapor in flue gas at any given location, (For example in Figure (1) the wall temperature goes below the dew point temperature at approximately 50% down the length of the exchanger), the water vapor in the flue gas stream will start condensing.

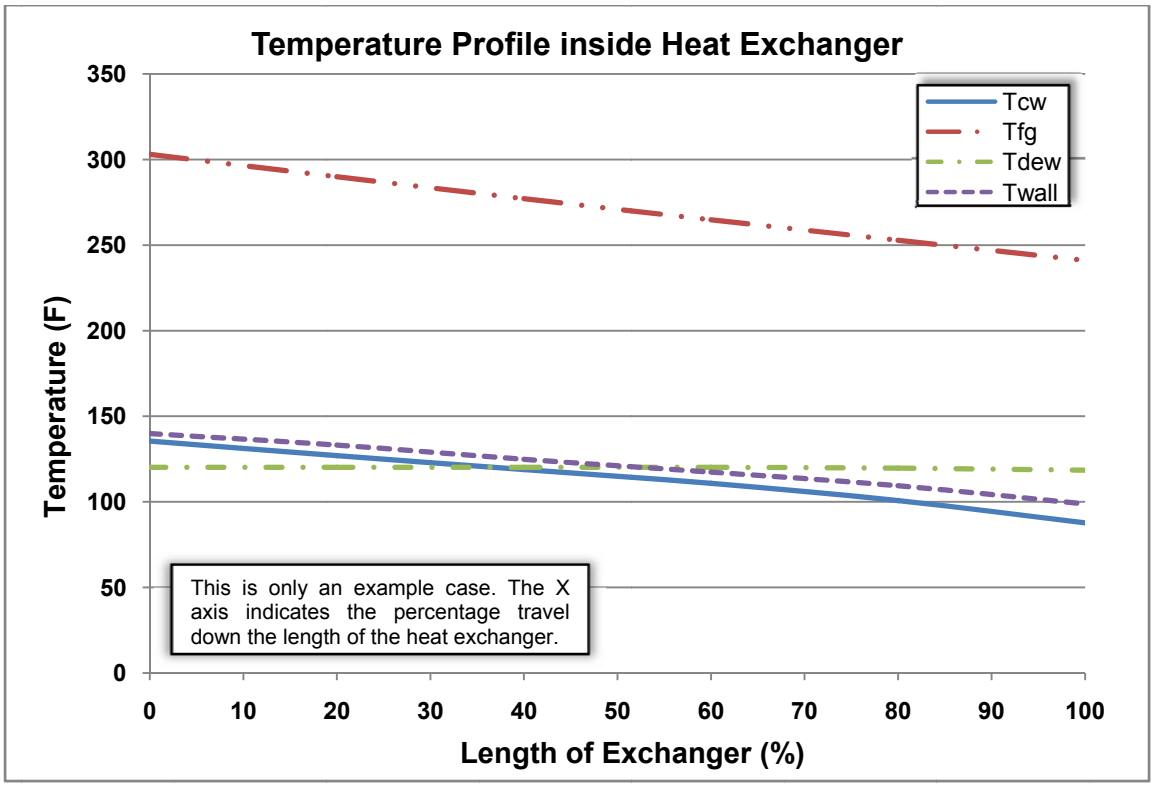

Figure 1 - Typical temperature distributions inside a heat exchanger

As a result of the vapor condensation phenomenon, both sensible and latent heat transfers are observed in the system. In 1934, Colburn and Hougen developed a fundamental transport equation for condensation in the presence of non-condensable gases (4):

$$h_{fg}(T_{fg} - T_i) + k_m h_l (y_{H_2O} - y_i) = U_0 (T_i - T_{cw})$$

In the above equation, on the left hand side, the first term represents the sensible heat transfer from flue gas to tube and the second term represents the latent heat transfer due to vapor condensation. h_{fg} is the convective heat transfer coefficient on wet flue gas side; T_{fg} and T_i are the bulk temperature of flue gas and gas-condensate film interfacial temperature, respectively. The parameters k_m and h_l are the mass transfer coefficient and latent heat of water vapor, respectively. y_{H_2O} and y_i are the mole fraction of water vapor in bulk and at the gas-condensate interface of flue gas, respectively, and T_{cw} is the temperature of cooling water. U_0 is the overall heat transfer coefficient expressed as shown below:

$$\frac{1}{U_0 A_{eff}} = \left[\frac{1}{h_{cw}} + R_{fl}\right]\frac{1}{A_i} + R_{wall} + \frac{1}{h_f A_o}$$

where, A_{eff} is the effective area and is assumed to be the same as tube outer surface Area A_o, and, A_i is the tube inner surface area. R_{fl} is the thermal resistance due to fouling on the inside of the tube. h_{cw} and h_f are the convective heat transfer coefficient for cooling water and the condensate film formed on the outer surface of the tube. R_{wall} is the thermal resistance of the tube wall and depends on the tube material as well as the inner and outer diameters.

$$R_{wall} = \frac{ln\left(d_o/d_i\right)}{2\pi k_w L}$$

where, d_o and d_i are the outer and inner diameters of the tube, k_w is the thermal conductivity of the tube material and L is the overall length of the tube.

In most cases, when using a clean source of cooling water, very little or no fouling is observed inside the tubes and hence thermal resistance due to tube fouling can be neglected. Further, the thickness of the condensate film on the tube outer surface is negligible and thus the thermal resistance due to the condensate film can also be neglected. Substituting the surface area as the product of the circumference and the overall length of the tube, L, and solving for U_0, the equation reduces to:

$$U_0 = \frac{1}{\frac{r_o}{r_i}\frac{1}{h_{cw}} + \frac{r_o}{k_w} ln\frac{r_o}{r_i}}$$

Substituting the value of U_0 from above in the Colburn-Hougen equation and rearranging, the expression for Ti can be deduced as follows:

$$T_i = \frac{\left[h_{fg}T_{fg} + \left(\frac{1}{\frac{r_o}{r_i}\frac{1}{h_{cw}} + \frac{r_o}{k_w} ln\frac{r_o}{r_i}}\right) * T_{cw} + k_m h_l\left(y_{H_2O} - y_i\right)\right]}{\left[\left(\frac{1}{\frac{r_o}{r_i}\frac{1}{h_{cw}} + \frac{r_o}{k_w} ln\frac{r_o}{r_i}}\right) + h_{fg}\right]}$$

In the absence of condensation, the interfacial temperature T_i is replaced by the outer tube wall temperature T_{ow} and the mass transfer term can be dropped from the Colburn-Hougen equation. The rate of heat transfer reduces to a simple equation:

$$q = \frac{T_{fg} - T_{cw}}{R_{total}}$$

where, R_{total} is the total thermal resistance of the control volume and is the sum of the individual thermal resistance of flue gas, tube wall and cooling water.

$$R_{total} = R_{flue\ gas} + R_{wall} + R_{cooling\ water}$$

and,

$$R_{flue\ gas} = \frac{1}{h_{fg}A_o} = \frac{1}{2\pi r_o L h_{fg}}$$

$$R_{cooling\ water} = \frac{1}{h_{cw}A_i} = \frac{1}{2\pi r_i L h_{cw}}$$

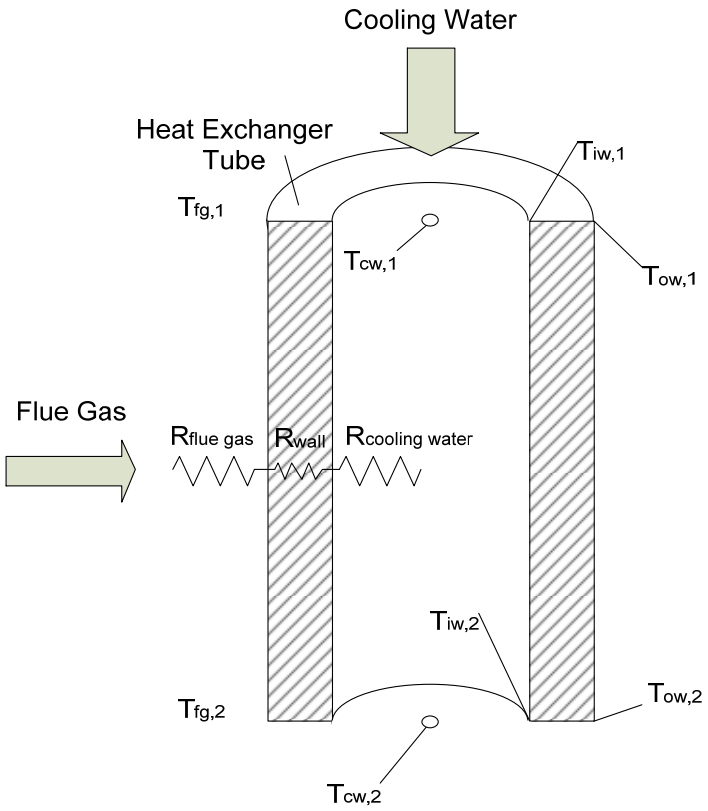

Figure 2 - Thermal resistances between flue gas and cooling water in the absence of condensation

The heat is first transferred from flue gas to the tube wall and then from the wall to the cooling water. It is necessary to discretize the heat exchanger and calculate the tube inner and outer wall temperature for each discrete cell as the flue gas and cooling water temperatures change through the length of the heat exchanger as indicated in Figure (1). Consider that the tube section shown in Figure (2) represents a discretized cell, for the first iteration, the total thermal resistance and the inlet conditions for flue gas and cooling water are known. Assuming no condensation at the beginning of the heat exchanger (the first cell), the heat transferred to the tube wall from flue gas is given by:

$$q = h_{fg} A_{oc} (T_{fg} - T_{ow})$$

where, A_{oc} is the tube outer wall surface area for the cell and T_{ow} is the temperature of the tube outer wall. The equation can be rearranged to obtain an expression for initial tube outer wall temperature as:

$$T_{wo} = T_{fg} - \frac{q}{h_{fg} A_{oc}}$$

The wall temperatures thus calculated for the first cell and the flue gas and cooling water temperatures can be used as the inlet conditions to the next successive cell. At any i^{th} cell along the length of the tube, the law of conservation of energy between the change in enthalpy of the flue gas and the heat transferred to the tube wall can be applied to calculate the flue gas temperature at the exit of the new cell by using the $T_{fg,2}$, $T_{cw,2}$, $T_{ow,2}$, $T_{iw,2}$ from the $(i-1)^{th}$ cell as the inlet conditions to the i^{th} cell.

$$\dot{m}_{fg} C_{p,fg} (T_{fg,2} - T_{fg,1}) = h_{fg} (T_{fg} - T_{ow,1}) A_{oc}$$

where, T_{fg} is the mean of the flue gas inlet and exit temperature for the cell. Rearranging,

$$T_{fg,2} = \frac{(\dot{m}_{fg} C_{p,fg} - 0.5 * h_{fg} A_{oc}) * T_{fg,1} + h_{fg} A_{oc} T_{ow,1}}{\dot{m}_{fg} C_{p,fg} + 0.5 * h_{fg} A_{oc}}$$

Similarly, from energy balance, the total change in enthalpy of the cooling water should be equal to the total heat transferred to the wall from the flue gas. Thus for the same i^{th} cell:

$$h_{fg} (T_{fg} - T_{ow,1}) A_{oc} = \dot{m}_{cw} C_{p,cw} (T_{cw,2} - T_{cw,1})$$

rearranging, $T_{cw,2} = T_{cw,1} - h_{fg}(T_{fg} - T_{ow,1})A_o/\dot{m}_{cw}C_{p,cw}$

In the presence of condensation, it is necessary to modify the above equation using Colburn-Hougen relation and the wall temperature $T_{ow,1}$ is replaced by the temperature of the gas-condensate interface, $T_{i,1}$. The temperatures $T_{fg,2}$ and $T_{cw,2}$ can be rewritten as:

$$T_{fg,2} = \frac{(\dot{m}_{fg}C_{p,fg} - 0.5 * h_{fg}A_{oc}) * T_{fg,1} + h_{fg}A_{oc}T_{i,1}}{\dot{m}_{fg}C_{p,fg} + 0.5 * h_{fg}A_{oc}}$$

$$T_{cw,2} = T_{cw,1} - \frac{[h_{fg}(T_{fg} - T_{i,1}) + k_m h_l(y_{H_2O} - y_i)]A_{oc}}{\dot{m}_{cw}C_{p,cw}}$$

The enthalpy change in cooling water can then be used to calculate the temperature of the tube inner wall. From the law of conservation of energy, the convective heat transfer from the wall to the cooling water should be equal to the change in enthalpy of the cooling water as expressed below:

$$h_{cw}A_{ic}(T_{iw,2} - T_{cw,2}) = \dot{m}_{cw}C_{p,cw}(T_{cw,1} - T_{cw,2})$$

rearranging,

$$T_{iw,2} = T_{cw,2} + \frac{\dot{m}_{cw}C_{p,cw}(T_{cw,1} - T_{cw,2})}{h_{cw}A_{ic}}$$

Lastly, the outer wall temperature at the exit of the cell can be obtained from energy balance between the enthalpy change in cooling water and rate of heat transfer between the tube outer and inner wall.

$$q = \frac{(T_{ow,2} - T_{iw,2})}{R_{wall}} = \dot{m}_{cw}C_{p,cw}(T_{cw,2} - T_{cw,1})$$

Substituting the expression for R_{wall} in the above expression and rearranging,

$$T_{ow,2} = T_{iw,2} + \frac{\dot{m}_{cw}C_{p,cw}(T_{cw,1} - T_{cw,2})\ln {}^{r_o}/_{r_i}}{2\pi k_w L}$$

It must be noted here that the temperature of both the inner and the outer wall depend only on the change in temperature of the cooling water. Thus, these equations apply irrespective of water condensation outside the tube.

For the calculation of all the temperatures described in the equations above, it is necessary to calculate the water vapor mole fraction at the interface as well as the convective heat transfer coefficients for flue gas and cooling water. All the thermodynamic properties described below are calculated at each discrete cell and then averaged over the entire tube length. For exchanger with bank to bare tubes in inline arrangement, an empirical relation to calculate the Nusselt number was proposed by Zukauskas (5).

$$Nu_{fg} = CRe_{fg,max}^{m} Pr^{0.36} \left(\frac{Pr}{Pr_s}\right)^{1/4}$$

where, Pr is the Prandtl number and Pr_s is the Surface Prandtl number. All variables except Pr_s are calculated at the bulk of flue gas. The variables C and m depend on the Reynold's number. For the range $10^3 \leq Re_{fg,max} \leq 2 \times 10^5$, C is typically 0.27 and m is evaluated graphically based on experimental data from Zukauskas (5). The convective heat transfer coefficient for flue gas can be calculated as:

$$h_{fg} = \frac{Nu_{fg} k_{fg}}{d_o}$$

On the cooling water side, the Nusselt number is obtained from the expression by Gnielinski (6)

$$Nu_{cw} = \frac{(f/8)(Re_{cw} - 1000)Pr}{1 + 12.7(f/8)^{1/2}\left(Pr^{2/3} - 1\right)}$$

where, the friction factor f is calculated for $3 \times 10^3 \leq Re_{cw} \leq 5 \times 10^6$ from the Moody Diagram by using the relationship (7),

$$f = (0.79 ln Re_{cw} - 1.64)^{-2}$$

The convective heat transfer coefficient for cooling water is calculated using the Nusselt number for cooling water as:

$$h_{cw} = \frac{Nu_{cw} k_{cw}}{d_i}$$

The water vapor mole fraction y_i at the interface is calculated and the beginning of each cell using the Antoine equation (8)

$$y_i = \frac{e^{\left(a-\frac{b}{T_i+c}\right)}}{P_{tot}}$$

where, a = 16.262, b = 3799.89 and c = 226.35 and P_{tot} is the total pressure of flue gas.

As the two fluids, flue gas and cooling water, travel through the heat exchanger, they experience pressure drops. The drop in pressure on the flue gas side and the cooling water side determines the additional power required by the ID fan and cooling water circulation pump. It is assumed that the flow both inside and outside the tubes is fully developed and remains turbulent throughout the length of the heat exchanger.

Zukauskas developed a relationship to determine Pressure drop on the flue gas side for an exchanger with tubes in inline arrangement as a function of the Longitudinal and Transverse Pitch, number of tube rows and the maximum Reynold's number of the flue gas flow (5) as:

$$\Delta p_{fg} = N_L \chi \left(\frac{\rho_{fg} V_{max}^2}{2}\right) f$$

where, N_L is the total number of rows, χ is the correction factor, ρ_{fg} is the density of flue gas, Vmax is the maximum velocity between the tubes and f is the friction factor. The correction factor depends on the tube longitudinal and transverse pitch while the density velocity and friction factor are calculated for each cell and then averaged for the entire heat exchanger. Assuming that the fan works as an isentropic compressor, the additional power required is obtained from the pressure drop by using simple thermodynamic equation:

$$\Delta\, Fan\ Power = \frac{\dot{m_{fg}} C_{p,fg} \left[\left(\frac{P_{out}}{P_{in}}\right)^{\frac{k-1}{k}} - 1\right]}{\eta_{fan}}$$

where, P_{in} is atmospheric pressure, P_{atm} and P_{out} is the sum of P_{atm} and the pressure drop calculated above, k is the ratio of specific heat at constant pressure and constant volume, η_{fan} is the efficiency of the fan.

On the cooling water side, a large proportion of the pressure drop is observed through the length of the tube and can be calculated using the Darcy-Weisbach equation (9):

$$\Delta p_l = f \frac{L}{d_i} \frac{\rho_{cw} V_{avg}^2}{2}$$

where, Δp_l is the pressure loss along the length of the tube, f is the friction factor and can be obtained from the Moody Diagram (7), L is the total length of the tube, ρ_{cw} is the density of cooling water and d_i is the inner diameter of the tube.

. Besides this, minor pressure losses are also observed in the inlet and the outlet header, in the 180° elbows and due to sudden contraction and expansion of the cooling water. The details of the pressure loss calculations are available in Hazell's thesis (3). Given the total volume flow rate of cooling water, Q, and the pump efficiency,η_{pump}, the total pump power required to pump the cooling water through the tubes can then be calculated from the total pressure drop as:

$$W_{pump} = \frac{Q \Delta p_{total}}{\eta_{pump}}$$

2.2.Water-to-Water Heat Exchanger

HX1 described above is essentially a bank of tubes placed directly in the existing flue gas duct. The tubes move up and down through the height of the exchanger with 180° bends at each end till they reach the other end of the exchanger. In contrast to HX1, the water-to-water heat exchanger, or HX2, is modeled as a typical shell and tube heat exchanger with two tube passes and one shell. Cooling water enters HX2 from the top, as illustrated in Figure (3), and Boiler Feed Water flows inside the tubes such that the two fluids move in a counter cross flow fashion.

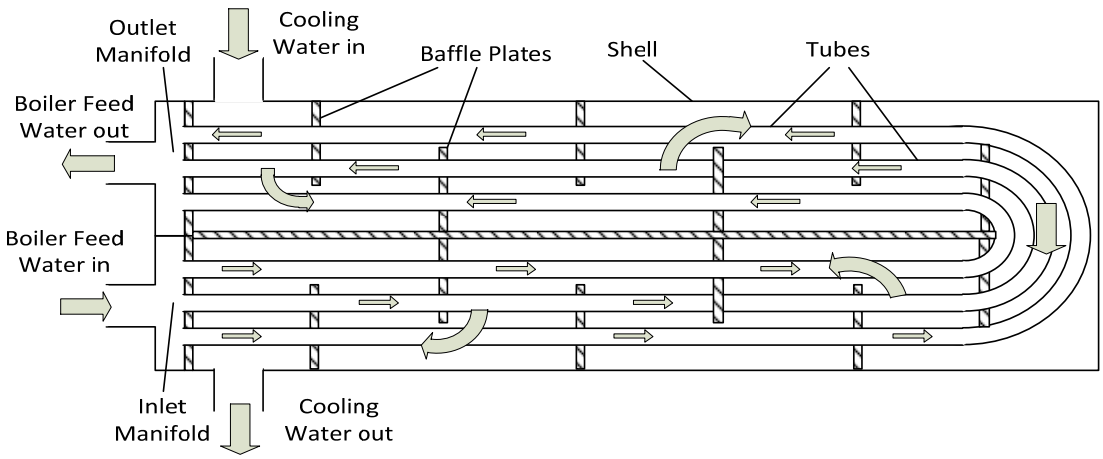

Figure 3 - Water-to-Water Heat Exchanger Model

For HX2, we know the inlet and exit temperature of cooling water and the inlet temperature of boiler feed water. We use the NTU method for calculating the effectiveness of the heat exchanger. The exit temperature of boiler feed water is then calculated from the heat exchanger effectiveness. The heat exchanger effectiveness is defined as a function of the number of transfer units as (10):

$$\varepsilon = \frac{1 - e^{-N_{tu}\left(1-\frac{C_{min}}{C_{max}}\right)}}{1 - \left(\frac{C_{min}}{C_{max}}\right) e^{-N_{tu}\left(1-\frac{C_{min}}{C_{max}}\right)}}$$

where, C_{min} and C_{max} are the minimum and maximum of the heat capacity of cooling water and the boiler feed water, and, N_{tu} is the number of transfer units and is given as:

$$N_{tu} = \frac{N * U_0 A_{eff}}{C_{min}}$$

In the above equation, N is the total number of tubes, U_0 is the overall heat transfer coefficient and A_{eff} is the effective surface area of each tube. For the ease of calculation, it is assumed the A_{eff} is the same as the outer surface area A_o of the tube.

Similar to the thermal resistances in condensing heat exchanger as shown in Figure (2), the rate of heat transfer equation for the water-to-water heat exchanger can also be represented as the sum of thermal resistances:

$$\frac{1}{U_0} = R_{cooling\ water} + R_{wall} + R_{boiler\ feedwater}$$

where $R_{cooling\ water}$, R_{wall} and $R_{boiler\ feedwater}$ are the thermal resistance of the cooling water, the tube wall and the boiler feed water, respectively, and are given as:

$$R_{cooling\ water} = \frac{1}{h_{cw} A_o} = \frac{1}{2\pi r_o L h_{cw}}$$

$$R_{wall} = \frac{ln\left({}^{r_o}/_{r_i}\right)}{2\pi k_w L}$$

$$R_{boiler\ feedwater} = \frac{1}{h_{bfw} A_i} = \frac{1}{2\pi r_i L h_{bfw}}$$

here, h_{cw} and h_{bfw} are the convective heat transfer coefficient for cooling water and boiler feed water, r_o and r_i are the outer and inner radii of the water-to-water heat exchanger tube, and L is the total length of the tube.

For the calculation of the convective heat transfer coefficients for the cooling water and the boiler feed water, it is necessary to calculate the Nusselt number first. Nusselt number for the cooling water can be obtained by using the relation given by Zukauskas (5) for heat transfer across a tube bank:

$$Nu_{cw} = CRe_{cw,max}^{m} Pr^{0.36} \left(\frac{Pr}{Pr_s}\right)^{1/4}$$

where Re is the Reynold's number, Pr is the Prandtl number, Pr_s is the surface Prandtl number. It must be noted here that, although the equation is the same as that used for calculation of convective heat transfer for flue gas in HX1, but, unlike HX1 all the physical variables are calculated at the mean of the inlet and exit temperatures of cooling water. Also, Pr_s is assumed to be the same as Pr to simplify the calculations. The constants C and m depend on the maximum Reynold's number for the cooling water and are obtained graphically from the experimental data by Zukauskas (5). The maximum velocity in a flow across tube bank occurs between two successive tubes and is given as:

$$V_{cw,max} = V_{cw} * \frac{S_t}{S_t - d_o}$$

here, V_{cw} is the velocity of the fluid before it approaches the tube bank, S_t is the transverse pitch between the tubes, and d_o is the tube outer diameter.

The convective heat transfer coefficient for cooling water can be calculated as:

$$h_{cw} = \frac{Nu_{cw} k_{cw}}{d_o}$$

The calculations for heat transfer coefficient for boiler feed water flowing inside the heat exchanger tubes are similar to those for cooling water for the condensing heat exchanger with Nusselt number obtained from equation given by Gnielinski (6) as:

$$Nu_{bfw} = \frac{(f/8)(Re_{bfw} - 1000)Pr}{1 + 12.7(f/8)^{1/2}\left(Pr^{2/3} - 1\right)}$$

Where f is the friction factor and is calculated from the Moody diagram. All the physical variables for boiler feed water are calculated at the inlet temperature of boiler feed water since the exit temperature is unknown.

The convective heat transfer coefficient for boiler feed water can be calculated as:

$$h_{bfw} = \frac{Nu_{bfw} k_{bfw}}{d_i}$$

The effectiveness of a heat exchanger is defined as the ratio of actual heat transfer to the maximum possible heat transfer and can be represented as:

$$\varepsilon = \frac{q_{actual}}{q_{max}} = \frac{C_{bfw}(T_{bfw,out} - T_{bfw,in})}{C_{min}(T_{cw,in} - T_{bfw,in})}$$

where, C_{bfw} is the heat capacity rate of boiler feed water and effectiveness ε is calculated from the N_{tu} relationship given above.

The expression can then be rearranged to obtain $T_{bfw,out}$ as:

$$T_{bfw,out} = \frac{\varepsilon * C_{min}(T_{cw,in} - T_{bfw,in})}{C_{bfw}} + T_{bfw,in}$$

Similar to the condensing heat exchanger, cooling water and boiler feed water fluid streams experience pressure drop as they flow through the heat exchanger. The calculation of these pressure drops is important in estimating the pump power required to circulate the two fluids through the exchanger. The pressure drop on the shell side or the drop in pressure of the cooling water as it flows across the tube bank depends on the type of tube arrangement-inline/staggered, tube spacing, number of rows of tube in the bank, and flow velocity and is given as:

$$\Delta p_{cw} = Eu \frac{\rho V_{cw,max}^2}{2} N_L$$

Here, Eu is the Euler's constant. It depends on the tube transverse and longitudinal pitch and is obtained from the experimental correlations given by Zukauskas and Ulinskas (11) in the power law form as:

$$Eu = \sum_{i=0}^{4} \frac{c_i}{Re^i}$$

where, c_i depends on the tube geometry and the Reynolds number of flow and is provided in the table below. Here, a and b are the ratio of Transverse and longitudinal pitch w.r.t. the tube outer diameter. $a=S_t/d_o$, $b=S_l/d_o$.

Table 1 - Coefficients, c_i, for calculating Euler's constant for in-line square banks (11).

a = b	Re Range	C_0	C_1	C_2	C_3	C_4
1.25	3-2 X 10^3	0.272	0.207 X 10^3	0.102 X 10^3	0.286 X 10^3	-
1.25	2 X 10^3 - 2 X 10^6	0.267	0.249 X 10^4	-0.927 X 10^7	0.10 X 10^{11}	-
1.5	3-2 X 10^3	0.263	0.867 X 10^2	-0.202 X 10^1	-	-
1.5	2 X 10^3 - 2 X 10^6	0.235	0.197 X 10^4	-0.124 X 10^8	0.312 X 10^{11}	-0.274 X 10^{14}
2	7 - 800	0.188	0.566 X 10^2	-0.646 X 10^3	0.601 X 10^4	-0.183 X 10^5
2	800 - 2 X 10^6	0.247	-0.595	0.15	-0.137	0.396

The pressure drop on the shell side is directly proportional to the number of baffle plates provided in the shell. The pressure drop calculated from the above relations is the drop observed in a heat exchanger without baffles. Therefore, for a heat exchanger shell with N_b number of baffles the total pressure drop is given by:

$$\Delta p_{cw,total} = \Delta p_{cw} * (N_b + 1)$$

The flow losses due to leakage across the baffle plates, as indicated in Figure (4a.), were neglected. Here the stream B is the main cross flow stream while the streams A, C and E are tube to baffle hole leakage stream, bundle bypass stream and baffle to shell leakage stream, respectively. The number of baffle plates, their size and spacing between the plates has not been optimized at this stage and the pressure loss due to formation of eddies, Refer Figure (4b, 4c), is also neglected. Also, the losses at the inlet and exit and any other minor losses were neglected.

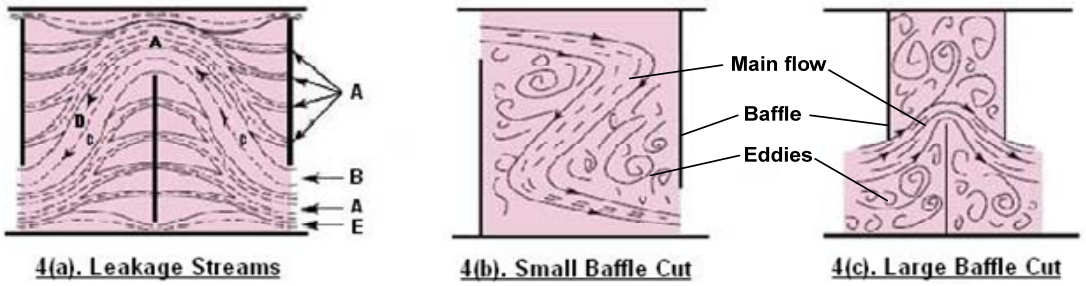

Figure 4 - Shell Side Leakage Streams and Eddy Formation due to Baffles

The tube side pressure drop for boiler feed water is obtained from Darcy Weisbach equation (9):

$$\Delta p_{bfw} = f \frac{L}{d_i} \frac{\rho_{bfw} V_{bfw,avg}^2}{2}$$

where, Δp_{bfw} is the pressure loss along the length of the tube, f is the friction factor and can be obtained from the Moody Diagram (7), L is the total length of the tube, ρ is the density of boiler feed water and d_i is the inner diameter of the tube.

Beside the pressure drop along the tube length, some minor pressure losses are observed in the inlet and outlet manifolds as the fluid suddenly contracts and expands, respectively, and the pressure drop in the inlet manifold is given as (9):

$$\Delta p_{inlet} = K_L \frac{\rho_{bfw} V_{inlet}^2}{2}$$

where, K_L is the loss coefficient and for the case of sudden contraction at sharp edges, KL is usually assumed to be 0.5.

At the outlet header, sudden expansion is observed and the pressure drop can be calculated as (9):

$$\Delta p_{outlet} = \left(1 - \frac{A_1}{A_2}\right)^2 \frac{\rho_{bfw} V_{exit}^2}{2}$$

here, the term $\left(1 - \frac{A_1}{A_2}\right)^2$ is the loss coefficient and depends on the ratio of the area of cross-section of the tube to the manifold. The minor losses are added to the pressure drop in the tube to obtain the overall pressure drop for boiler feed water.

Minor losses in the 180° tube bends and any other leakage losses were neglected. The total addition power required for the pump can then be calculated from the total pressure drop as:

$$W_{pump} = \frac{Q\Delta p_{total}}{\eta_{pump}}$$

here, Q is the total flow rate of boiler feed water or cooling water and Δp_{total} is the total pressure drop in the fluid.

2.3. Estimation of Cost

The heat exchangers can be used in variety of configurations. A few of them will be discussed in detail in Section 5. Each of these configurations has its own set of advantages and the size of these heat exchangers can quickly grow very large if we try to recover maximum possible heat or water from the flue gas stream. As such, it becomes necessary to take into account the economics of the heat exchanger. Heat exchangers have two types of costs associated with them, the capital cost and the operating cost.

2.3.1. Capital Cost

The capital cost, also referred to as fixed cost, consists of the cost of material and the manufacturing and installation cost for the shell and the tubes. Since a condensing heat exchanger is essentially a tube bundle placed in the flue gas duct, this exchanger does not require a shell. Therefore, the capital cost of condensing heat exchangers is primarily the cost of the tube material and their production/installation. In studies done on cost estimation of shell and tube heat exchangers (12), it was observed that with the increase in size of the heat exchangers, the cost of manufacturing/labor cost remained more than the cost of material even though the cost of material starts increasing with size while the fabrication costs decreases steadily with increase in size.

The type of tube material used for the tubes also plays a key role. Assuming that the same technology and labor skills are required to manufacture tubes irrespective of the tube material, the use of expensive materials like Nickel alloy 22 results in higher material cost than the fabrication cost. For condensing heat exchangers, Nickel alloy 22 is used as tube material up-to the point where water starts condensing out to save the tubes from acid corrosion and stainless steel SS304 is used thereafter. The choice of materials is based on the detailed study done by Hazell

(3). Hazell also obtained quotations from suppliers of stainless steel and Nickel alloy 22 tubes. Assuming negligible hike in the pricing since his study, the same pricing of $14.89/ft for manufacturing and installation cost for both SS304 and nickel alloy 22 tubes of 2" diameter NPS and 0.195" thickness has been used. The cost of material was assumed to be $10.69/ft for SS304 tubes and $110.71/ft for Nickel alloy 22 tubes of 2" diameter NPS and 0.195" thickness.

Assuming the life expectancy of 20 years for the heat exchanger, over which a loan would be raised to build the heat exchanger, and an annual rate of interest of 5% be levied on the loan, a monthly payment factor was calculated using the equation (13):

$$PF = \frac{i(1+i)^n}{(1+i)^n - 1}$$

where, PF is the monthly payment factor, i is the monthly rate of interest and n is the period of loan in months. The annual fixed cost of the heat exchanger can then be calculated from the total fixed cost as:

$$AFC = (12 * PF + TIF) * (Total\ Fixed\ Cost)$$

where, AFC is the annual fixed cost and TIF is the taxes and insurance factor and has been assumed to be 0.015 in this study.

Unlike the condensing heat exchanger, for the water-to-water heat exchanger, we will need a shell and the tube material has been assumed to be Seamless Low alloy 213 T11 for higher thermal conductivity. The cost analysis for the shell and the tubing has not been done at this stage.

2.3.2. Operating Cost

The operating cost is the annual expenses that would be observed upon bringing the heat exchanger into operation. As explained in Section 2.1 and Section 2.2 of this report, there is pressure drop observed in both the streams on either side of the tubes. To assist flow, pumps are employed to run the cooling water through the tubes and additional power is required by the ID fan to blow the flue gas out into the stack. The additional power requirements can be calculated from the pressure drop (also explained in above sections). Assuming that the heat exchanger will

remain in service for 7000 hours per year and the cost of electricity is $60/MWhr, the annual operating cost is given as:

$$AOC = Power\ (in\ MW) * \frac{7000\ hrs}{year} * {\$60}/{MWhr}$$

Here, AOC is the Annual Operating Cost and Power is the total power required to operate the heat exchanger.

3. Effects of Operating Conditions

The use of boiler feed water instead of a secondary cooling water loop comes with an added advantage. Not only is it possible to recover water from the flue gas stream but the heat absorbed from the flue gas can be used to improve the unit heat rate. In a previous study by Hazell (3), the impacts of varying mass flow rate ratio of cooling water and flue gas and the cooling water inlet temperature were studied. These results show that the size of the exchanger increases rapidly for higher heat transfer rates.

The mass flow rate of boiler feed water is typically less than that of flue gas. In other parts of this study, the ratio of the mass flow rate of boiler feed water and flue gas was assumed to be constant at 0.443. But, in a study conducted by Jonas (14), it was shown that the mass flow rate of boiler feed water is proportional to the targeted temperature of the boiler feed water as it exits the heat exchanger.

For the 600MW power plant analyzed here, the temperature of boiler feedwater flowing from the condenser hot well is at a temperature of 87°F, as obtained from the supercritical steam cycle used by Jonas (15) provided in Appendix-A Figure (A.1), and, the temperature of feed water is raised to ~500°F before it enters the economizer. The boiler feed water is passed through a series of feed water heaters where it is heated using steam extracted from various stages of the turbine. As a result of using the condensing heat exchanger to preheat the feed water, the duty on the feed water heaters is reduced. As a result, steam, which would have otherwise been extracted for the heaters, now passes through the turbine and adds to the total turbine power output. If more steam passes through the LP turbine into the condenser, the boiler feed water flow rate will increase accordingly.

Jonas developed an ASPEN model to determine the relationship between turbine cycle heat rate, change in net power output and mass flow rate of boiler feed water with respect to the temperature of the boiler feed water at the exit of the condensing heat exchangers. See Figure (5), Figure (6) and Figure (7) below.

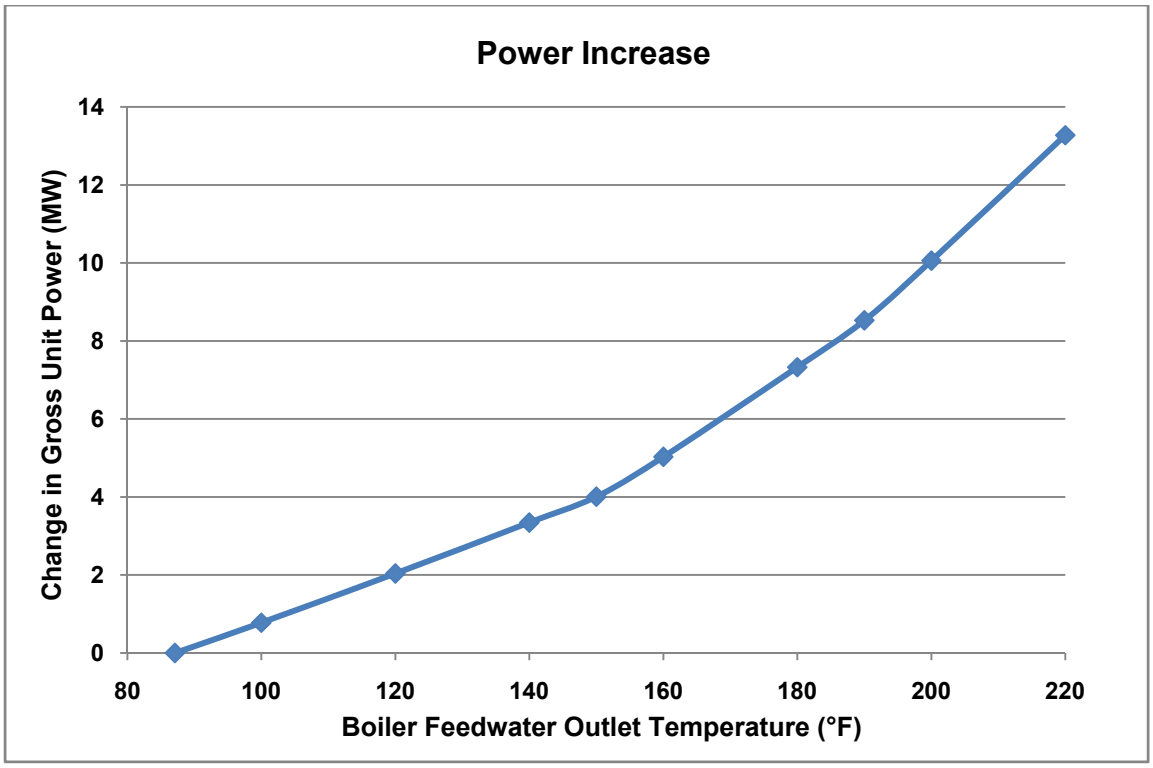

Figure 5 - Change in Gross Unit Power output with Boiler Feed Water Temperature at exit of Heat Exchanger (14)

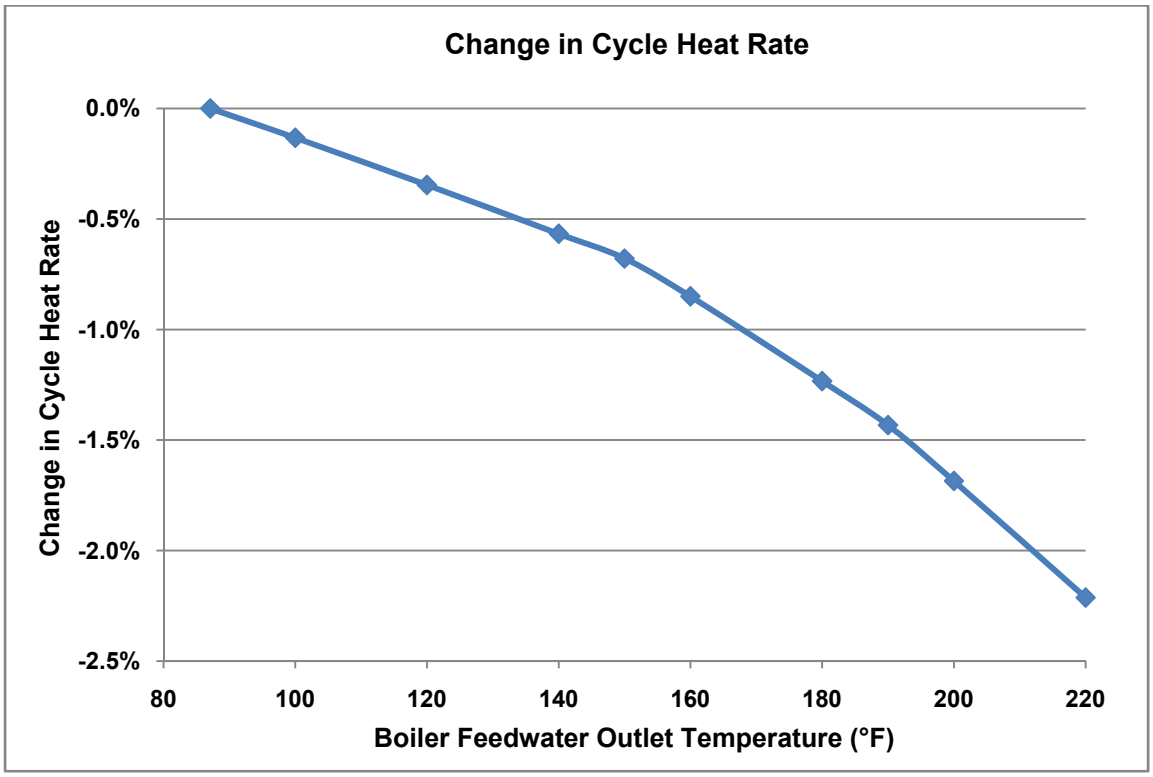

Figure 6 - Change in Cycle Heat Rate with Boiler Feed Water Temperature at exit of Heat Exchanger (14)

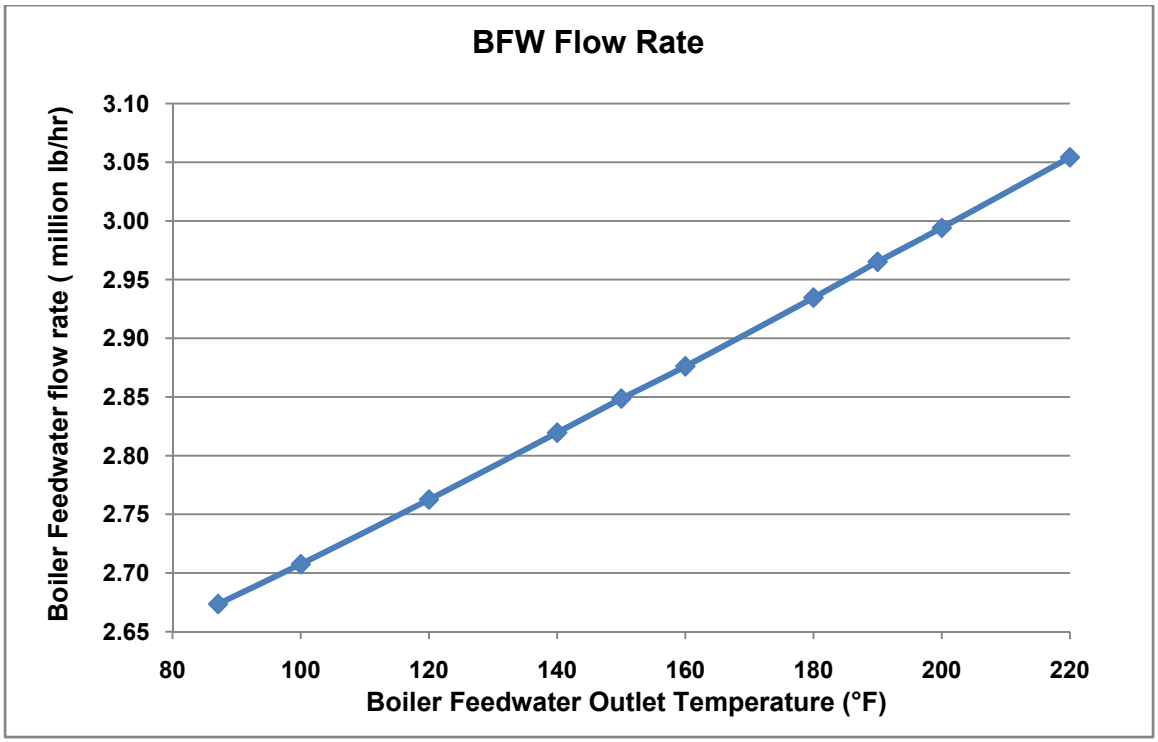

Figure 7 - Change in Boiler Feed Water Flow Rate with Boiler Feed Water Temperature at exit of Heat Exchanger

From the Figures (5) and (6), it is clear that with the increase in temperature of boiler feedwater at the exit of the heat exchanger, the change in net power increases steadily and the heat rate improves. Further in Figure (5), we can identify two knee points on the curve at 150°F and 190°F at which the slope of the curve increases slightly indicating higher change in net power for the same increase in boiler feedwater exit temperature. This can be explained by looking at the supercritical cycle used by Jonas (14), refer Appendix A Figure A.1, which indicates that at a temperature of 153°F, the FWH1 can be completely taken off and similarly FWH2 can be completely taken off at feedwater temperature of 193°F. Also, from Figure (7), it is observed that the curve for mass flow rate of boiler feedwater with respect to feedwater temperature is a straight line indicating that the mass flow rate of boiler feed water is directly proportional to the feedwater exit temperature.

Unless stated otherwise, the above observations were taken into account in this study and the feed water flow rate was changed with respect to the temperature of feed water coming out of the condensing heat exchanger.

4. Effect of Tube Diameter on Performance and Cost

The choice of tube diameter is an important issue. The Reynold's number of the flow is inversely proportional to tube diameter and the pressure drop observed as the fluid passes though the tube or the across the tube bank is directly proportional to the tube inner and outer diameter, respectively. For the condensing flue gas heat exchanger, the density of flue gas is much lower than the cooling water circulating inside the tubes. As a result, the pressure drop observed in flue gas stream is much less than in cooling water. Analyses were performed to determine how the increase in tube diameter would influence the total heat transferred to the cooling water from flue gas and also the cost impact of it.

A set of simulations were run for different tube diameters and for various ratios of mass flow rate of cooling water and flue gas. In each case it was assumed that the tubes will have standard dimensions as per ASME B36.19 and the tube thickness will match Schedule 40S.

Through a series of experiments, Zukauskas (5) established that the heat transfer in bank of tubes depends on the tube spacing parameters defined as:

$$a = {}^{S_t}/_{d_o} \qquad \& \qquad b = {}^{S_l}/_{d_o}$$

where, S_t and S_l are the transverse and longitudinal pitch, respectively. The possible range of 'a' and 'b' is obtained from empirical formulas as:

$$1.20 \leq a \leq 2.70 \qquad \& \qquad 1.25 \leq b \leq 2.60$$

Since the diameter of the tube is varied for different simulations, the tube wall thickness was also varied. Further, the cross-sectional dimensions of the duct were kept constant at 40' X 40'. As a result, the number of rows and columns for a given length of the duct also changed. The transverse pitch (S_t) was kept constant at 6.17" while the values of 'b' were kept at minimum in the above range and the longitudinal pitch (S_l) was calculated for each tube diameter. Refer to the Tables below for details of the fixed and variable process conditions and heat exchanger geometry.

Table 2 - Fixed Process Conditions for studying the impact of Tube Diameter

Fixed Inlet Conditions			
M_{fg} (lbm/hr)	T_{fg} (°F)	T_{bfw} (°F)	y_{H2O} (%)
6.31E+06	135	87	17.4

Table 3 - Fixed Heat Exchanger Geometry for studying the impact of Tube Diameter

Fixed Heat Exchanger Geometry				
Tube Wall Thickness	S_t (in)	S_l (in)	Duct Depth (ft)	Duct Height (ft)
Schedule 40S	6.17	1.25 X Tube OD	40	40

Table 4 - Variable Parameters for studying the impact of Tube Diameter

Variable Parameter		
Duct Length (ft)	Flow Ratio	Tube Diameter NPS (in)
5	0.443	2
7	1	2.5
10	1.5	3
12		3.5
15		
20		

For the mass flow rate ratio of 0.443, the tube diameter was not increased, as increasing the tube diameter beyond 2" NPS resulted in a decrease in Reynold's number with the flow becoming laminar, which is undesirable. But, still it was interesting to compare the results from exchangers with larger diameter tubes and higher flow ratio with those for flow ratio of 0.443 and tube diameter 2" NPS.

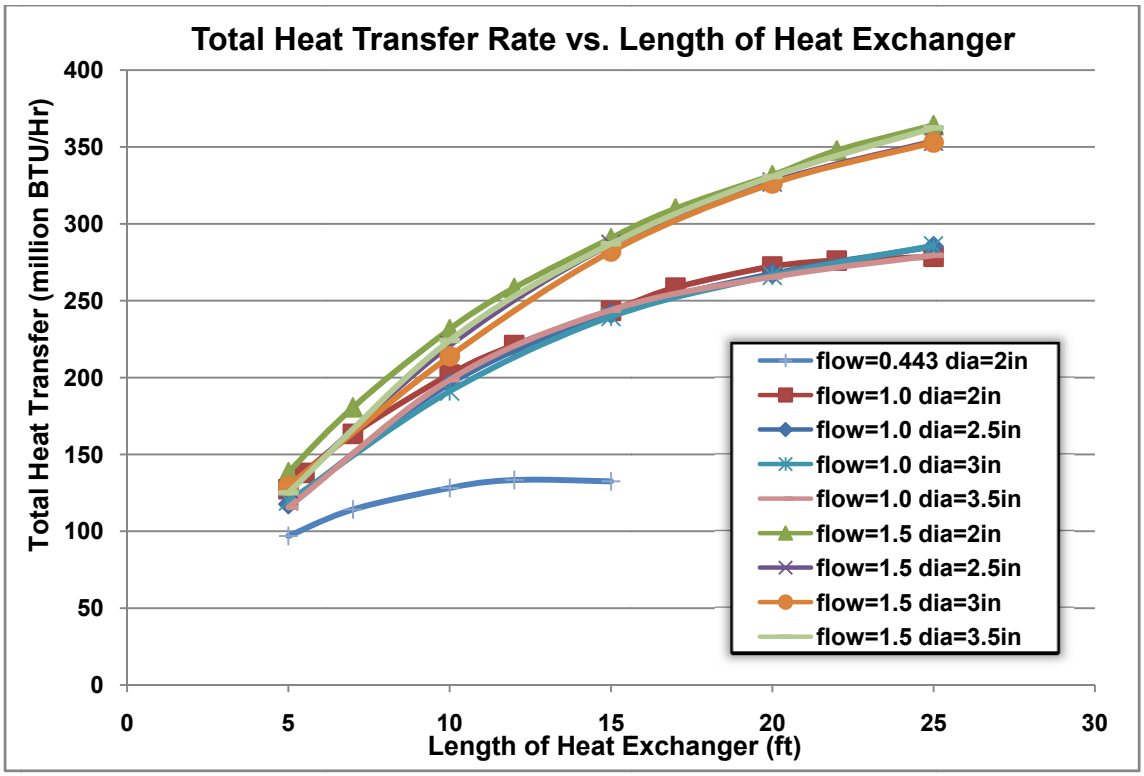

Figure 8 - Impact of Tube Diameter on Total Heat Transfer

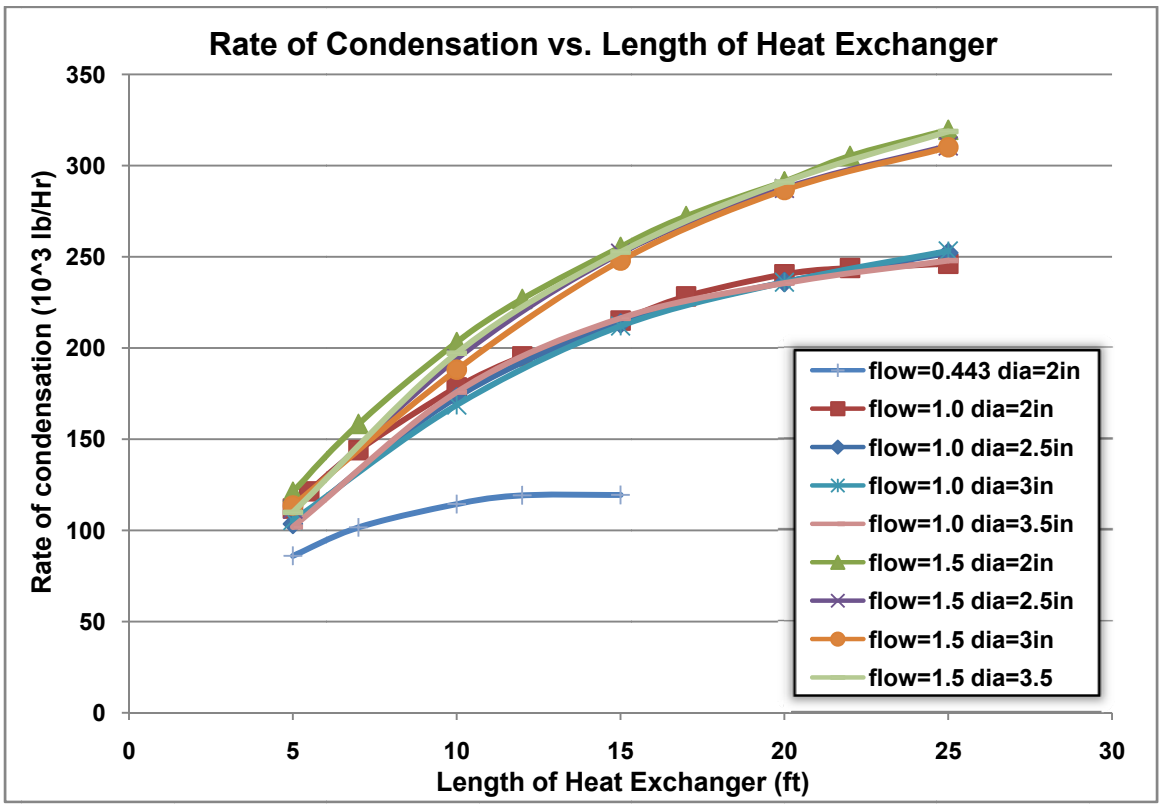

Figure 9 - Impact of Tube Diameter on Rate of Condensation

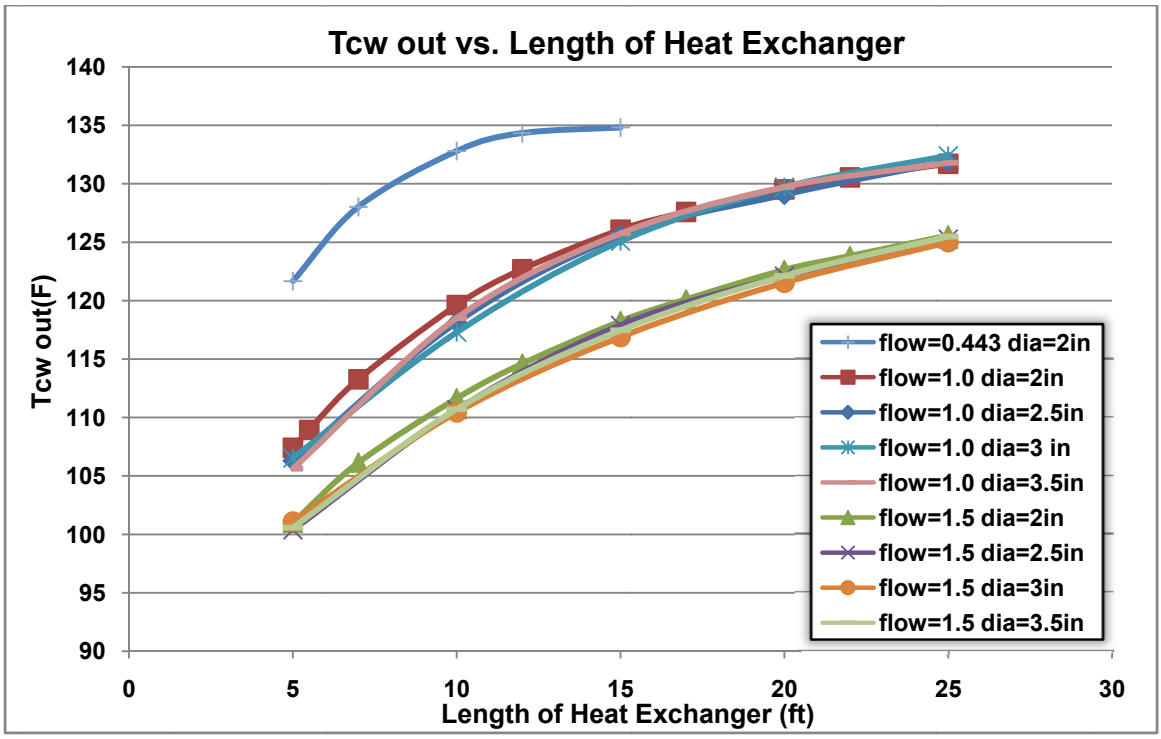

Figure 10 - Impact of Tube Diameter on Cooling Water Temperature at exit of Heat Exchanger

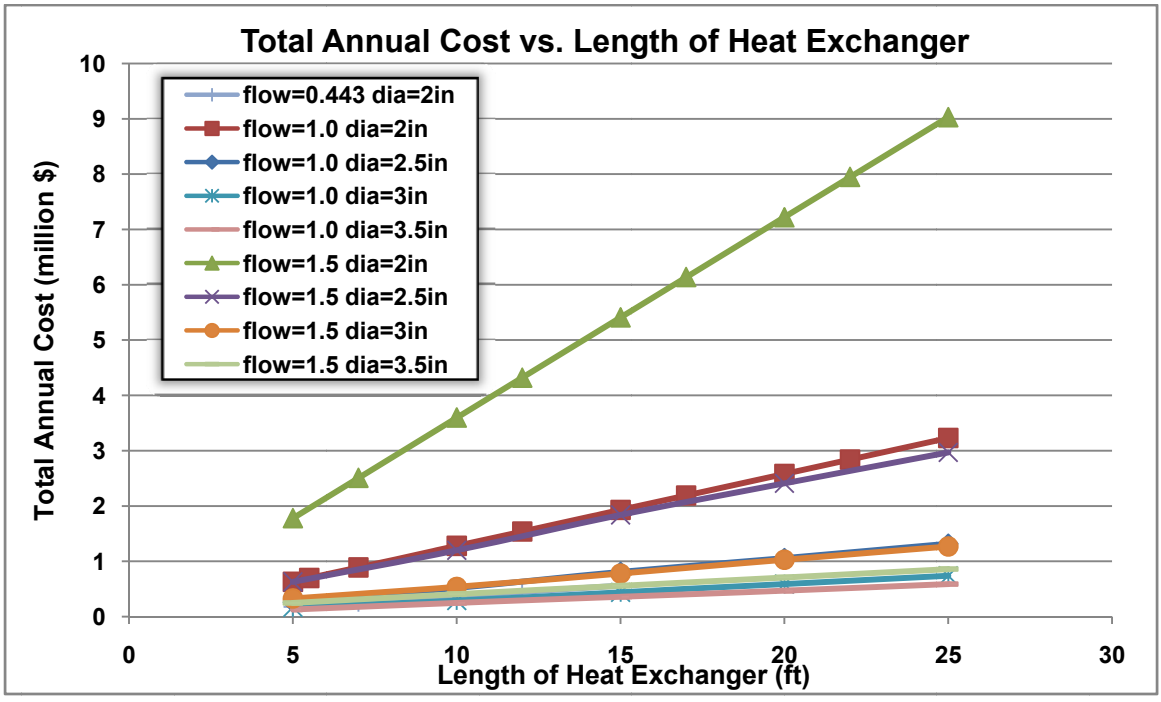

Figure 11 - Impact of Tube Diameter on Total Annual Cost of Heat Exchanger

From the Figures (8), (9), and (10), it is evident that for a given flow rate ratio and size of the heat exchanger (Duct Length), the total heat transfer rate, rate of condensation and the

temperature of the cooling water at the exit of the heat exchanger remain nearly the same with increase in tube diameter. The reason for this observation is that the overall surface area of the tubes for each diameter is nearly the same. Even though the number of tubes decreases due to the fixed cross-section of the duct, the likely reduction in surface area is compensated by the increase in diameter of the tubes. But, from Figure (11), it can be observed that the total annual cost is greatly reduced for a given mass flow rate with the increase in tube diameter. This observation can be attributed to the reduction in pressure drop in the cooling water, as it passes through the heat exchanger tubes, with increase in tube diameter.

The total annual cost of the heat exchanger comprises of fixed cost and annual operating cost as explained in Section 2.3. The details of the annual operating costs and total fixed costs as well as the pressure drop in flue gas and cooling water streams are available in Tables (5) and (6) below, respectively. It must be noted that the Tables (5) and (6) are provided only for heat exchangers of Duct Length 20ft as from the above figures it is reasonable to assume that the curves for rate of condensation, total heat transfer and Temperature of cooling water at the exit of heat exchanger become nearly flat.

Table 5 - Impact of Tube Diameter on Pressure Drop for 20ft Heat Exchanger Length

Cooling Water to Flue Gas Mass Flow Rate Ratio = 1.0					
Tube Diameter (NPS)	Cooling Water Δp	Flue Gas Δp	ID Fan Power	Cooling Water Pump Power	Total Power
(in)	(psi)	(psi)	KW	KW	KW
2	696.897	0.046	25.21	4774.40	4799.61
2.5	203.078	0.057	34.72	1391.28	1425.99
3	66.201	0.081	55.25	453.54	508.79
3.5	36.173	0.117	86.18	247.82	334.01
Cooling Water to Flue Gas Mass Flow Rate Ratio = 1.5					
Tube Diameter (NPS)	Cooling Water Δp	Flue Gas Δp	ID Fan Power	Cooling Water Pump Power	Total Power
(in)	(psi)	(psi)	KW	KW	KW
2	1540.297	0.045	24.32	15828.74	15853.06
2.5	447.017	0.056	33.48	4593.74	4627.22
3	145.504	0.079	53.35	1495.26	1548.61
3.5	79.671	0.114	82.81	818.73	901.54

Table 6 - Impact of Tube Diameter on Total Annual Cost for 20ft Heat Exchanger Length

Cooling Water to Flue Gas Mass Flow Rate Ratio = 1.0						
Tube Diameter (NPS)	Cond. Rate	Total HT	Total Capital Cost	Annual Fixed Cost	Annual Operating Cost	Total Annual Cost
(in)	[10^3 lb/hr]	[10^6 BTU/hr]	$ million	$ million	$ million	$ million
2	240.34	272.29	5.98	0.56	2.02	2.58
2.5	236.10	267.40	4.9	0.46	0.6	1.06
3	235.98	266.38	3.98	0.38	0.21	0.59
3.5	235.50	265.41	3.52	0.33	0.14	0.47
Cooling Water to Flue Gas Mass Flow Rate Ratio = 1.5						
Tube Diameter (NPS)	Cond. Rate	Total HT	Total Capital Cost	Annual Fixed Cost	Annual Operating Cost	Total Annual Cost
(in)	[10^3 lb/hr]	[10^6 BTU/hr]	$ million	$ million	$ million	$ million
2	291.31	331.55	5.98	0.56	6.66	7.22
2.5	287.49	327.22	4.9	0.46	1.94	2.41
3	286.58	326.21	3.98	0.38	0.65	1.03
3.5	291.00	330.79	3.52	0.33	0.38	0.71

From the above tables, assuming a 20ft long heat exchanger, the total power required and the total annual cost were plotted for different tube diameters at different mass flow rate ratios. Refer Figure (12) and Figure (13) below.

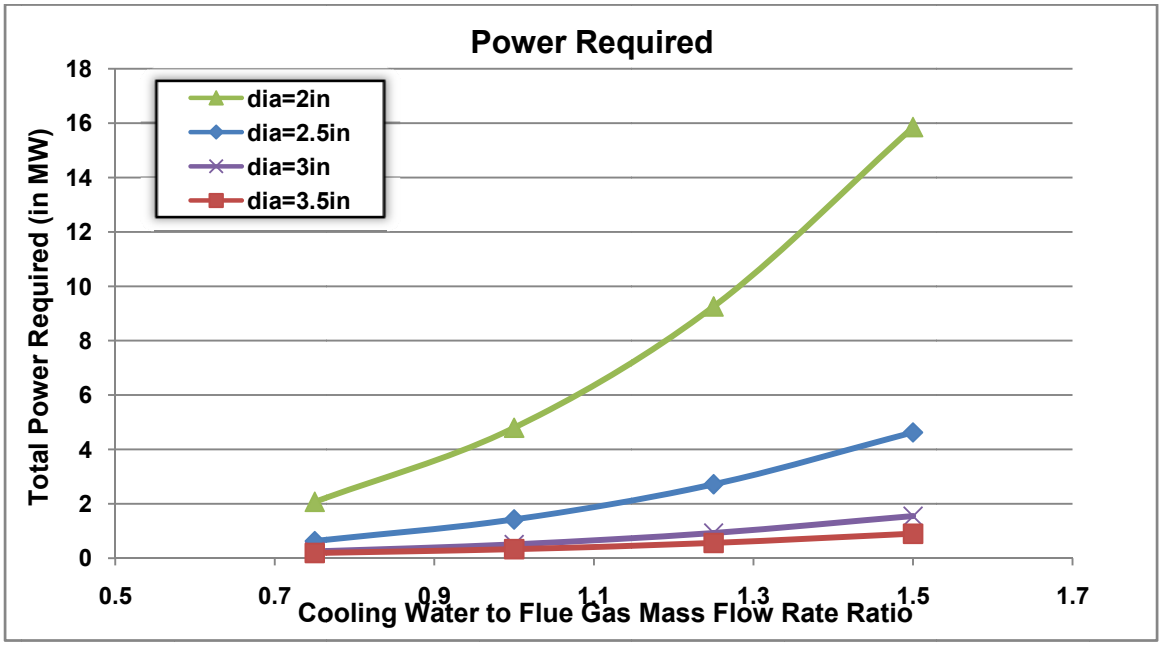

Figure 12 - Impact of Diameter on Power Requirements for 20ft long Heat Exchanger

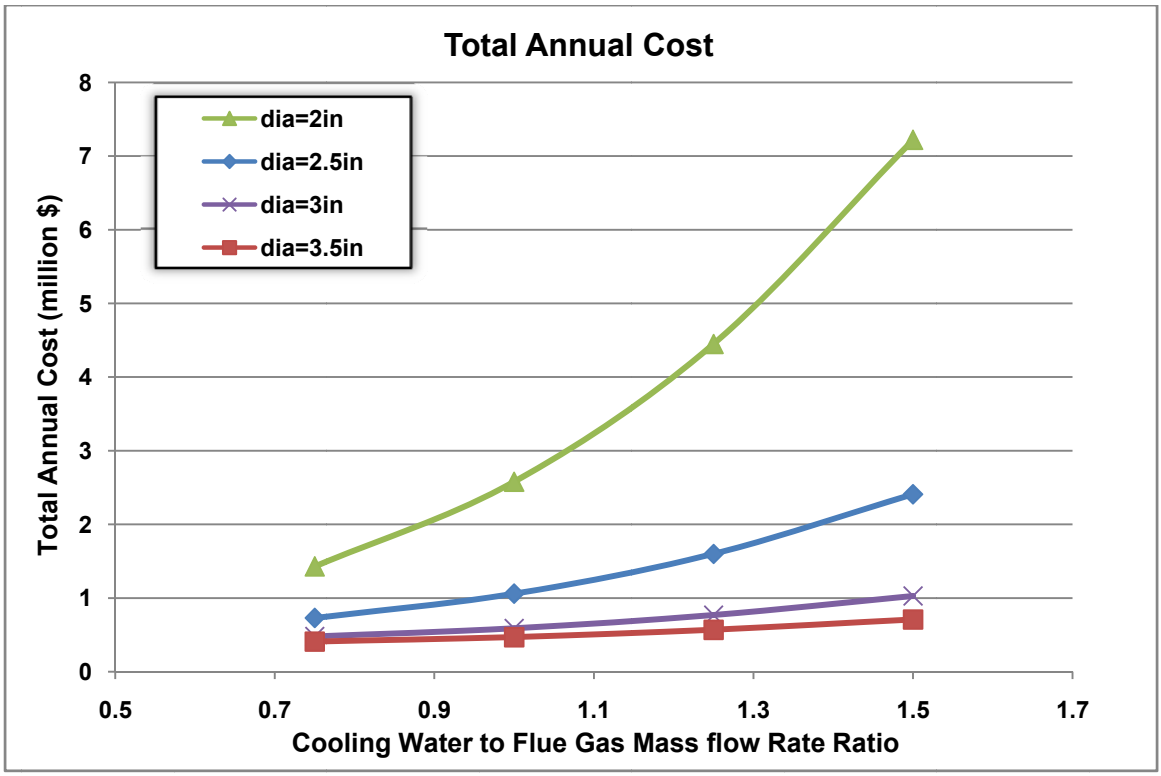

Figure 13 - Impact of Diameter on Total Annual cost for 20ft long Heat Exchanger

Assuming that the pricing of tube per lbm is same for different diameter tubes considered here, it is observed in Table (6) that the fixed cost decreases with increase in tube diameter. This can be attributed to lesser material requirement for larger diameter tubes keeping same surface area. Further, it is also observed that the total power consumed by the system reduces with increase in diameter of tubes due to reduction in overall pressure drop. Thus, the total annual cost associated with the heat exchanger also decreases as can be seen in Figure (13).

5. Heat Exchanger Arrangements

Flue gas entering the condensing heat exchanger can be cooled down using air or water. A detailed study on condensing water from flue gas using air is described by Kessen in his dissertation (15). The present study concentrates on water cooled condensing heat exchangers with flue gas flowing outside the exchanger tubes and water flowing inside the tubes. For the cooling water, we have the option of using boiler feedwater from the steam circuit or cooling water from another external source. For the 600 MW unit described here, the boiler feedwater extracted before the first feedwater heater is at a temperature of nearly 87°F. The use of boiler feedwater serves in recovering water from the flue gas and also improves the power plant heat rate by using the recovered heat to preheat boiler feedwater. If a separate source of cooling water is used, the condensed flue gas moisture can be routed through the cooling tower. As a third possibility, a combination of boiler feed water and cooling water can be used such that the cooling water flows through the tubes of the condensing heat exchanger and then transfers the heat absorbed from the flue gas to the boiler feedwater in a separate shell and tube heat exchanger. The details of these models are provided in the subsequent sections.

For all the models discussed, the inlet conditions of flue gas were based on a 600MW conventional coal-fired power plant unit burning PRB coal with flue gas flow rate of 6.3 million lb/hr after the ESP. If the system has a wet FGD unit, the flue gas will be saturated with water, thus increasing the mass flow rate to 6.716 million lb/hr. The increased mass flow rate of flue gas for a system with FGD has been taken into account in all heat exchanger arrangements discussed in this study, unless otherwise noted. Further details of the process conditions are provided in subsequent sections.

5.1.Heat Exchanger placed Upstream of Wet FGD, Flue gas at 303°F

It is not an uncommon practice for power plants to use a low sulfur coal and avoid altogether wet FGD unit while still abiding by the emission limits issued by EPA. For a coal fired power plant, flue gas after the ESP is usually at temperatures close to 300°F. The mass flow rate

of flue gas is around 6.3 million lb/hr with a moisture content of roughly 12%. The heat exchangers placed in flue gas stream, upstream of the wet FGD unit, are exposed to corrosive environment due to the presence of H_2SO_4 in flue gas. As a result, it becomes necessary to use corrosion resistant Nickel alloy 22 material for the heat exchanger tubes until the tube wall temperature reaches below the dew point temperature of moisture in the gas stream. The choice of material and its impact on cost and total heat transfer were studied in detail by Hazell (3). Hazell also discussed the effect of temperature of cooling water at the inlet of the heat exchanger and the effect of ratio of mass flow rate of cooling water to flue gas on rate of condensation, total heat transfer and the total annual cost associated with the system. In this study, we looked at the impact of using high temperature boiler feed water coming out of different feed water heaters by assuming that the heat exchanger is placed before low pressure feedwater heater 1,2 or 3.

The temperature and flow rate ratio of boiler feedwater to flue gas depends on where, in the steam circuit, the feed water is extracted from and how much heat is intended to be recovered from the flue gas as explained in Section 3. Different process conditions were analyzed based on mass flow rate of boiler feedwater as obtained from Jonas' ASPEN model (14).

For these analyses of heat exchangers upstream of the FGD unit, pipe size was kept constant at 2" diameter and tube wall thickness of 0.195" was assumed. Larger diameter, which was identified as advantageous in Section 4, was not used for tubes in these analyses since the effects of tube ID were investigated only for heat exchangers downstream of the FGD unit. The tube spacing of S_t = 6.17" and S_l = 2.97" were used based on the optimization analysis done by Hazell (3). The fixed process conditions and heat exchanger geometry are summarized in Table (7) and Table (8), respectively. The variable parameters are provided in Table (9).

Table 7 - Fixed Process Conditions for Heat Exchanger Placed Upstream of Wet FGD

Inlet Conditions		
M_{fg} (lb/hr)	y_{H2O} (%)	T_{fg} (°F)
6.31E+06	11.6	303

Table 8 - Fixed Heat Exchanger Geometry for Heat Exchanger Placed Upstream of Wet FGD

Fixed Heat Exchanger Geometry					
Tube Diameter NPS (in)	Tube Wall Thickness (in)	S_t (in)	S_l (in)	Duct Depth (ft)	Duct Height (ft)
2	0.195	6.17	2.97	40	40

Table 9 - Various Process Conditions for Heat Exchanger Placed Upstream of Wet FGD

Variable Process Conditions		
Sub-Case	BFW Inlet Temp (°F)	Flow ratio
A	98	0.462
B	87	0.437
C	87	0.45
D & E	152	0.503
F	194	0.503

Six different subcases were studied. Each case had a distinct inlet temperature of boiler feedwater and boiler feedwater to flue gas mass flow rate ratio. A summary of the input parameters of these subcases is provided in Table (9) above. It must be noted here that case 'D' and 'E' have same inlet process conditions but they have different target temperature of boiler feedwater at the exit of heat exchanger which can be attained by increasing the heat exchanger duct length, or equivalently, the surface area. The detailed process conditions of each case are provided in Appendix-A Table (A.1). For these subcases, trends for rate of condensation, the temperature of boiler feedwater at the exit of the heat exchanger and the total annual cost are analyzed for different heat exchanger lengths are provided below in Figure (14), Figure (15) and Figure (16), respectively.

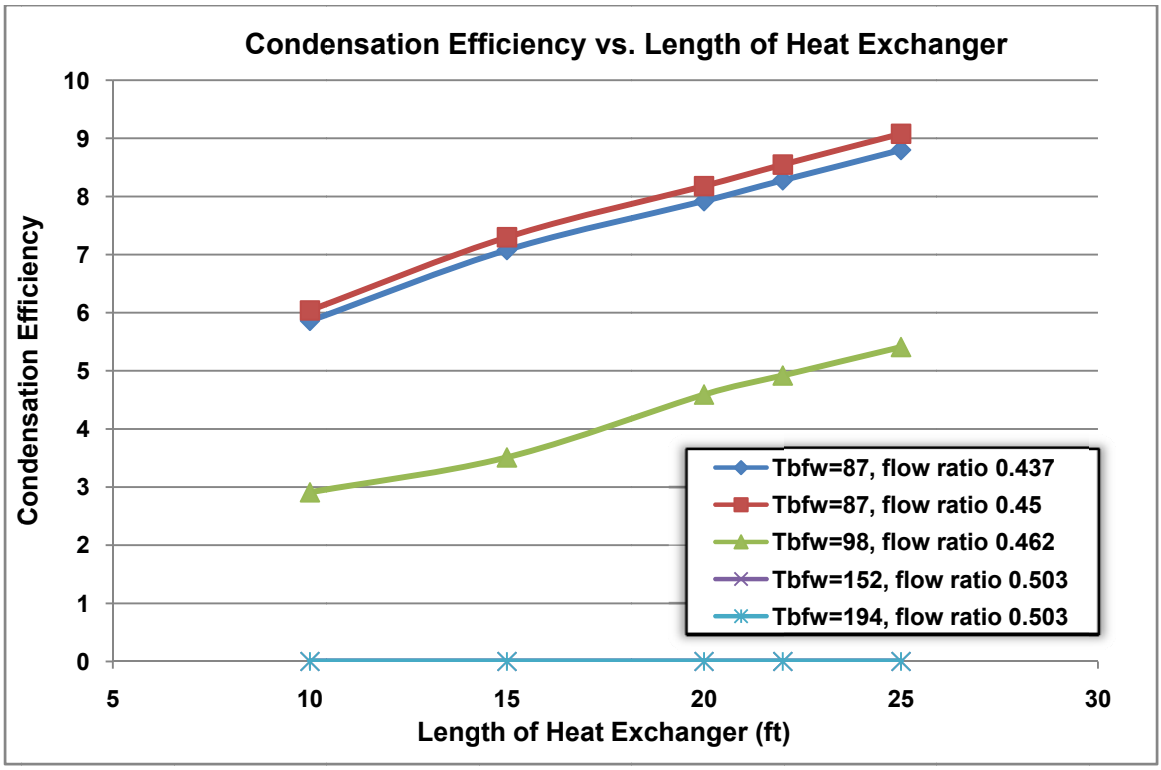

Figure 14 - Impact of using high temperature BFW on Condensation Efficiency of Heat Exchanger placed Upstream of Wet FGD

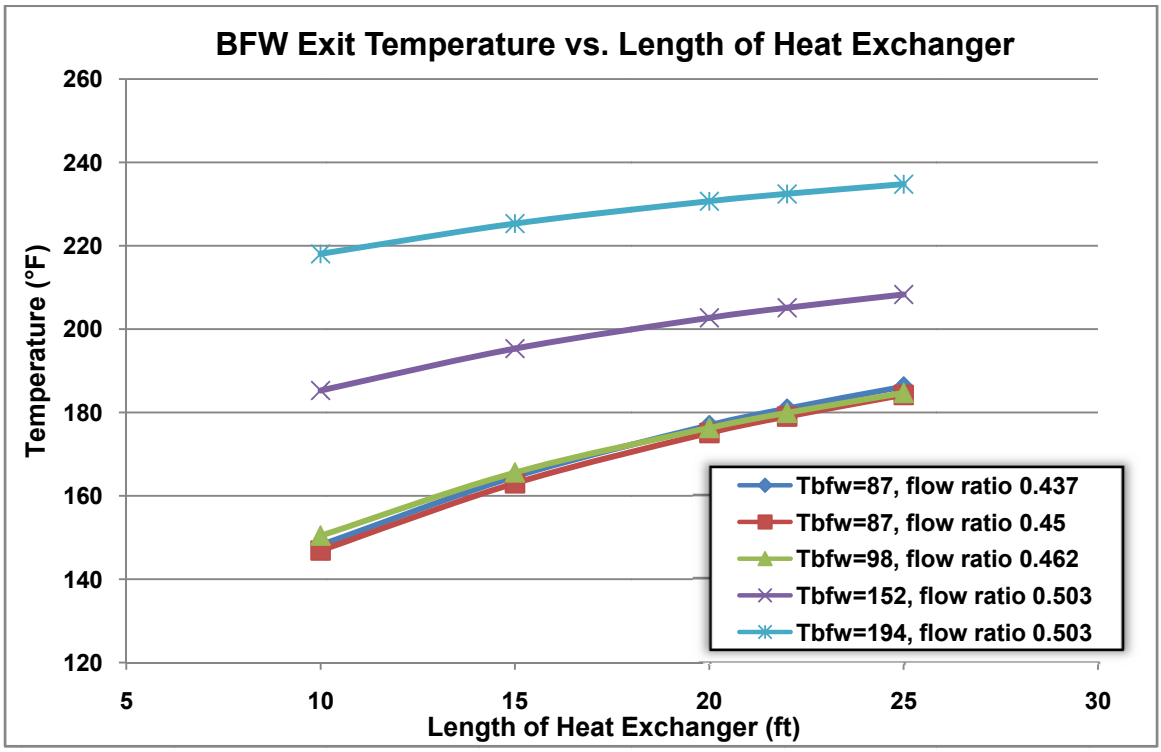

Figure 15 - Impact of high temperature BFW on temperature of BFW at the exit of Heat Exchanger, placed Upstream of Wet FGD

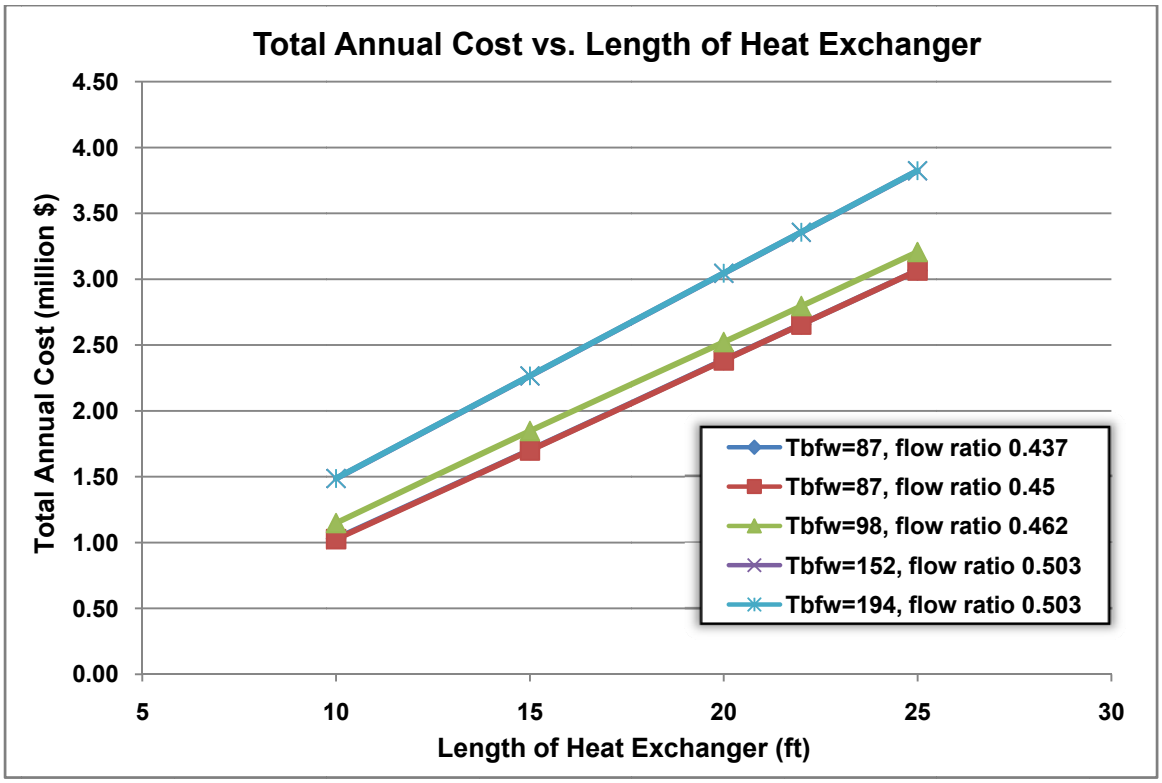

Figure 16 - Impact of high Temperature BFW on Total Annual Cost of Heat Exchanger Placed Upstream of Wet FGD

From the above plots, it can be observed that for a given length of the heat exchanger, condensation efficiency decreases with increase in temperature of boiler feedwater at the inlet of heat exchanger and for the boiler feedwater inlet temperatures of 152°F and 192°F, there is no condensation observed at all. Assuming a 20ft long heat exchanger, the temperature profiles for these subcases are provided below in Figures (17 a-e) below:

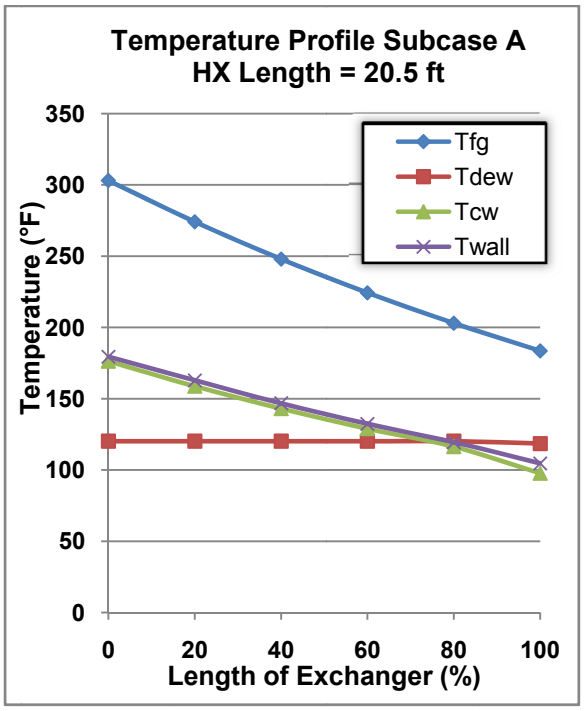

17(a) - Tbfw_in = 98°F

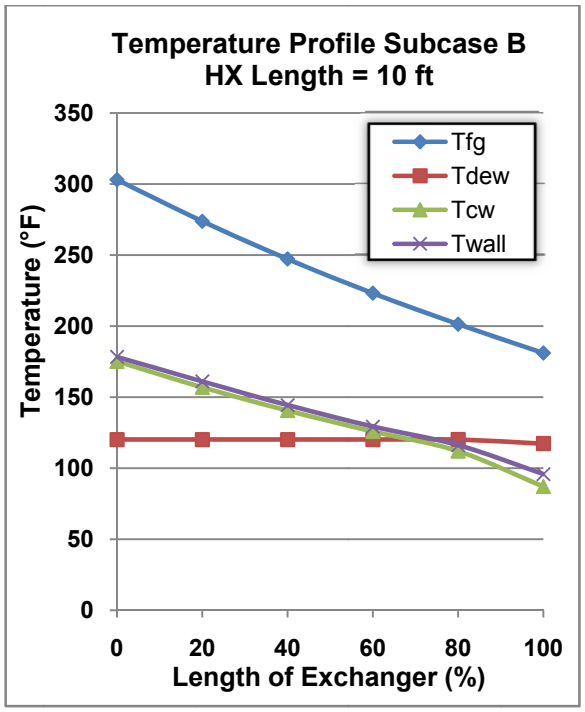

17(b) - Tbfw_in = 87°F

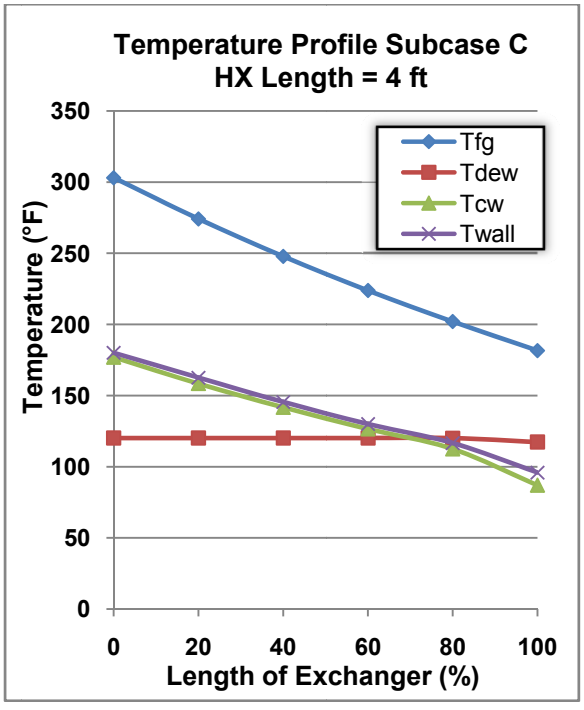

17(c) - Tbfw_in = 87°F

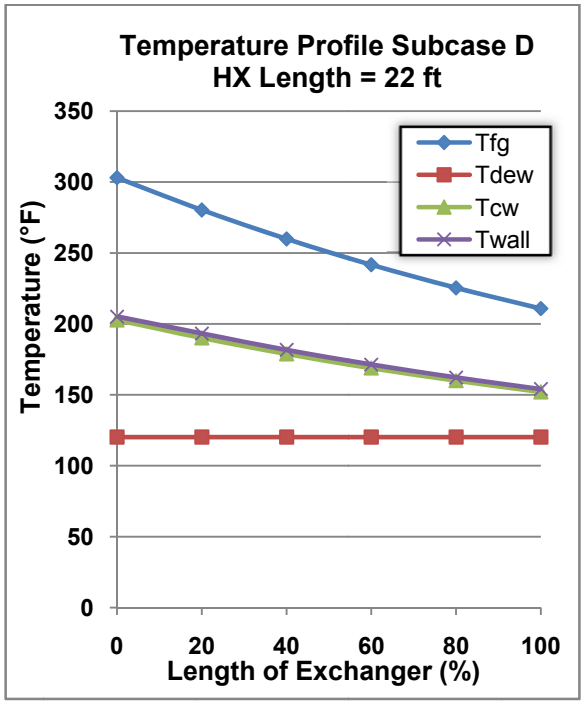

17(d) - Tbfw_in = 152°F

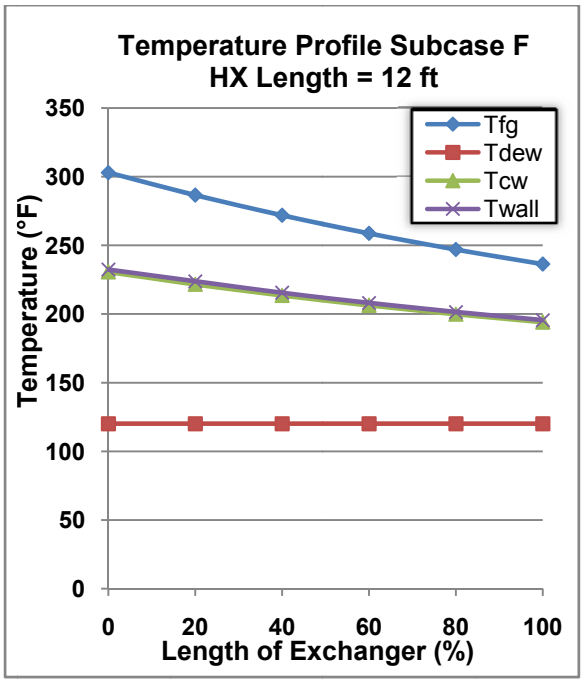

17(e) - Tbfw_in = 194°F

Figure 17 - Temperature Profiles for subcases with variable BFW inlet temperatures for heat exchanger upstream of wet FGD

From the above plots of temperature profiles, it is evident that the point of condensation moves further down the length of the heat exchanger duct with the increase in temperature of boiler feedwater at the inlet of the heat exchanger resulting in lower condensation efficiency. Further, movement of condensation point away from the upstream end of the heat exchanger also means that the length of tubes made from Nickel alloy 22 material will increase to ensure higher corrosion resistance which results in an increase in total annual cost of the heat exchanger, as can be seen in Figure (16).

Further, the results obtained from Jonas (14) indicate that the flow rate ratio depends on the target exit temperature of the boiler feedwater. Simulations were run to design heat exchangers to obtain specific boiler feedwater exit temperatures for ratios of mass flow rate of boiler feedwater to flue gas as provided in Appendix-A Table (A.1). Results from the simulations for these exchangers are given below in Table (10).

Table 10 - Simulation results for the sub-cases A-F for Heat Exchanger placed upstream of the Wet FGD Unit

		Sub-Case A	Sub-Case B	Sub-Case C	Sub-Case D	Sub-Case E	Sub-Case F
Length of HX	**ft**	20.5	10	4	22	7.5	12
m° FG	**[10^6 lb/hr]**	6.309	6.309	6.309	6.309	6.309	6.309
m° BFW	**[10^6 lb/hr]**	2.914	2.839	2.757	3.173	3.173	3.173
Ratio	**BFW/FG**	0.462	0.45	0.437	0.503	0.503	0.503
Cond. Point	**% length from upstream end of HX**	79.01	60.38	21.18	100.00	100.00	100.00
Cond. Rate	**lb/hr**	20892.34	27029.65	18965.83	0.00	0.00	0.00
Capture Efficiency	**%**	4.67	6.04	4.24	0.00	0.00	0.00
T_{fg} in	**(°F)**	303	303	303	303	303	303
T_{fg} out	**(°F)**	182.09	221.71	265.53	206.24	254.55	253.68
T_{bfw} In	**(°F)**	97.66	86.89	87.36	152.00	151.97	194.02
T_{bfw} Out	**(°F)**	177.22	146.89	118.46	205.14	178.86	221.23
BFW Δp	**(psi)**	159.40	74.21	27.93	199.63	67.68	108.62
FG Δp	**(psi)**	0.058	0.029	0.011	0.064	0.022	0.035
Total Installed Cost	**$ Million**	25.08	9.79	1.96	32.37	10.54	17.32
Total Power Req.	**kW**	540.55	247.58	91.25	729.04	248.20	398.84
Annual Operating Cost	**$ Million**	0.23	0.10	0.04	0.31	0.10	0.17
Total Annual Cost	**$ Million**	2.59	1.03	0.22	3.36	1.10	1.80

From the above table, it was observed that the total annual cost associated with heat exchangers placed before the FWH1 were lowest. It was also apparent that, for boiler feedwater at a given temperature at the inlet of the heat exchanger, the total annual cost depends on the temperature to which boiler feedwater is heated in the heat exchanger. In order to identify the most appropriate target temperature to which boiler feedwater should be heated in the condensing heat exchangers, four more heat exchangers with duct length 20ft, 15ft, 7ft and 3ft, and, process

conditions similar to those for the heat exchangers placed before the FWH1, detailed in Table (10) above, were simulated. More detailed process conditions for these additional sub-cases numbered 1-4, as obtained from Jonas (14) are provided in Appendix-A Table (A.2). The results from these subcases including the ones with least total annual cost are provided in Table (11).

Table 11 - Simulation results for the sub-cases 1 – 4 for Heat Exchanger placed upstream of the Wet FGD Unit

		Sub-Case 1	Sub-Case 2	Sub-Case B	Sub-Case 3	Sub-Case C	Sub-Case 4
Length of HX	**ft**	20	15	10	7	4	3
m° FG	**[10^6 lb/hr]**	6.309	6.309	6.309	6.309	6.309	6.309
m° BFW	**[10^6 lb/hr]**	2.922	2.894	2.839	2.801	2.757	2.732
Ratio	**BFW/FG**	0.463	0.459	0.45	0.44	0.437	0.433
Cond. Rate	**lb/hr**	36595.46	31677.44	27029.65	21954.34	18965.83	18313.9
Cond. Point	**% length from upstream end of HX**	73.27	69.62	60.38	51.45	21.18	0.75
Capture Efficiency	**%**	8.18	7.08	6.04	4.91	4.24	4.09
T_{fg} in	**(°F)**	303	303	303	303	303	303
T_{fg} out	**(°F)**	181.02	198.43	221.71	240.97	265.53	275.28
T_{bfw} In	**(°F)**	87.03	86.59	86.89	87.70	87.36	86.88
T_{bfw} Out	**(°F)**	175.09	164.64	146.89	135.47	118.46	111.53
BFW Δp	**(psi)**	148.16	105.12	74.21	49.08	27.93	20.84
FG Δp	**(psi)**	0.056	0.043	0.029	0.020	0.011	0.008
Total Installed Cost	**$ Million**	23.11	16.55	9.79	6.00	1.96	0.79
Total Power Req.	**kW**	491.74	341.89	247.58	160.37	91.25	67.95
Annual Operating Cost	**$ Million**	0.21	0.14	0.10	0.07	0.04	0.03
Total Annual Cost	**$ Million**	2.38	1.70	1.03	0.63	0.22	0.10

From the above simulation results, it is observed that the cost of material plays a major role in variation of the total annual cost. The temperature distribution for each heat exchanger is provided in Figure (18 a-d), respectively.

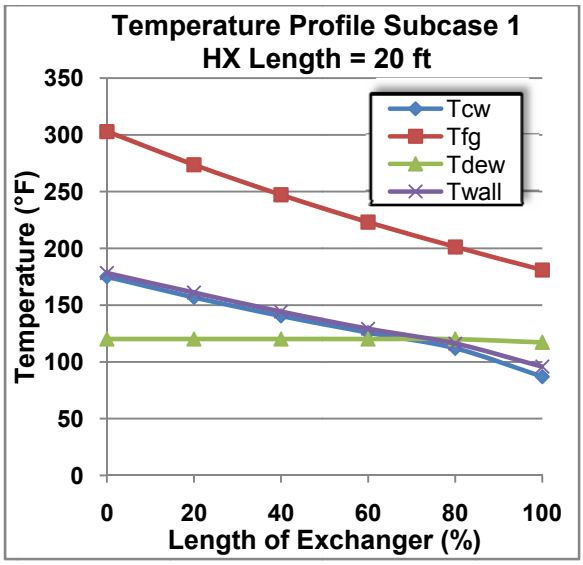

18(a)

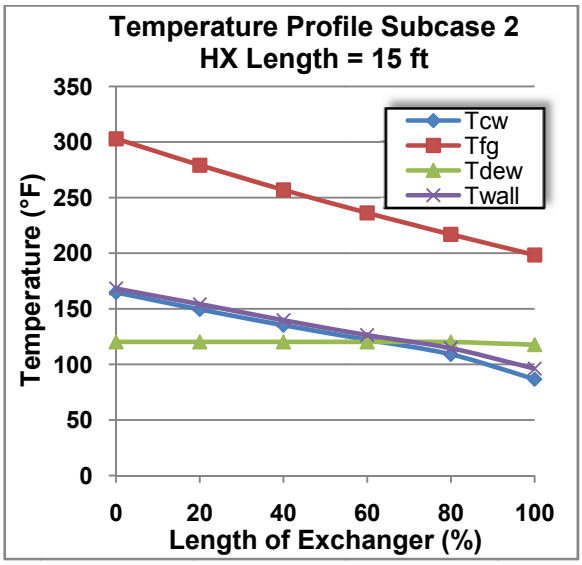

18(b)

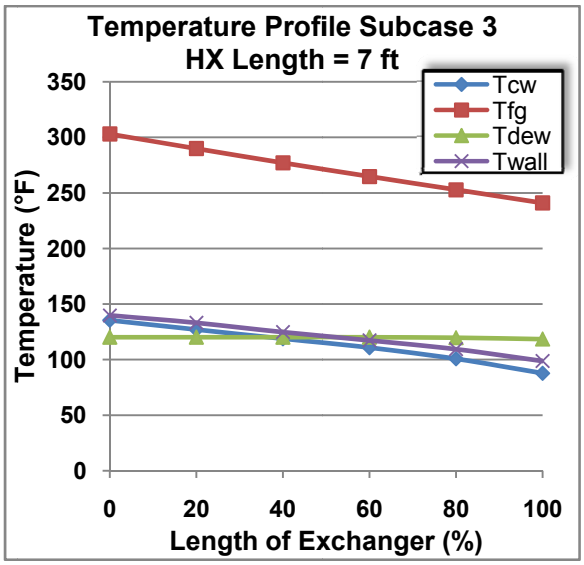

18(c)

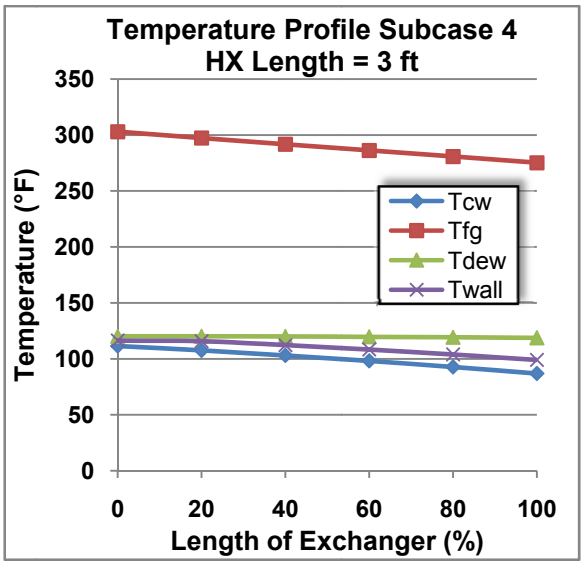

18(d)

Figure 18 - Temperature Profiles for Subcases 1-4, Model 1, System without FGD

From the Table (11), it can be noticed that the total length of the heat exchanger duct reduces with decrease in temperature of boiler feedwater at the exit of the heat exchanger. Also, the point of condensation moves closer to the beginning of the heat exchanger. This reduces the

quantity of expensive Nickel alloy 22 material for tubes. The overall Cost-benefit analysis for these sub-cases was done by Jonas (14) as illustrated in Figure (19) and Figure (20) below.

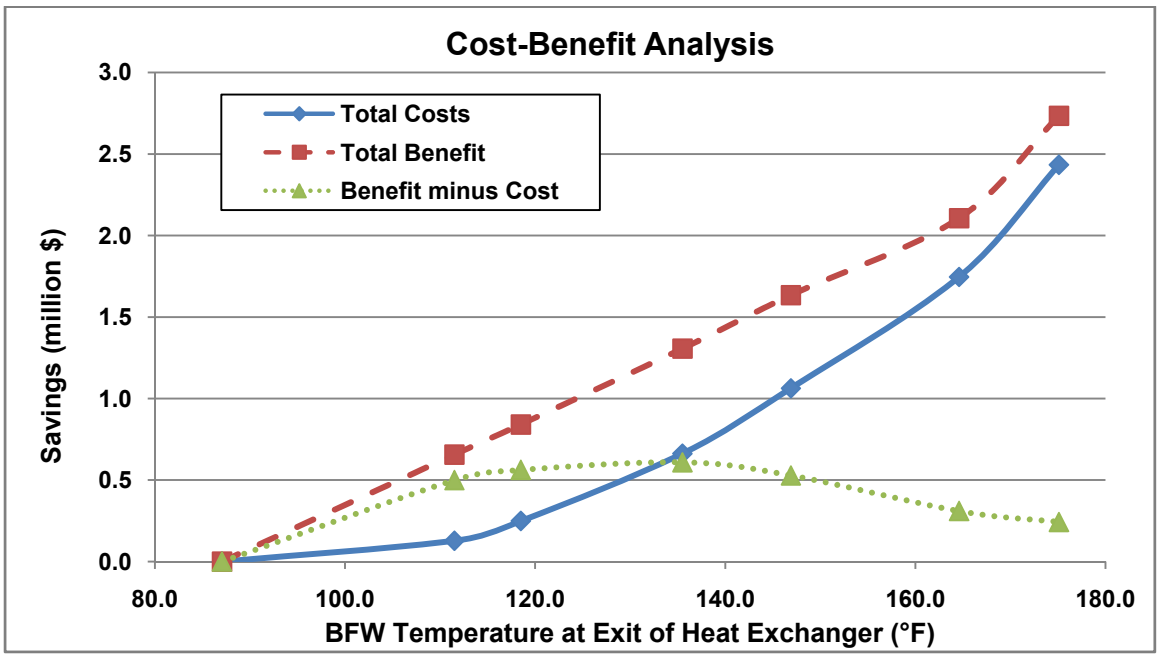

Figure 19 - Cost Benefit Analysis of Heat Exchanger placed before Wet FGD and Boiler Feedwater extracted before FWH1 (14)

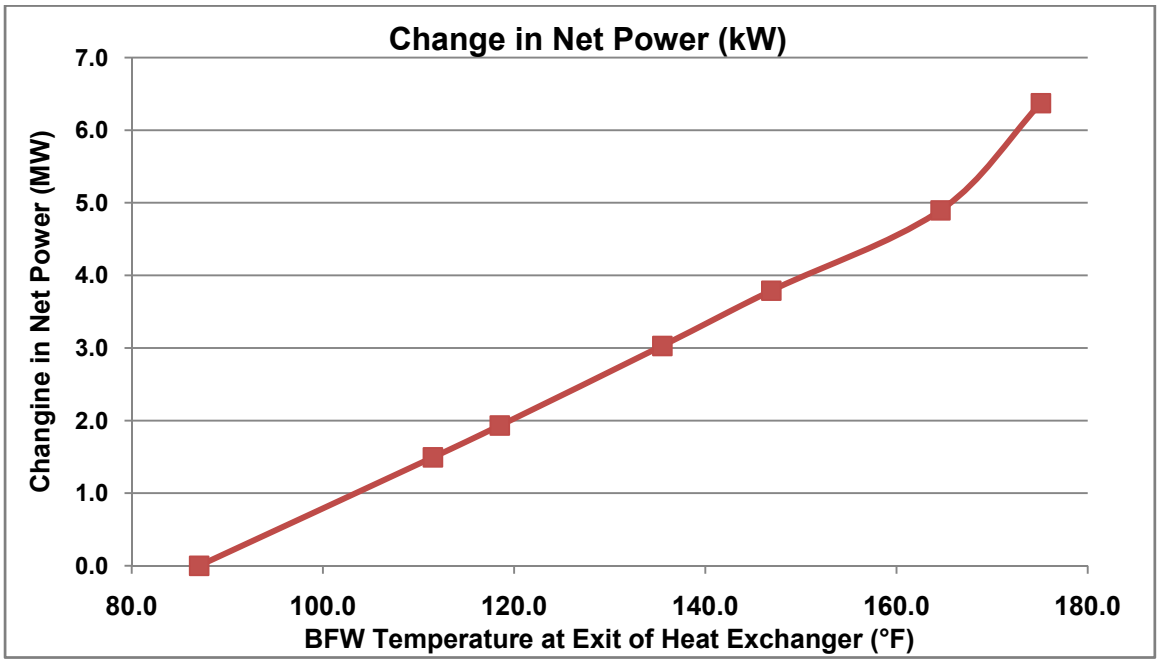

Figure 20 - Change in Net Power for Heat Exchanger placed before Wet FGD and Boiler Feedwater extracted before FWH1 (14)

From the Figure (19), it can be inferred that the total profits associated with heat exchangers increases steadily with increase in the temperature of boiler feedwater at the exit reaching a maximum at approx. 135° F and then declines.

5.2.Heat Exchanger placed Downstream of Wet FGD, Flue Gas at 135°F

Wet FGD units are used after the ESP to remove SO_2 from the flue gas stream. The flue gas stream coming out of the FGD is at a temperature of approximately 135°F and is saturated with water, i.e., the mole fraction of water vapor is 17.4%. For a 600MW plant, the mass flow rate of flue gas leaving the wet FGD was assumed to be around 6.3 million lb/hr,

The impact of increase in the ratio of mass flow rate of cooling water to flue gas as well as the temperature of the cooling water at the inlet of the heat exchanger on rate of condensation and the rate of heat transfer were studied by Hazell (3). In this study, we looked at the impact of changing the transverse pitch between the tubes.

Although the ratio of mass flow rate boiler feedwater to flue gas is typically in the range of 0.4 - 0.5, for these analyses it was assumed to be 1.5 with cooling water entering the heat exchanger at a temperature of 87°F. The tubes were assumed to be 2" diameter NPS with wall thickness of 0.195". The fixed process conditions and heat exchanger geometry for this analysis are summarized in Table (12) and Table (13), respectively. The variable parameters are provided in Table (14) below. It must be noted here that there is only a relatively small window of opportunity to recover heat from the flue gas, since the flue gas is at a temperature of 135°F as compared to 300°F upstream of FGD unit.

Table 12 - Fixed Process Conditions for Heat Exchanger placed Downstream of Wet FGD

Inlet Conditions				
M_{fg} (lbm/hr)	M_{bfw} (lbm/hr)	y_{H2O} (%)	T_{fg} (°F)	T_{bfw} (°F)
6.31E+06	9.46E+06	17.4	135	87

Table 13 - Fixed Heat Exchanger Geometry for Heat Exchanger placed Downstream of Wet FGD

Fixed Heat Exchanger Geometry				
Tube Diameter NPS (in)	Tube Wall Thickness (in)	S_l (in)	Duct Depth (ft)	Duct Height (ft)
2	0.195	2.97	40	40

Table 14 - Variable Parameter for Heat Exchanger placed Downstream of Wet FGD

Variable Parameters
Transverse Pitch S_t (in)
4.88
5.14
6.17

While choosing the values of Transverse Pitch as mentioned in Table (14), it was made sure that the tube spacing parameter 'a' as determined by Zukauskas (5) , given by, $a = {S_t}/{d_o}$, is within the specified range of values established empirically as $1.20 \leq a \leq 2.70$

The condensation efficiency, temperature of cooling water at the exit of heat exchanger and the total annual cost were analyzed for different heat exchanger lengths as illustrated in Figure (21), Figure (22) and Figure (23) below:

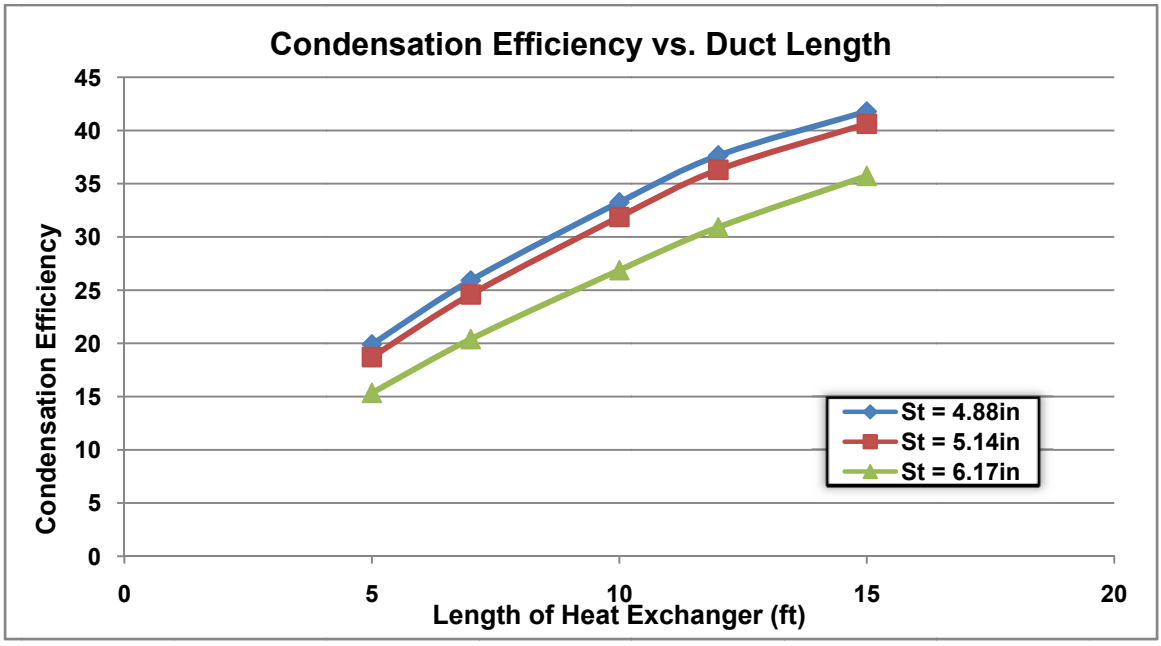

Figure 21 - Impact of Transverse Pitch on Condensation Efficiency of Heat Exchanger placed Downstream of Wet FGD

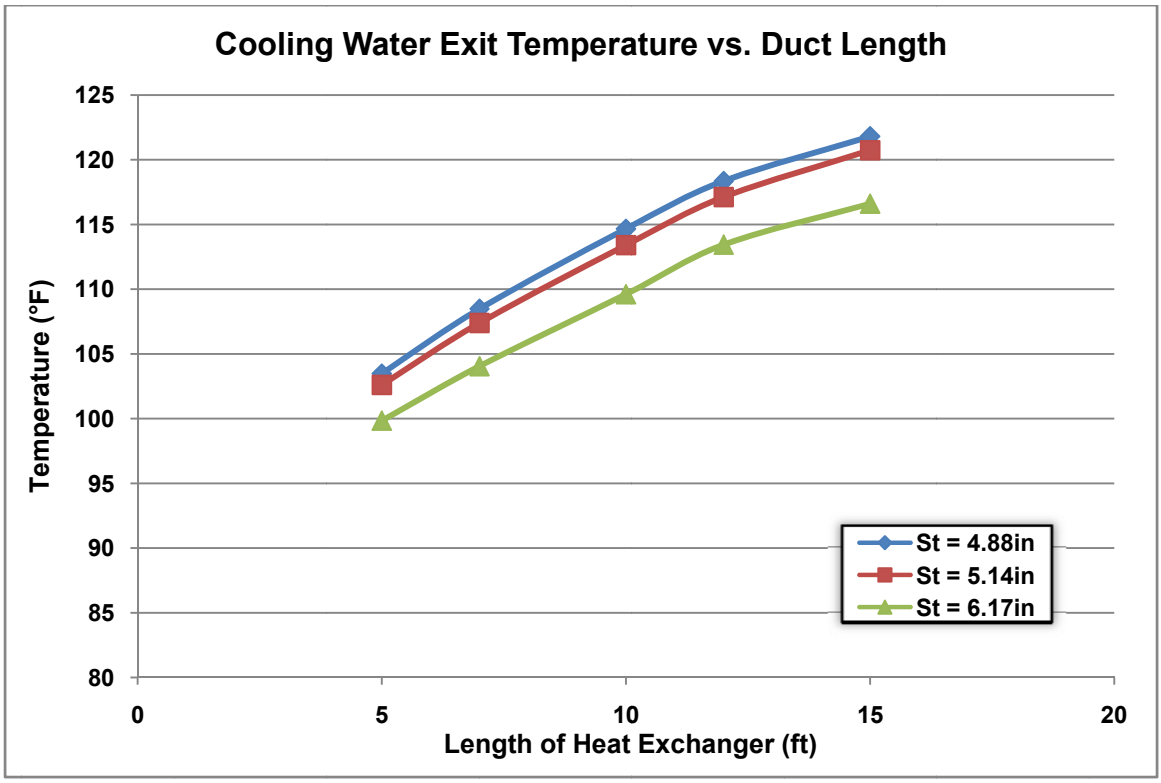

Figure 22 - Impact of Transverse Pitch on Temperature of Cooling Water at the Exit of Heat Exchanger placed Downstream of Wet FGD

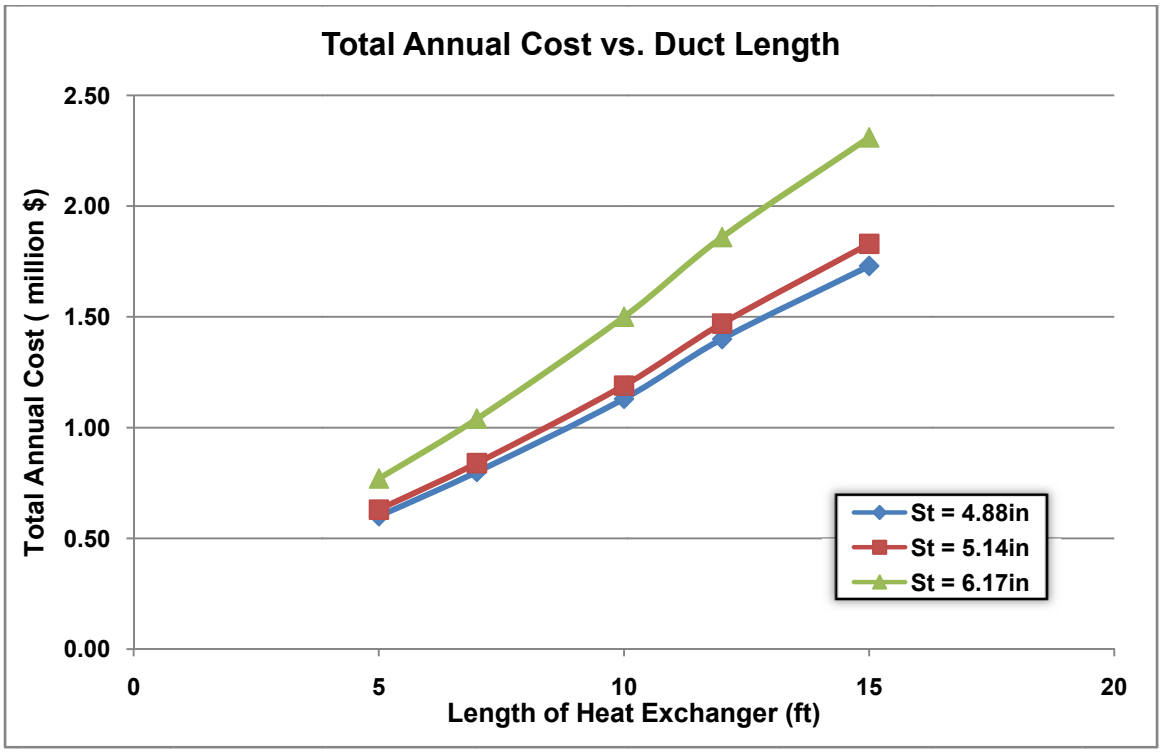

Figure 23 - Impact of Transverse Pitch on Total Annual cost of Heat Exchanger placed Downstream of Wet FGD

From the Figure (21) and (22), it can be noticed that the rate of condensation and the temperature of cooling water at the exit of the heat exchanger increase with decrease in transverse pitch. This can be attributed to the increase in total surface area of the tubes as the total number of tubes in the bank increases, for a given size duct, due to reduction in the spacing between the tubes. This also means that the total cost of material and the manufacturing and installation cost will increase. Further, due to a more packed geometry for lower transverse pitch, there is some increase in the pressure drop in flue gas stream. But, due to the increase in number of tubes, the total mass flow rate of cooling water per tube is reduced, resulting in decrease in pressure drop on cooling water side. This decrease in pressure drop for cooling water dominates the annual operating cost, thus bringing the total annual cost down, as can be seen in the Figure (23).

5.3.Precooled Flue Gas using Water Spray, Flue Gas at 155°F

Flue gas always contains some mole fractions of SO_2 and SO_3. Although SO_3 reacts with moisture in flue gas to form vapors of sulfuric acid and condenses out with moisture in flue gas, FGD unit are required to remove SO_2. In this section, we analyzed the impact of spraying low temperature water in the flue gas stream to precool it to a temperature of 155°F on condensation efficiency and total annual cost in comparison to that of a heat exchanger placed upstream or downstream of a wet FGD without spraying.

For a 600MW plant, the mass flow rate of flue gas increases from 6.31 million lb/hr to 6.54 million lb/hr as a result of spraying additional water into the gas stream and the mole fraction of water vapor in flue gas increased from 11.6% to 16.4%. The mass flow rate of feedwater was 2.83 million lb/hr for this model resulting in a flue gas to feedwater mass flow rate ratio of 0.443. It was assumed that the mass flow rate of feedwater remains constant for all heat exchanger geometries analyzed, irrespective of the temperature of boiler feedwater at the exit of the heat exchanger. The tubes were assumed to be 2” diameter NPS with wall thickness of 0.195”. The fixed process

conditions and heat exchanger geometry for this configuration are summarized in Table (15) and Table (16), respectively. The variable parameters are provided in Table (17). The detailed process conditions as obtained from Jonas (14) are provided in Appendix-A Table (A.3).

Table 15 - Fixed Process Conditions for Precooled Flue Gas using Water Spray

Inlet Conditions				
M_{fg} (lbm/hr)	M_{bfw} (lbm/hr)	y_{H2O} (%)	T_{fg} (°F)	T_{bfw} (°F)
6.54E+06	2.839E+06	16.4	155	87

Table 16 - Fixed Heat Exchanger Geometry for Precooled Flue Gas using Water Spray

Fixed Heat Exchanger Geometry					
Tube Diameter NPS (in)	Tube Wall Thickness (in)	S_t (in)	S_l (in)	Duct Depth (ft)	Duct Height (ft)
2	0.195	6.17	2.97	40	40

Table 17 - Variable Parameter for Heat Exchanger for Precooled Flue Gas using Water Spray

Variable Parameter	
Duct Length (ft)	Surface Area (ft^2)
5	3.35E+04
10	7.08E+04
15	1.08E+05
20	1.45E+05

The results obtained for this configuration were compared with those for heat exchangers with same geometry and mass flow rate of boiler feedwater, but, without precooling the flue gas stream using water spray and placed upstream of FGD (UHX) as well as downstream of FGD (DHX). The fixed process conditions for these systems are provided below in Table (18) and Table (19), respectively.

Table 18 - Fixed Process Conditions for UHX without using Water Spray for Precooling Flue Gas

Inlet Conditions				
M_{fg} (lbm/hr)	M_{bfw} (lbm/hr)	y_{H2O} (%)	T_{fg} (°F)	T_{bfw} (°F)
6.309E+06	2.838E+06	11.6	303	87

Table 19 - Fixed Process Conditions for DHX without using Water Spray for Precooling Flue Gas

Inlet Conditions				
M_{fg} (lbm/hr)	M_{bfw} (lbm/hr)	y_{H2O} (%)	T_{fg} (°F)	T_{bfw} (°F)
6.76E+06	2.848E+06	17.4	135	87

Condensation efficiency, temperature of boiler feedwater at the exit of heat exchanger and total annual cost for heat exchanger with precooled flue gas were compared with those for UHX and DHX with regular flue gas. The plots for the same are provided below in Figure (24), Figure (25) and Figure (26), respectively.

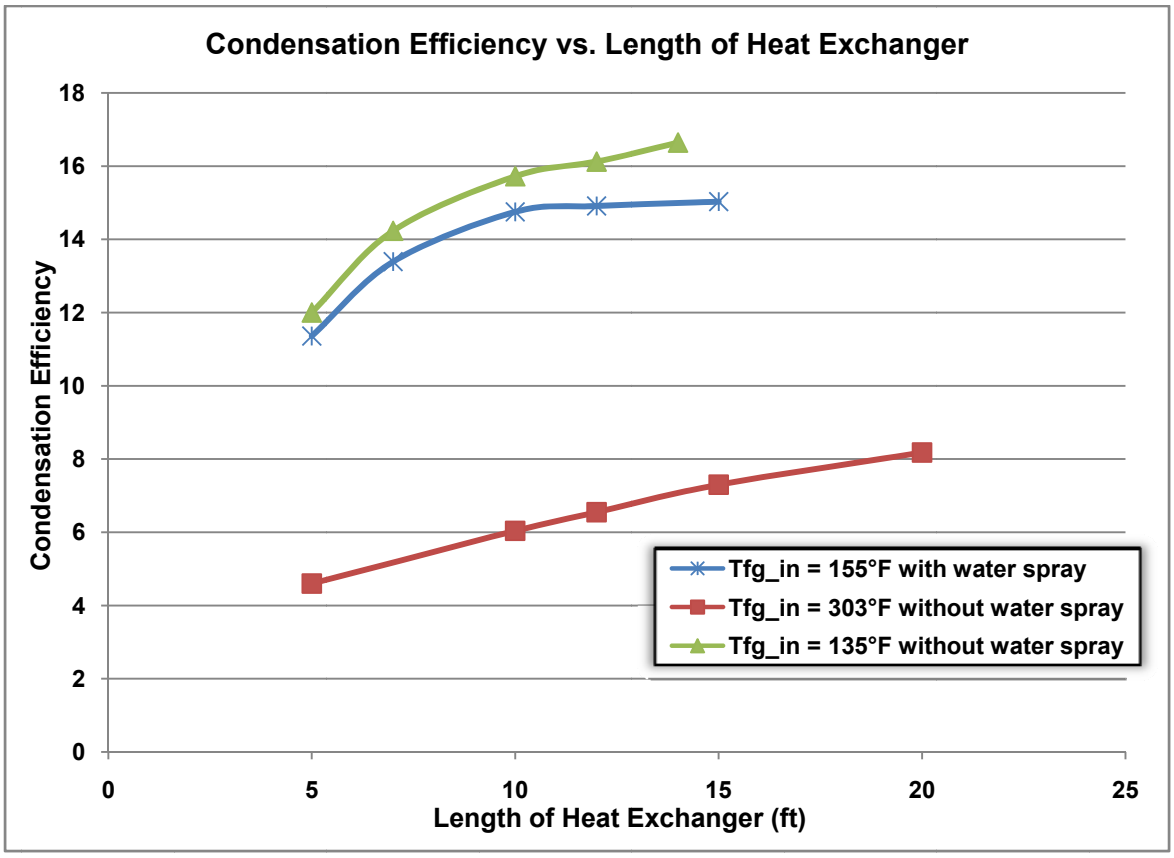

Figure 24 - Condensation Efficiency for Heat Exchanger with Precooled Flue Gas compared to UHX and DHX

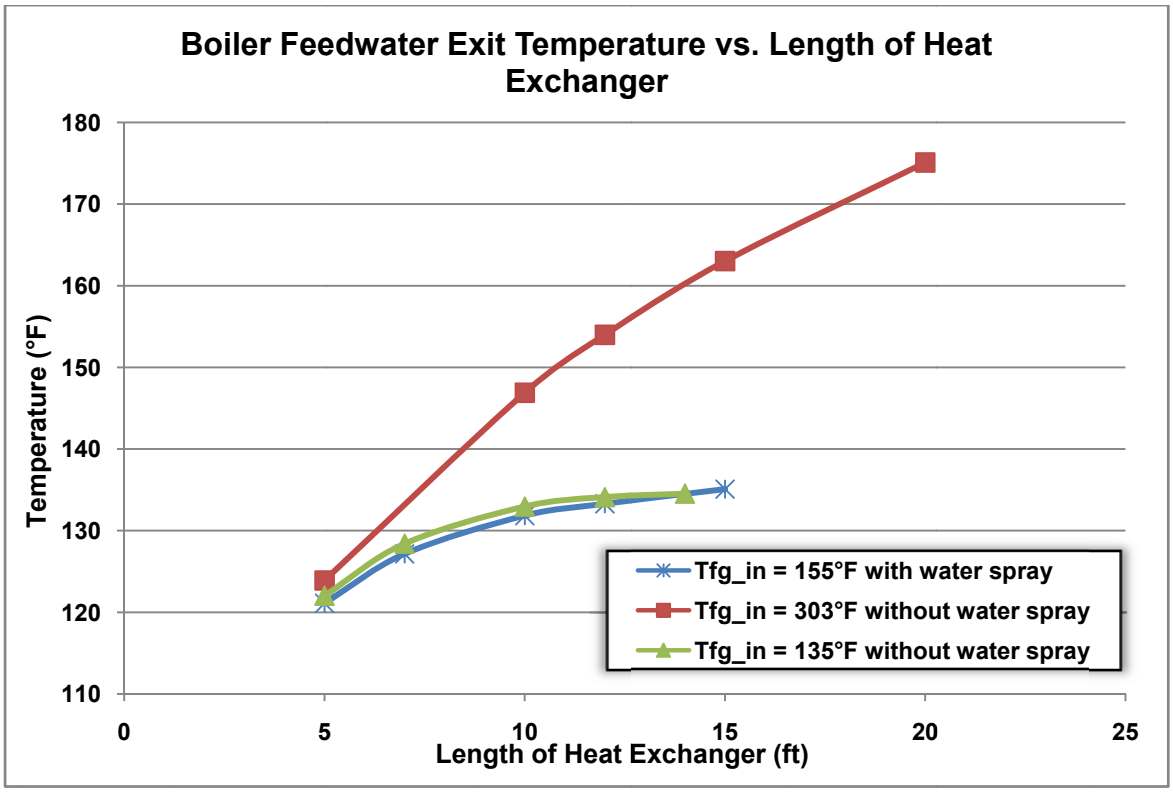

Figure 25 - Boiler Feedwater Exit Temperature for Heat Exchanger with Precooled Flue Gas compared to UHX and DHX

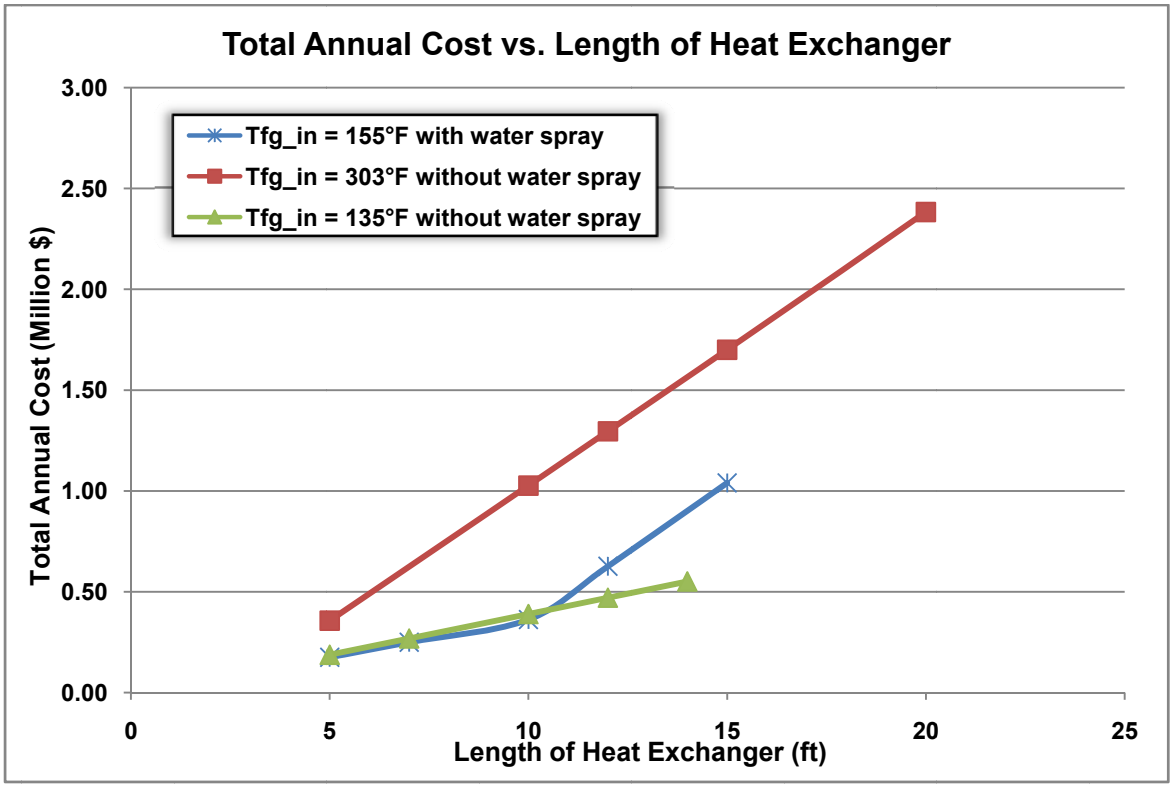

Figure 26 - Total Annual Cost for Heat Exchanger with Precooled Flue Gas compared to UHX and DHX

From Figure (24) it is noticed that the condensation efficiency for precooled flue gas remains lower than that for DHX. This can be explained by the fact that the flue gas downstream of FGD is saturated with water at 135 °F with water vapor mole fraction of 17.4% while the precooled flue gas at 155°F has water vapor mole fraction of 16.4% only, which indicated that the flue gas is not saturated. As a result more water condensation will be observed in DHX, thus, higher condensation efficiency. It is interesting to note from Figure (25) that the rise in temperature and thus total heat transfer for heat exchanger with precooled flue gas and DHX are nearly equal while that for UHX without water spraying is much higher. This can be attributed to higher temperature of flue gas for UHX. On the contrary, though the precooled flue gas has higher temperature than that for DHX, the nearly same heat transfer can be explained by the difference in mass flow rate of flue gas for precooled flue gas and DHX. The higher temperature of flue gas compensates for the lower mass flow rate of precooled flue gas.

This is also the reason for nearly same total annual cost for heat exchangers up-to a size of 10ft as indicated in Figure (26). Up-to a size of 10ft, even though the heat exchanger for precooled flue gas utilizes Nickel alloy 22 for tube material for some tube length, the higher cost for material is compensated by the lower operating cost of the heat exchanger due to lesser pressure drop. Beyond the size of 10ft, the cost of material becomes substantial and the heat exchangers for precooled flue gas tend to have higher total annual cost.

It is also possible that the spraying of water into flue gas stream might have an impact on the duty associated with FGD unit. This aspect has not been looked into at this stage.

5.4.Coupled Heat Exchanger, Flue gas at 135°F

Sometimes a thermal power plant is spread over a large area of land and the boiler unit is at some distance from the turbine floor resulting in a large distance between the flue gas duct after the ESPs and the boiler feedwater line after the condenser. Thus, the possibility of using boiler feedwater as the cooling fluid for the condensing heat exchanger becomes questionable due to the distance, space and arrangement inconvenience. In this model, we looked at the option of using two sets of heat exchangers coupled together using cooling water as intermediate fluid which

absorbs heat from the flue gas in condensing heat exchanger (HX1) and afterwards rejects the heat to boiler feedwater in the second heat exchanger (HX2). Since both the hot and the cold fluid for HX2 are water, namely cooling water and boiler feedwater, in this study, HX2 is also referred to as water-to-water heat exchanger. The basic system arrangement is provided below in Figure (27). It must be noted here that the temperatures of cooling water in the Figure (27) are for cooling water to boiler feedwater mass flow rate ratio of 0.75 only.

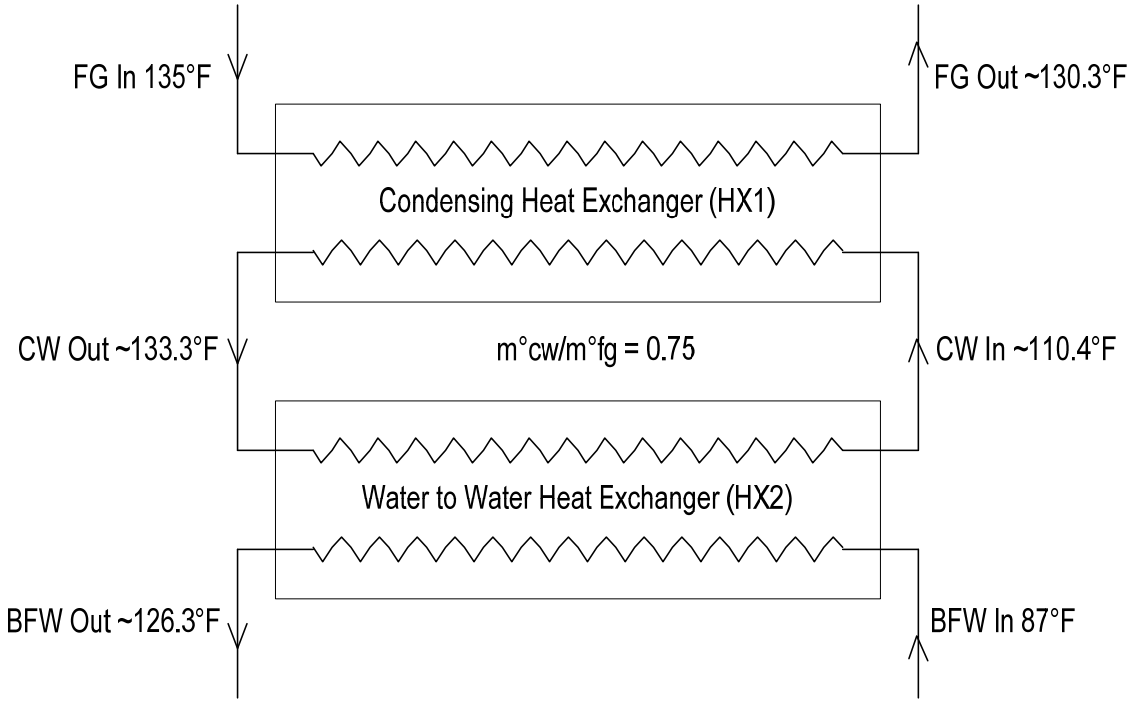

Figure 27 - Flow diagram for Coupled Heat Exchanger Arrangement

The detailed design of the water-to- water heat exchanger has been described in Section 2.2. There exists a limit on the maximum mass flow rate ratio of boiler feedwater that can be obtained by altering the duty on low pressure FWHs. All the extractions from the low pressure turbine eventually combine and this water is then pumped back into the steam circuit after the first feedwater heater (FWH1) using the drain pump. The detailed steam cycle ASPEN Model as used by Jonas (16) is available in Appendix-A, Figure (A.1). For a 600MW plant with FGD unit, the maximum mass flow rate ratio of boiler feedwater to flue gas is limited to 0.503 after FWH1, as observed from results obtained from Jonas (14). Assuming that the mass flow rate of flue gas after the FGD is 6.31 million lb/hr, and HX2 is placed before FWH1, the mass flow rate of boiler

feedwater available is nearly 2.79 million lb/hr. The boiler feedwater enters HX2 at a temperature of 87°F and the flue gas enters HX1 at 135°F and is saturated with water vapor. i.e, the mole fraction of water is 17.4%. Cooling water is continuously circulated between the two heat exchangers and energy and mass balance equations are used to calculate cooling water temperatures at the inlet and exit of HX1.

To simplify the calculations, HX2 is assumed to be a shell and tube heat exchanger with a shell of rectangular cross-section 10'X4' with a horizontal separating plate at a height of 5' dividing the exchanger into two passes for cooling water flowing outside the heat exchanger tubes. Boiler feed water flows inside the tubes. The tubes are assumed to be 1" NPS diameter with a wall thickness 0.133" matching Schedule 40S as per ASME B36.19.

For HX1, the length of the duct was kept constant at 20'. The tube diameter was assumed to be 3.5" with a wall thickness of 0.226" matching Schedule 40S as per ASME B36.19. The choice of tube diameter was based on the results obtained from the study of impacts of tube diameter as explained in Section 4 of this report.

Three different cases were evaluated with mass flow rate ratios of 0.75, 1.0 and 1.5 between cooling water and flue gas. Separate calculations were also done for condensing heat exchangers with boiler feedwater and cooling water as cooling fluids and the results were compared to those obtained for coupled heat exchangers. There are three possibilities compared in this section:

1. Using boiler feedwater at water to flue gas mass flow rate ratio of 0.443.

For the possibility of using only the boiler feedwater as cooling fluid, the mass flow rate of boiler feedwater is kept constant at 2.79 million lb/hr. For a 600MW unit, flue gas is at a temperature of 135°F downstream of the FGD unit. As a result, there is a limitation on the maximum amount of heat that can be recovered from the flue gas. A heat exchanger in 15ft long duct was found to be appropriately long to heat boiler feedwater to nearly 134°F. The fixed process conditions and heat exchanger geometry for the system using boiler feedwater are summarized in below in Table (20) and Table (21), respectively.

Table 20 - Fixed Process Conditions for system using Boiler Feedwater for comparison with Coupled Heat Exchanger

Inlet Conditions for system using Boiler Feedwater				
M_{fg} (lbm/hr)	M_{bfw} (lbm/hr)	y_{H2O} (%)	T_{fg} (°F)	T_{bfw} (°F)
6.31E+06	2.79E+06	17.4	135	87

Table 21 - Fixed Heat Exchanger Geometry for system using Boiler Feedwater for comparison with Coupled Heat Exchanger

Fixed Heat Exchanger Geometry for system using Boiler Feedwater						
Tube Diameter NPS (in)	Tube Wall Thickness (in)	St (in)	Sl (in)	Duct Depth (ft)	Duct Height (ft)	Duct Length (ft)
2	0.195	6.17	2.97	40	40	15

2. Using cooling water at water to flue gas mass flow rate ratios of 0.75,1.0 and 1.5.

For the system using cooling water instead of boiler feedwater, a heat exchanger of length 23ft was identified to have a total surface area of 163052.00 ft^2 which is nearly the same as the combined surface area of HX1 and HX2 for coupled heat exchanger assembly as detailed in third possibility in this section. The mass flow rate ratio of cooling water to flue gas was varied. The fixed process conditions and heat exchanger geometry for the system using cooling water are summarized below in Table (22) and Table (23), respectively.

Table 22 - Fixed Process Conditions for system using Cooling Water for comparison with Coupled Heat Exchanger

Inlet Conditions for system using Cooling Water			
M_{fg} (lbm/hr)	T_{fg} (°F)	T_{bfw} (°F)	y_{H2O} (%)
6.31E+06	135	87	17.4

Table 23 - Fixed Heat Exchanger Geometry for system using Cooling Water for comparison with Coupled Heat Exchanger

Fixed Heat Exchanger Geometry for Cooling Water						
Tube Diameter NPS (in)	Tube Wall Thickness (in)	St (in)	Sl (in)	Duct Depth (ft)	Duct Height (ft)	Duct Length (ft)
3.5	0.226	6.17	2.97	40	40	23

3. Using coupled heat exchanger with cooling water to flue gas mass flow rate ratios of 0.75, 1.0 and 1.5.

For coupled heat exchanger arrangement, the geometry of HX2 was chosen from multiple trial and error combinations of duct height, depth and length and the tube diameter to obtain maximum heat transfer. Also, the tube material chosen for HX2 was low alloy carbon steel as it has a higher thermal conductivity compared to stainless steel and nickel alloy 22. The impact of the new tube material on the total annual cost has not been assessed at this stage. The surface areas of both the heat exchangers were kept constant i.e. 144,242.24 ft^2 for HX1 and 17,065.96 ft^2 for HX2 resulting in an overall total surface area of 161308.2 ft^2. The fixed process conditions and heat exchanger geometry for the coupled heat exchanger are summarized below in Table (24), Table (25) and Table (26), respectively.

Table 24 - Fixed Process Conditions for Coupled Heat Exchanger Assembly

Inlet Conditions for Coupled Heat Exchanger Assembly				
M_{fg} (lbm/hr)	M_{bfw} (lbm/hr)	y_{H2O} (%)	T_{fg} (°F)	T_{bfw} (°F)
6.31E+06	2.79E+06	17.4	155	87

Table 25 - Fixed Geometry for HX1 of Coupled Heat Exchanger Assembly

Fixed Heat Exchanger Geometry for HX1 of Coupled Heat Exchanger Assembly						
Tube Diameter NPS (in)	Tube Thickness (in)	St (in)	Sl (in)	Duct Depth (ft)	Duct Height (ft)	Duct Length (ft)
3.5	0.226	6.17	2.97	40	40	20

Table 26 - Fixed Geometry for HX2 of Coupled Heat Exchanger Assembly

Fixed Heat Exchanger Geometry for HX2 of Coupled Heat Exchanger Assembly						
Tube Diameter NPS (in)	Tube wall Thickness (in)	St (in)	Sl (in)	Duct Depth (ft)	Duct Height (ft)	Duct Length (ft)
1	0.133	1.7	1.7	4	5	27

The only variable parameter for a heat exchanger system using only cooling water and system using coupled heat exchangers is the mass flow rate ratio of cooling water to flue gas as provided in Table (27). The heat exchanger using only boiler feedwater, on the other hand, has fixed geometry and inlet process conditions.

Table 27 - Variable Process Condition for system using Cooling Water and Coupled Heat Exchanger

Variable Parameter	
M_{cw}/M_{fg}	M_{cw} (million lb/hr)
0.75	4.73
1.00	6.31
1.50	9.47

The condensation efficiency, temperature of boiler feedwater at the exit of heat exchanger and total pressure drop for the heat exchanger assembly were analyzed and compared to what was observed from analysis of heat exchangers with boiler feedwater and cooling water for cooling fluids. Refer below Figure (28), Figure (29) and Figure (30). It must be noted here that condensation efficiency for the assembly is actually the condensation efficiency of HX1 (since HX2 is a water-to-water heat exchanger) and the temperature of boiler feedwater, as depicted in Figure (28), is the temperature of boiler feedwater at the exit of HX2.

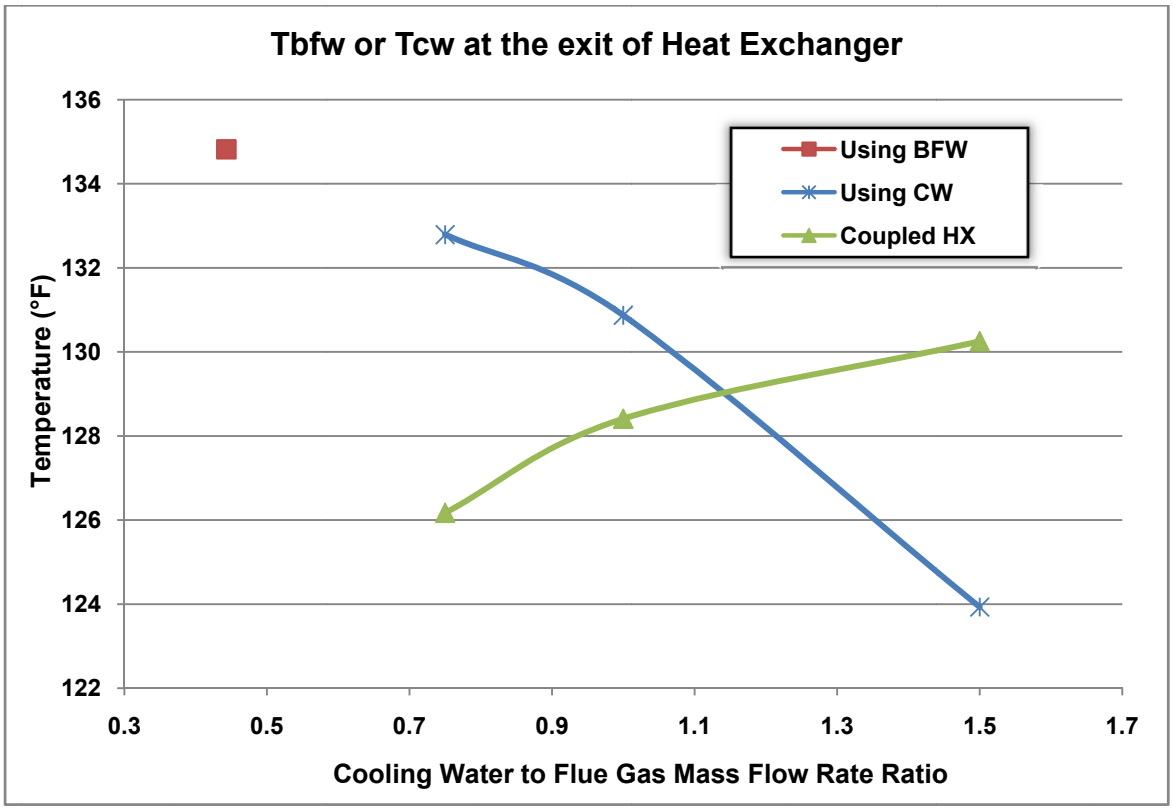

Figure 28 - Trend for Temperature of Feedwater at the exit of Coupled Heat Exchanger assembly compared to system using only Boiler Feedwater or only Cooling Water for various Cooling Water to Flue Gas Mass Flow Rate Ratios

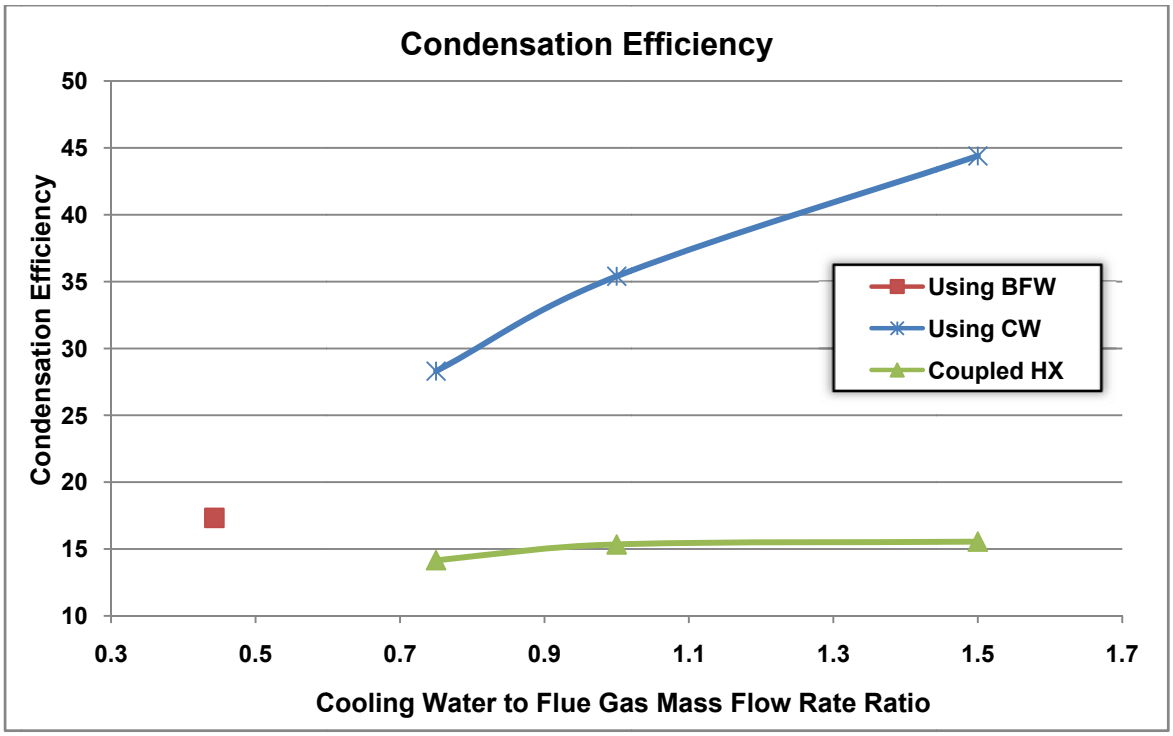

Figure 29 - Condensation Efficiency for Coupled Heat Exchanger assembly compared to system using only Boiler Feedwater or only Cooling Water for various Cooling Water to Flue Gas Mass Flow Rate Ratios

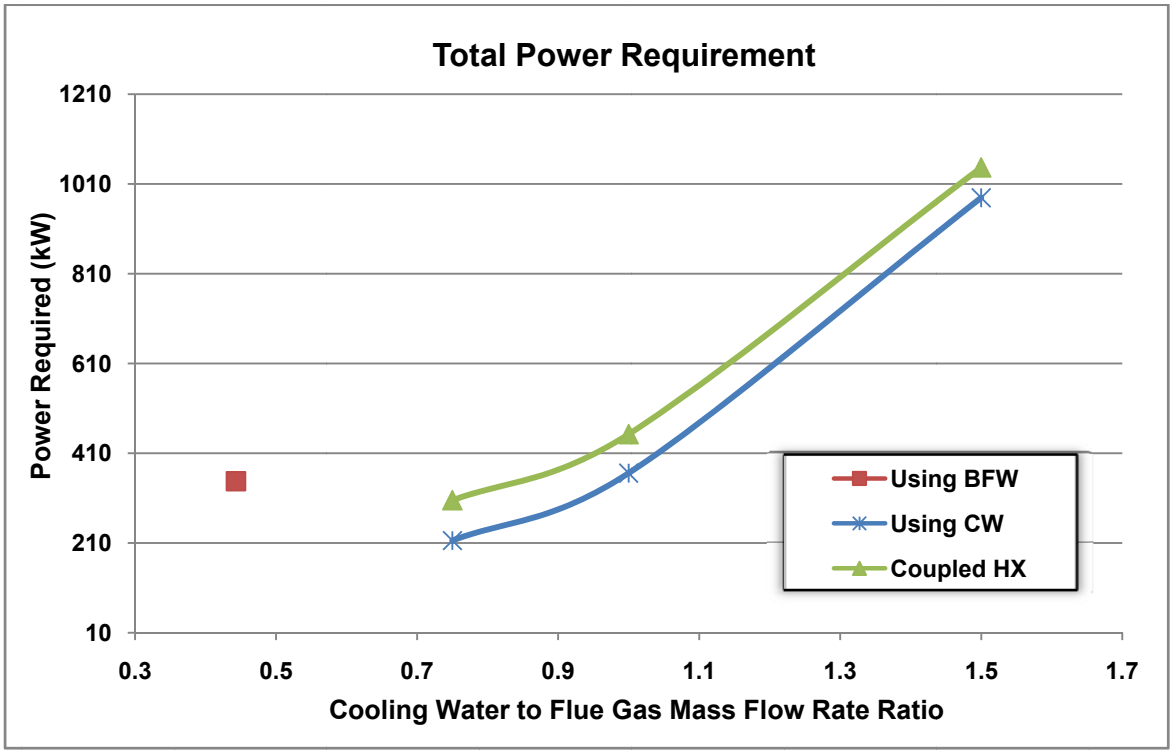

Figure 30 - Total power required for Coupled Heat Exchanger assembly compared to system using only Boiler Feedwater or only Cooling Water for various Cooling Water to Flue Gas Mass Flow Rate Ratios

From the Figure (28), it is observed that the temperature of feedwater at the exit of HX2 of coupled heat exchangers assembly increases with the increase in cooling water to flue gas mass flow rate ratio. This can be explained as the effectiveness of HX2 increases with increase in mass flow rate of cooling water. The trend for effectiveness is provided in Figure (31) below.

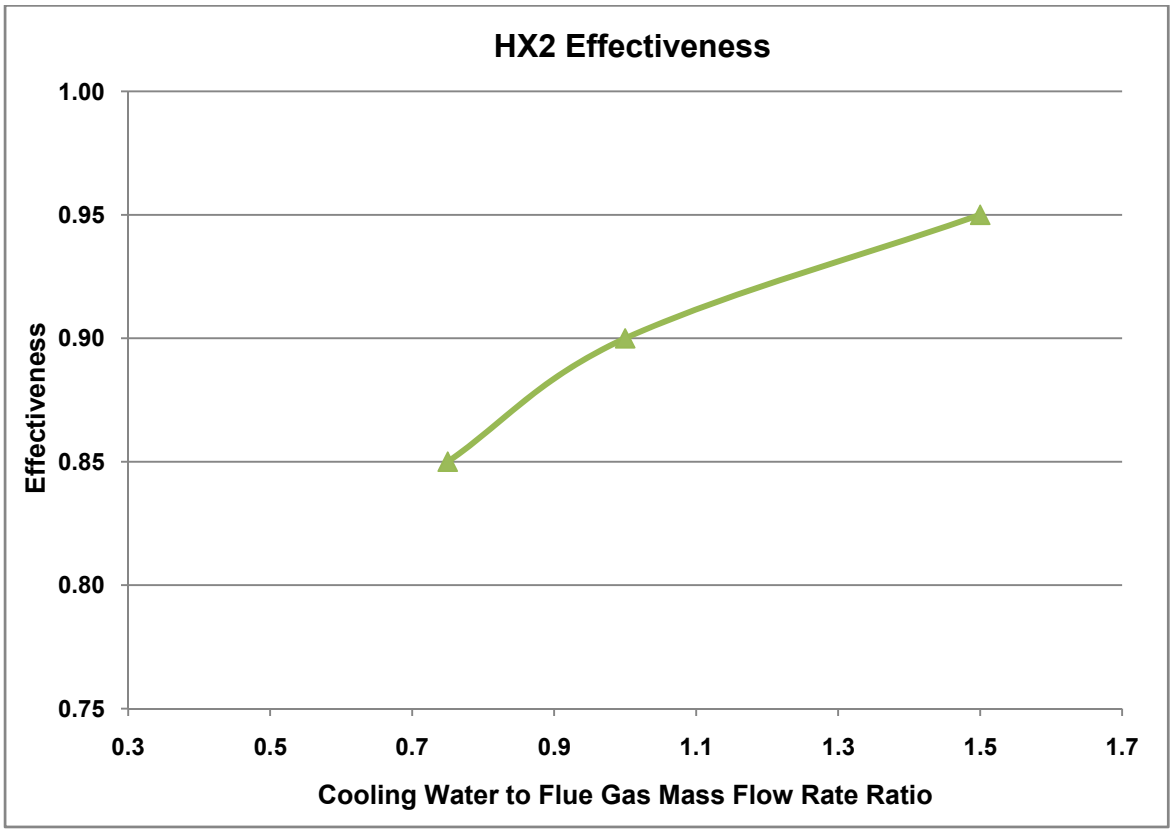

Figure 31 - Impact of cooling water to flue gas mass flow rate ratio on effectiveness of HX2 of Coupled Heat Exchanger Assembly

Further, it must be noted here that it gets harder to improve the effectiveness of HX2 above 0.95, and thus, increase the exit temperature of feedwater above 130°F. In contrast to the trends observed for coupled heat exchanger arrangement, for heat exchanger using cooling water, the temperature of cooling water at the exit of the heat exchanger decreases with increase in mass flow rate of cooling water. Moreover, even though the total rate of heat transfer increases with increase in mass flow rate of cooling water, the exit temperature of cooling water drops for the heat exchanger using only cooling water as can be seen in Figure (28).

If the aim of the heat exchanger is to condense out as much water from the flue gas as possible, clearly the best option is using only cooling water. The condensation efficiency for

coupled heat exchanger assembly is found to be lower compared to that of heat exchanger using either boiler feedwater or cooling water only as can be observed from Figure (29). This is due to the fact that in couplde heat exchangers, cooling water is at higher temperature at the inlet of HX1, and, the temperature further increases with increase in the cooling water to flue gas mass flow rate ratio. The trend for the temperature of cooling water at the inlet of HX1 is provided in Figure (32) below.

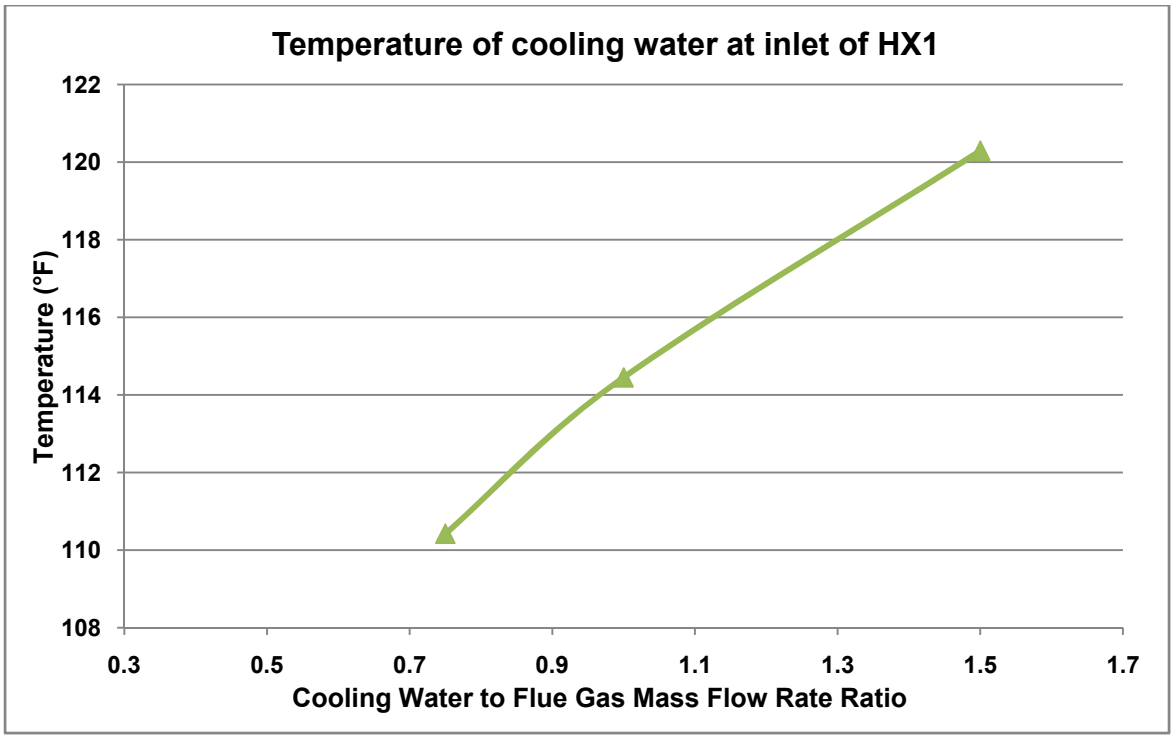

Figure 32 - Impact of Cooling Water to Flue Gas Mass Flow Rate Ratio on Temperature of Cooling Water at the inlet of HX1 of Coupled Heat Exchanger Assembly

The reason for increase in temperature of cooling water at the inlet of HX1 is that the cooling water is not routed through cooling tower to bring down its temperature; rather it is circulated continuously between HX1 and HX2. Any heat loss to the environment in the process of circulation has been neglected at this stage. Figure (33) and Figure (34) below depict the process flow diagram for coupled heat exchangers with cooling water to flue gas mass flow rate ratio of 1.0 and 1.5, respectively.

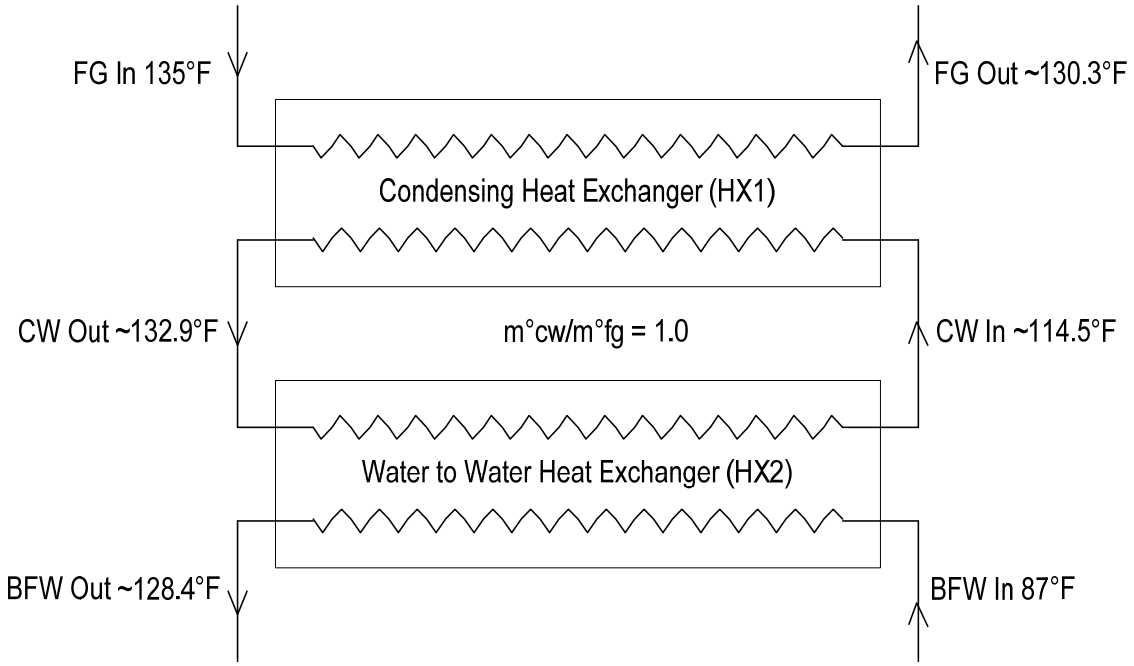

Figure 33 - Process Flow Diagram for Coupled Heat Exchanger with Cooling Water to Flue Gas Mass Flow Rate Ratio of 1.0

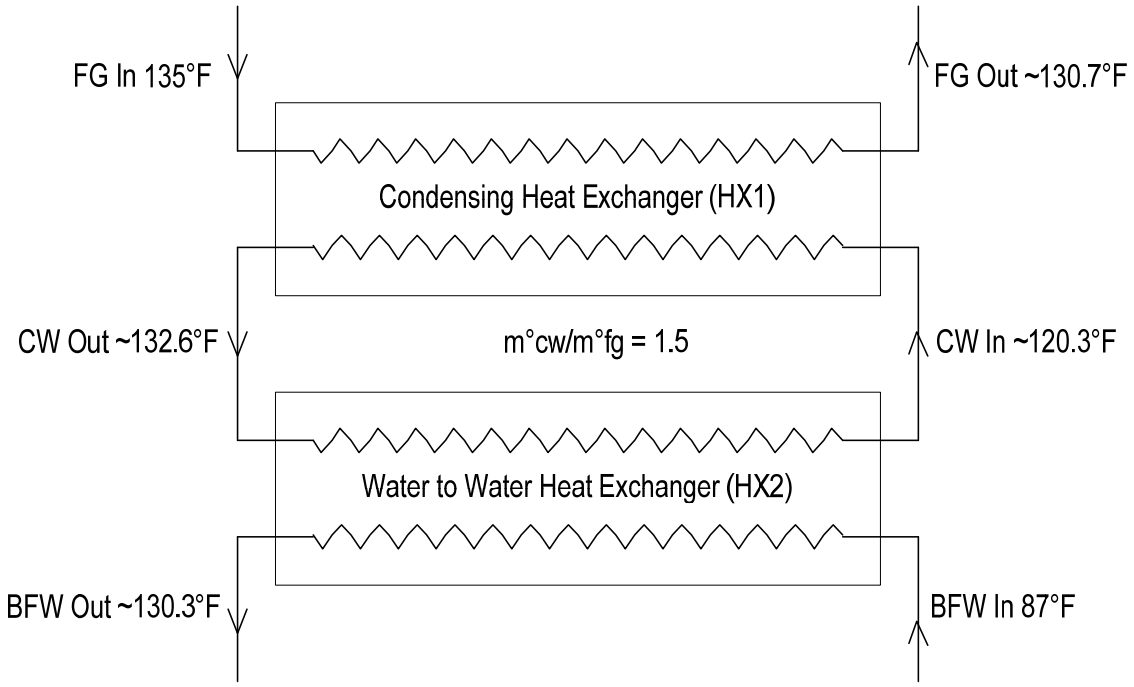

Figure 34 - Process Flow Diagram for Coupled Heat Exchanger with Cooling Water to Flue Gas Mass Flow Rate Ratio of 1.5

From the Figure (30), it can be noticed that the total power requirements for coupled heat exchanger assembly remains more than that for heat exchanger using only cooling water. The

increased power requirements can be attributed to the additional pressure drop due to usage of an additional heat exchanger in coupled heat exchangers assembly.

Overall, the use of feedwater directly with flue gas in condensing heat exchanger proves to be the ideal choice if the main aim of the system is to recover heat with reasonable power requirements, but, it is better to use cooling water at higher mass flow rates if we intend to condense out as much water as possible. The choice of coupled heat exchanger assembly is appropriate only, at higher mass flow rate ratios, when we have space constraints or the feed water line is at a distance from the flue gas duct after the ESP.

5.5.Cascaded Heat Exchanger, Flue Gas at 300°F -135°F

In this case, two heat exchangers are arranged in cascading across the FGD. The first heat exchanger, referred to as UHX, is placed upstream of the FGD and the second heat exchanger, referred to as DHX is placed downstream of the FGD. After the ESP, flue gas passes through the UHX and then enters the FGD where it is desulfurized. Saturated flue gas after the FGD enters the DHX. Boiler feedwater enters from downstream of the DHX, bypasses the FGD, and then re-enters the UHX such that an overall counter flow arrangement is obtained for both DHX and UHX. Refer Figure (35) below for the detailed process diagram.

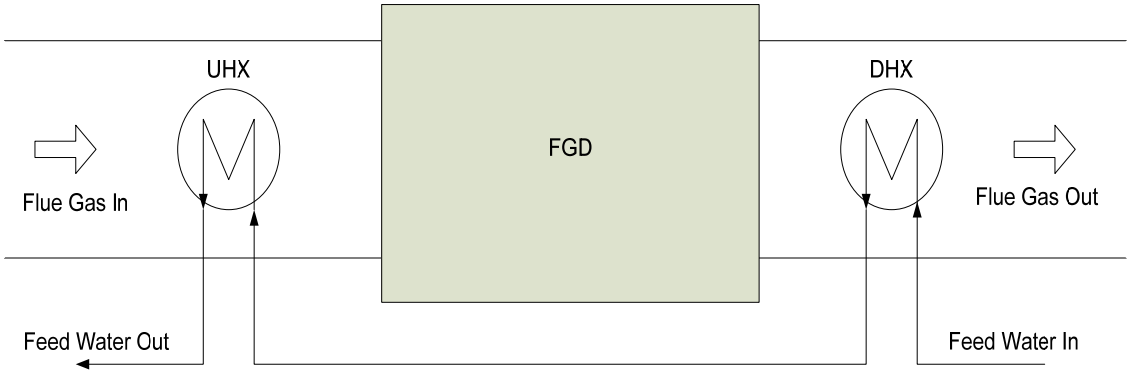

Figure 35 - Flow Diagram for Cascaded Heat Exchanger Arrangement

The analysis of this configuration was done in two stages. First, the DHX was optimized separately. It is possible to optimize DHX separately because irrespective of the temperature of flue gas at the exit of UHX, the inlet conditions of flue gas at the inlet of DHX will always remain

constant due to the presence of FGD. For a coal fired power plant, flue gas downstream of the FGD is saturated at a temperature of about 135°F. Keeping the temperature of boiler feedwater at the inlet of DHX fixed at 87°F, the only variable parameter is the mass flow rate of boiler feedwater. The mass flow rate of boiler feedwater depends only on the final temperature of boiler feedwater as it comes out of the UHX-DHX assembly, which decides the FWH duty required as explained in Section 3 of this report.

The flow rate of flue gas is 6.329 million lb/hr before it enters FGD, where it gets saturated and the flue gas flow rate increases to 6.716 million lb/hr due to the addition of water in FGD. The diameter of the tubes for DHX and UHX was kept constant at 2" NPS and wall thickness of 0.218". Setting a target temperature of boiler feedwater at the exit of UHX-DHX assembly, the mass flow rate of boiler feedwater was obtained from Jonas (14). Simulations were run by the author for multiple target temperatures of boiler feedwater and variable DHX duct lengths, and, the rate of condensation in DHX and total annual cost associated with DHX were obtained. A summary of the fixed process conditions and heat exchanger geometry for DHX is provided in Table (28) and Table (29) below:

Table 28 - Fixed Process Conditions for DHX of Cascaded Heat Exchangers Assembly

Inlet Conditions for DHX			
M_{fg} (lbm/hr)	T_{fg} (°F)	T_{bfw} (°F)	y_{H2O} (%)
6.72E+06	135	87	17.4

Table 29 - Fixed Heat Exchanger Geometry for DHX of Cascaded Heat Exchangers Assembly

Fixed Heat Exchanger Geometry for DHX					
Tube Diameter NPS (in)	Tube Wall Thickness (in)	S_t (in)	S_l (in)	Duct Depth (ft)	Duct Height (ft)
2	0.195	6.17	2.97	40	40

The variable boiler feedwater mass flow rates and the corresponding boiler feedwater temperature at the exit of the assembly are summarized below in Table (30).

Table 30 - Variable mass flow rate of boiler feedwater for DHX and UHX of Cascaded Heat Exchangers Assembly (14)

Variable Process Conditions	
T_{bfw} at exit of UHX-DHX (°F)	M_{bfw} (lb/hr)
140	2.82E+06
150	2.85E+06
160	2.88E+06
170	2.91E+06
180	2.93E+06
190	2.97E+06
200	2.99E+06

The plots for temperature of feedwater at the exit of DHX and rate of condensation in DHX as observed for variable feedwater mass flow rates listed in Table (30) are available below in Figure (36) and Figure (37), respectively.

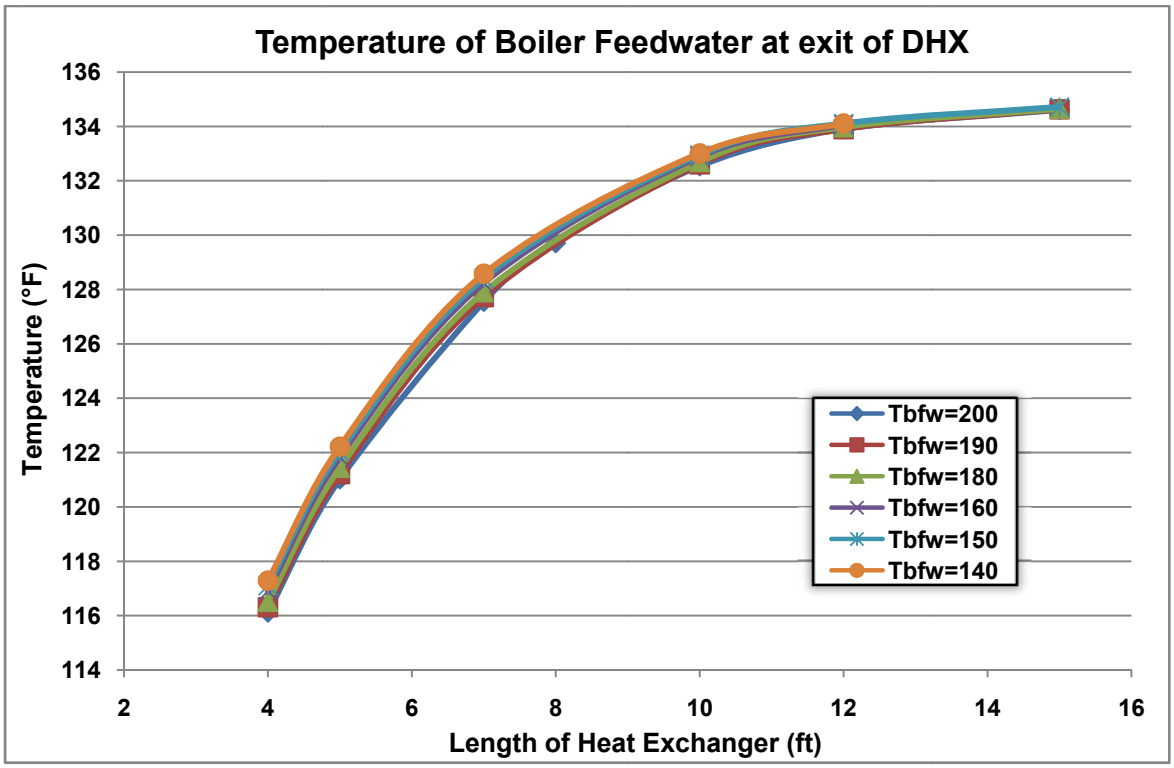

Figure 36 - Trend for Temperature of Boiler Feedwater at the Exit of DHX for various Target Feedwater Temperatures at the Exit of UHX-DHX Assembly.

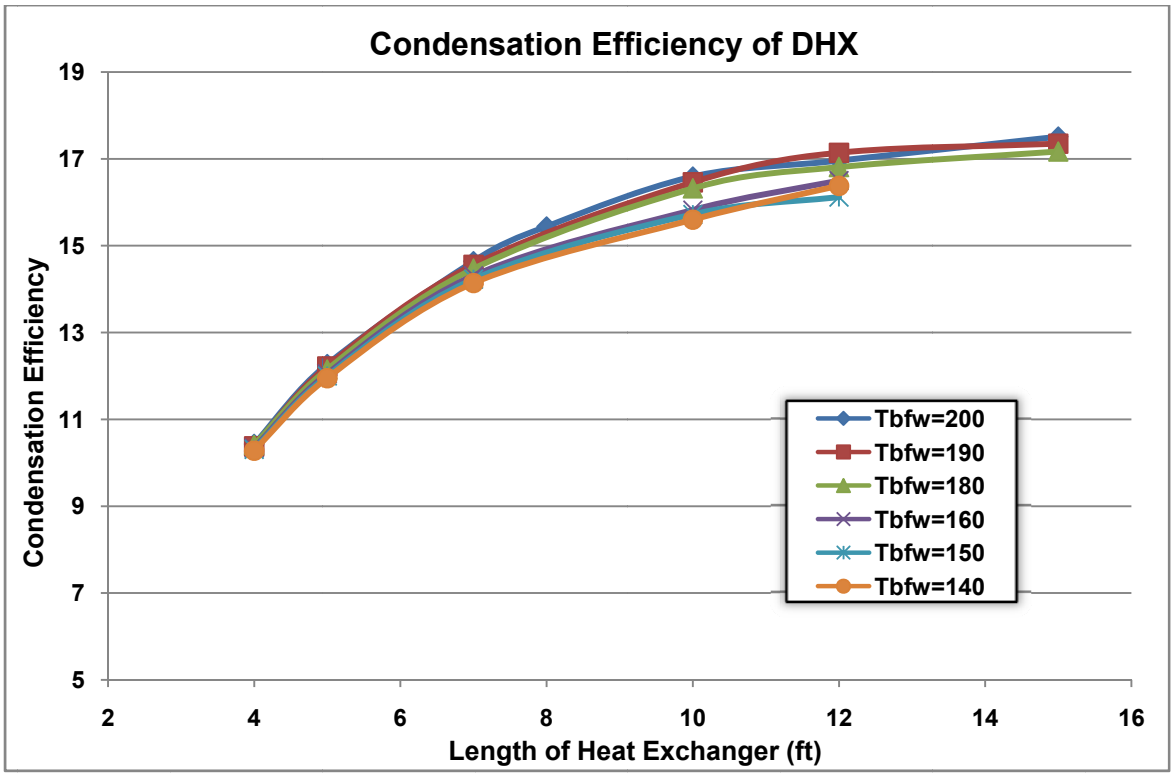

Figure 37 - Trend for Rate of Condensation in DHX for various Target Boiler Feedwater Temperatures at the Exit of UHX-DHX Assembly.

From Figure (36), it can be noticed that the temperature of boiler feedwater at the exit of DHX is nearly the same for all boiler feedwater mass flow rates simulated. The inlet temperature of flue gas and boiler feed water being constant for all the tests, the impact of slight changes in the mass flow rate of boiler feedwater is negligible on the total heat transferred from flue gas to boiler feedwater resulting in identical temperatures of boiler feedwater at the exit of DHX. Although, the change in mass flow rate of boiler feedwater results in condensation efficiency variation from 16.1% to 17.1% between the lowest and highest target temperature cases but the increase in condensation efficiency between two successive cases is negligible as can be seen in Figure (37).

Plots were also generated to identify the impact of variation in mass flow rate of boiler feedwater with target temperature of boiler feedwater at the exit of UHX-DHX assembly on the total capital cost as well as the annual operating cost. These plots are provided below in Figure (38) and Figure (39), respectively.

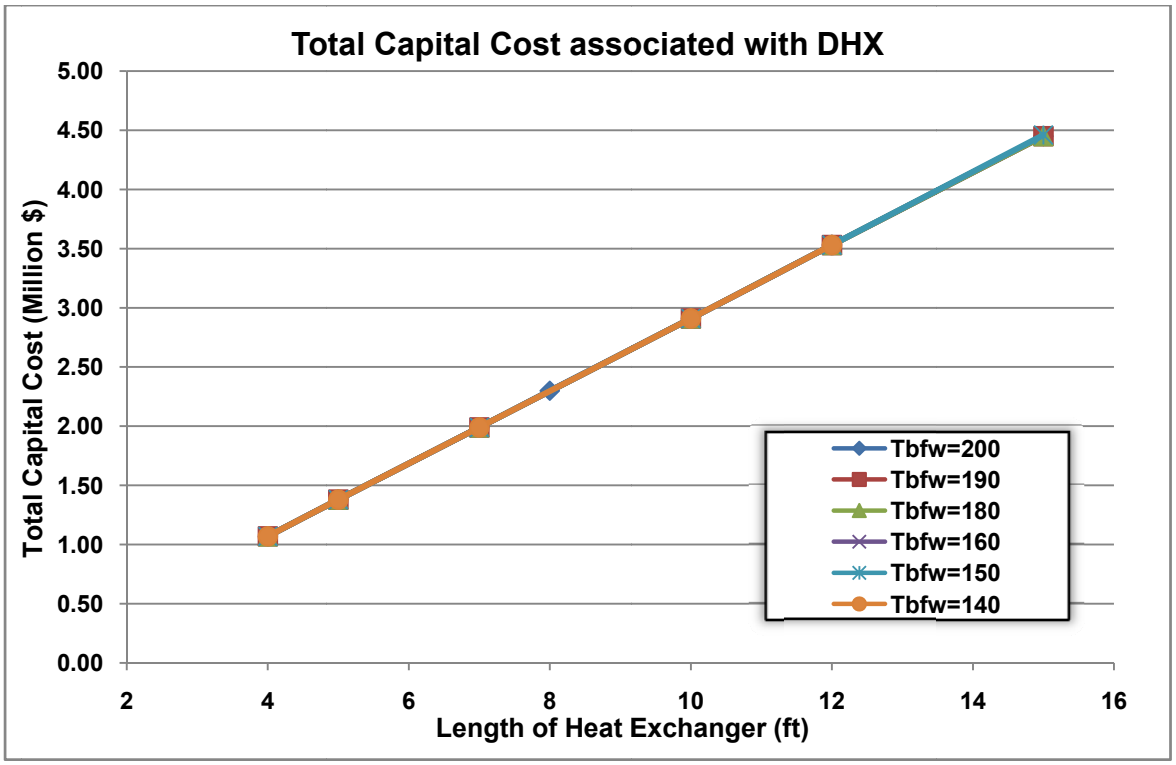

Figure 38 - Total Capital Cost associated with DHX for various Target Boiler Feedwater Temperatures at the Exit of UHX-DHX Assembly.

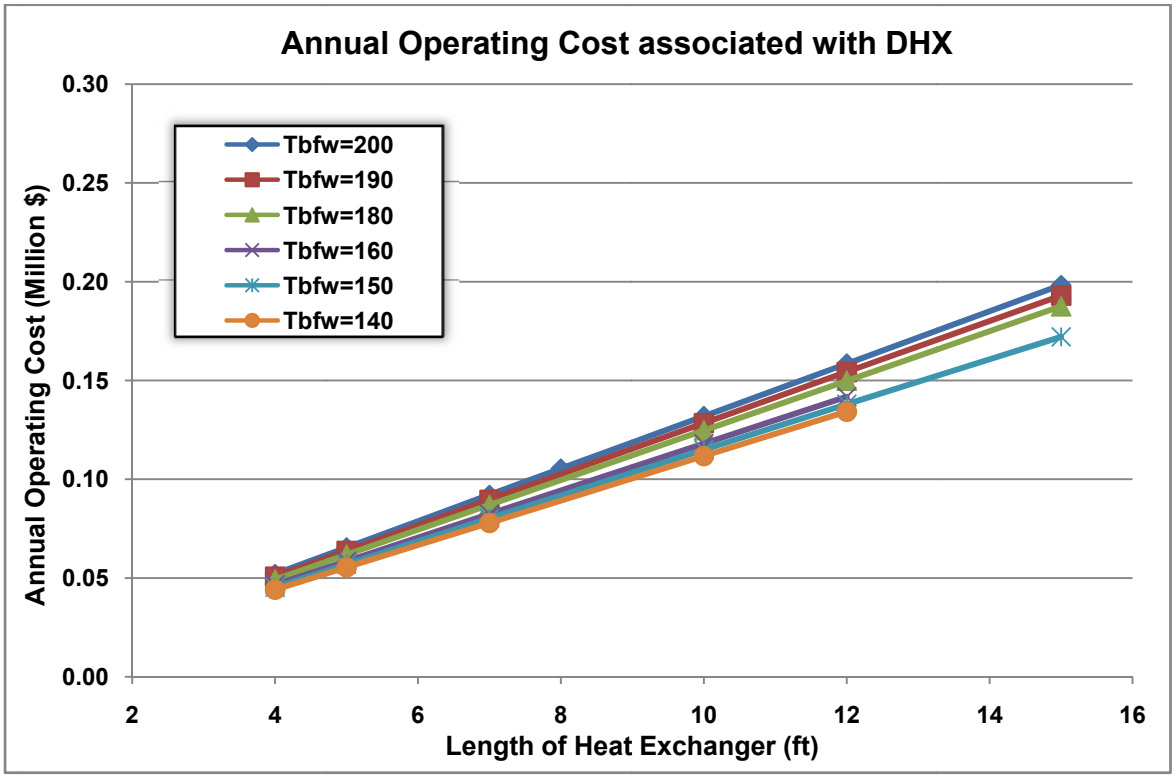

Figure 39 - Annual Operating Cost associated with DHX for various Target Boiler Feedwater Temperatures at the Exit of UHX-DHX Assembly

From Figure (38), it is observed that for a given duct length, the total capital cost remains the same irrespective of the target boiler feedwater temperature. This is expected because flue gas entering the DHX is saturated and therefore water vapor starts condensing as the flue gas enters the heat exchanger. Therefore, Nickel alloy 22 tubing is not required here. Thus, if we fix the length of the duct of the heat exchanger, the cost associated with manufacturing and installation and the tubing will remain constant irrespective of the mass flow rate of boiler feedwater. Further, the difference between the mass flow rates of boiler feedwater is quite small for different target temperatures of boiler feedwater at the exit of UHX-DHX assembly. As a result, the annual operating cost for all the cases simulated is nearly the same as can be seen in Figure (39) above.

Since, the total capital cost and operating cost associated with the DHX, of given duct length, were nearly the same, the resulting total annual cost for the DHX of that duct length was found to be approximately the same for all target temperatures at the exit of UHX-DHX assembly as can be seen below in Figure (40).

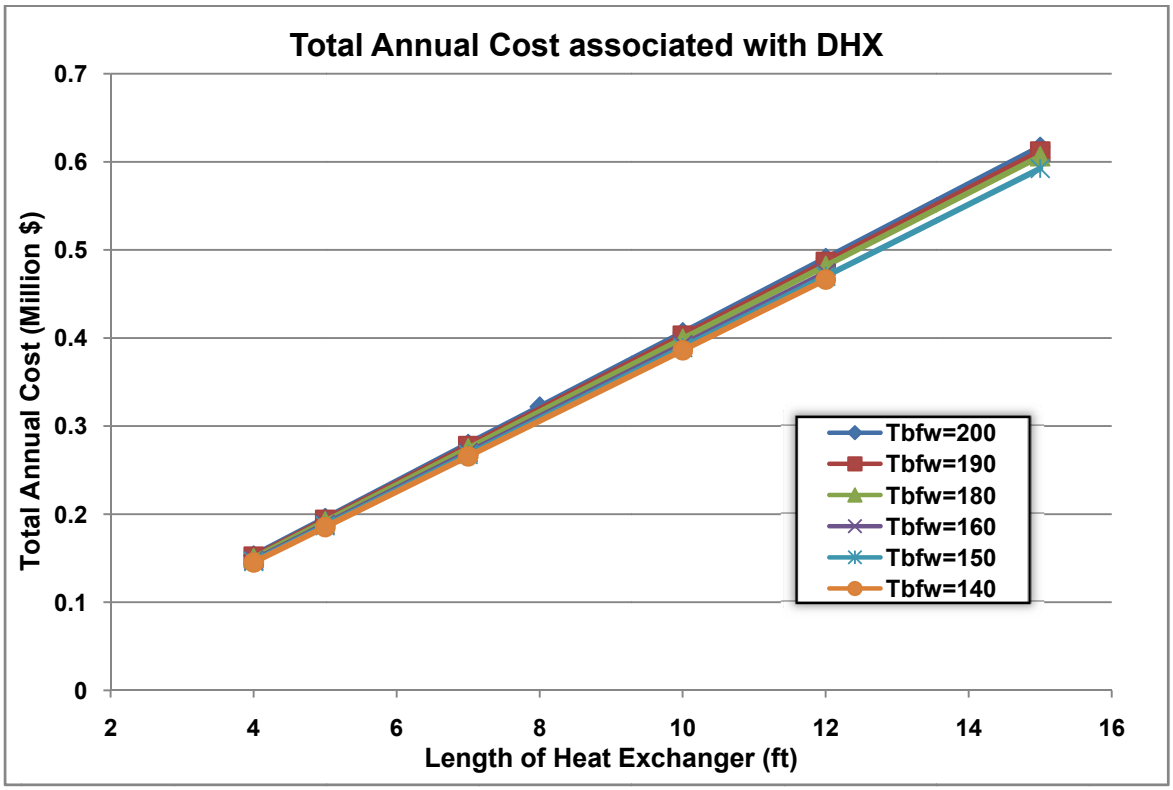

Figure 40 - Trend for Total Annual Cost associated with DHX for various Target Boiler Feedwater Temperatures at the Exit of UHX-DHX Assembly

Since the temperature of boiler feedwater at the exit of DHX, condensation efficiency in DHX and the total annual cost associated with DHX are nearly the same for different target temperatures of boiler feedwater at the exit of UHX-DHX assembly; it is acceptable to choose a fixed geometry of DHX in the UHX-DHX assembly.

Following the results analyzed above, DHX with a duct length of 12ft was selected. The total heat transfer, total annual cost, pressure drop etc associated with DHX of duct length 12 ft and various target temperatures of boiler feedwater at the exit of UHX-DHX assembly are provided below in Table (31).

Table 31 - Simulation results for DHX of Duct Length 12ft and various Boiler Feedwater Target Temperatures at the Exit of Cascaded Heat Exchanger Assembly

Tbfw_Target at the exit of UHX (°F)		200	190	180	170	160	150	140
Length of DHX	ft	12	12	12	12	12	12	12
m° Boiler Feedwater UHX-DHX	[10^6 lb/hr]	2.994	2.960	2.930	2.905	2.876	2.848	2.819
m° Flue Gas for DHX	[10^6 lb/hr]	6.720	6.720	6.720	6.720	6.720	6.720	6.720
Total Cond. Rate in DHX	[10^3 lb/hr]	124.35	125.7	123.29	122.14	121.01	118.22	120.11
Total Heat Transfer in DHX	[10^6 BTU/hr]	138.7624	140.3588	137.5914	136.2948	135.0164	131.7309	133.9525
DHX T_{fg} in	(°F)	135	135	135	135	135	135	135
DHX T_{fg} out	(°F)	129.06	128.96	129.11	129.17	129.23	129.4	129.27
DHX T_{bfw} In	(°F)	87	87	87	87	87	87	87
DHX T_{bfw} Out	(°F)	133.9	133.9	133.97	134.02	134.07	134.11	134.11
Boiler Feedwater Δp in DHX	(psi)	110.228	108.212	106.031	104.024	102.036	100.115	98.198
Flue Gas Δp in DHX	(psi)	0.031	0.031	0.031	0.031	0.031	0.031	0.031
Total Surface Area of DHX	ft^2	85720.06	85720.06	85720.06	85720.06	85720.06	85720.06	85720.06
Cond. Point in DHX	% distance from the upstream end of HX	0	0	0	0	0	0	0
y_{H2O}-EXIT of DHX		0.1489	0.1486	0.1491	0.1493	0.1496	0.1502	0.1498
Total Installed Cost for DHX	Million $	3.53	3.53	3.53	3.53	3.53	3.53	3.53
Annual Fixed Cost for DHX	Million $	0.33	0.33	0.33	0.33	0.33	0.33	0.33
ID Fan Power for DHX	kW	18.95	18.94	18.96	18.98	18.99	19.01	19
BFW Pump Power for DHX	kW	358.37	348.41	337.82	328.15	318.66	309.62	300.6
Total Power Req. for DHX	kW	377.33	367.35	356.78	347.12	337.65	328.63	319.6
Annual Operating Cost for DHX	Million $	0.1585	0.1543	0.1498	0.1458	0.1418	0.138	0.1342
Total Annual Cost for DHX	Million $	0.4906	0.4864	0.482	0.4779	0.474	0.4702	0.4664

Once the length of DHX was selected, simulations were performed for UHX to attain the target temperatures for boiler feedwater. It must be noted here that the target temperature of boiler feed water at the exit of UHX-DHX assembly is the temperature of boiler feedwater at the exit of UHX. The mass flow rate of flue gas upstream of the FGD is 6.329 million lb/hr with 12% moisture by mole fraction. The flue gas is at a temperature of 300°F upstream of the UHX. Assuming, no heat loss in pumping boiler feedwater around the FGD from DHX to UHX, boiler feedwater will enter the UHX at a temperature of 134°F which is the same temperature at which boiler feedwater exits DHX. A summary of the fixed process conditions and heat exchanger geometry for UHX is provided in Table (32) and Table (33) below. The mass flow rate of boiler feedwater for UHX will be the same as that for the DHX. Therefore the variable parameters for UHX will be the same as that for DHX as provided in Table (30).

Table 32 - Fixed Process Conditions for UHX of Cascaded Heat Exchanger Assembly

Inlet Conditions			
M_{fg} (lbm/hr)	T_{fg} (°F)	T_{bfw} (°F)	y_{H2O} (%)
6.33E+06	300	134	12

Table 33 - Fixed Heat Exchanger Geometry for UHX of Cascaded Heat Exchangers Assembly

Fixed Heat Exchanger Geometry					
Tube Diameter NPS (in)	Tube Wall Thickness (in)	S_t (in)	S_l (in)	Duct Depth (ft)	Duct Height (ft)
2	0.195	6.17	2.97	40	40

Simulations were run to identify the length of duct required for UHX so that the boiler feed water coming out of the UHX is heated to specific target temperatures. The changes in condensation efficiency and total annual cost, associated with UHX, with increase in target temperature of boiler feedwater at the exit of UHX were recorded. Table (34) below provides the details of total installed capital cost and annual operating cost as well as the fan and pump power requirements associated with UHX for various target temperatures of boiler feedwater at the exit of UHX.

Table 34 - Simulation results for UHX of UHX-DHX Assembly for various Boiler Feedwater Target Temperatures at the Exit of Cascaded Heat Exchanger Assembly

Tbfw_Target at the exit of UHX (°F)		200	190	180	170	160	150	140
Length of UHX	ft	26	18	13	9	6	3.5	1.9
m° Boiler Feedwater UHX-DHX	[10^6 lb/hr]	2.994	2.960	2.930	2.905	2.876	2.848	2.819
m° Flue Gas for UHX	[10^6 lb/hr]	6.329	6.329	6.329	6.329	6.329	6.329	6.329
Total Cond. Rate in UHX	[10^3 lb/hr]	0	0	0	0	0	0	0
Total Heat Transfer in UHX	[10^6 BTU/hr]	198.6517	166.1798	137.3053	106.7773	77.5051	46.1311	23.785
UHX T_{fg} in	(°F)	300	300	300	300	300	300	300
UHX T_{fg} out	(°F)	186.65	205.46	222.11	239.63	256.32	274.1	286.68
UHX T_{bfw} In	(°F)	133.89	133.88	133.9	133.89	133.71	133.72	133.46
UHX T_{bfw} Out	(°F)	200.16	189.89	180.68	170.65	160.67	149.92	141.91
Boiler Feedwater Δp in UHX	(psi)	236.728	160.579	113.423	76.789	49.936	28.214	15.407
Flue Gas Δp in UHX	(psi)	0.074	0.052	0.038	0.026	0.017	0.009	0.005
Total Surface Area of UHX	ft^2	190060.27	130437.29	93172.93	63361.44	41002.83	22370.65	11191.34
Cond. Point in UHX	% distance from the upstream end of HX	100	100	100	100	100	100	100
y_{H2O}-EXIT of UHX		0.12	0.12	0.12	0.12	0.12	0.12	0.12
Total Installed Cost for UHX	Million $	38.39	26.35	18.82	12.8	8.28	4.52	2.26
Annual Fixed Cost for UHX	Million $	3.62	2.48	1.77	1.21	0.78	0.43	0.21
ID Fan Power for UHX	kW	46.93	33.77	25.09	17.75	11.92	6.75	3.46
BFW Pump Power for UHX	kW	769.65	517.01	361.37	242.23	155.95	87.26	47.16
Total Power Req. for UHX	kW	816.57	550.78	386.46	259.99	167.87	94.01	50.63
Annual Operating Cost for UHX	Million $	0.34	0.23	0.16	0.11	0.07	0.04	0.02
Total Annual Cost for UHX	Million $	3.96	2.71	1.94	1.31	0.85	0.47	0.23

From Table (34), It can be noticed that total rate of condensation within UHX remains zero for all target temperatures of boiler feedwater at the exit of UHX. This can be attributed to the fact that the temperature of the tube wall always remains higher than the dew point temperature of moisture in flue gas stream as can be observed from the temperature distribution plots for UHX provided below in Figure (41 a-g) for each target temperature of boiler feedwater as provided in Table (30).

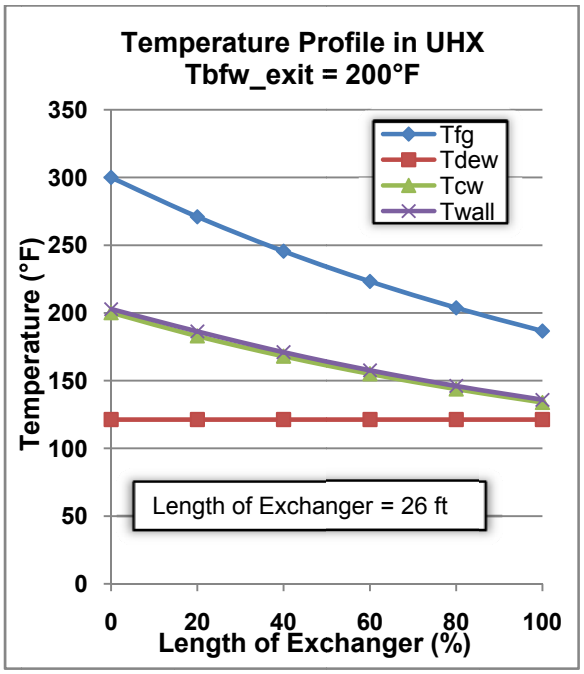

41(a) - Tbfw_Target = 200°F

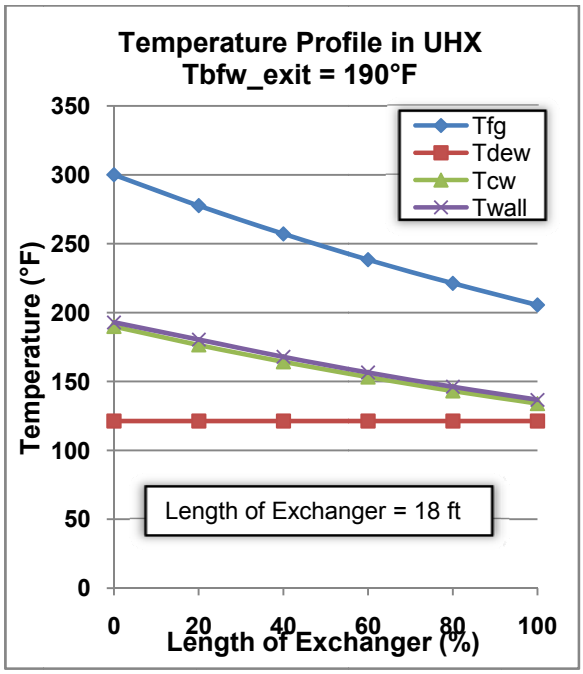

41(b) - Tbfw_Target = 190°F

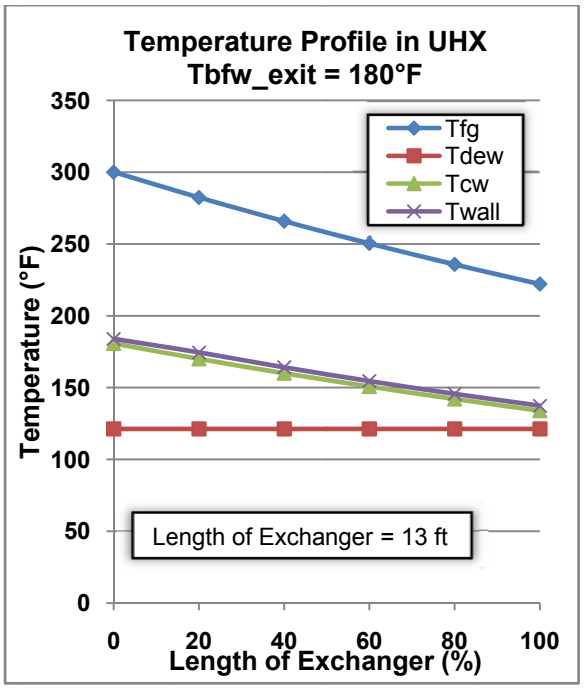

41(c) - Tbfw_Target = 180°F

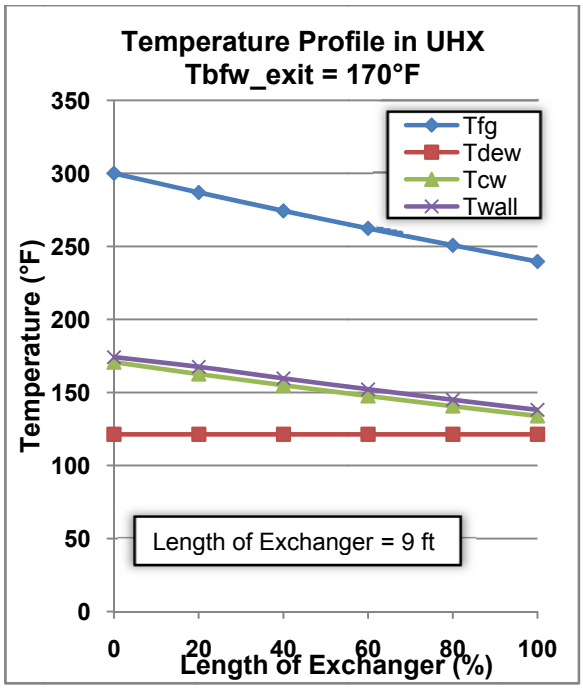

41(d) - Tbfw_Target = 170°F

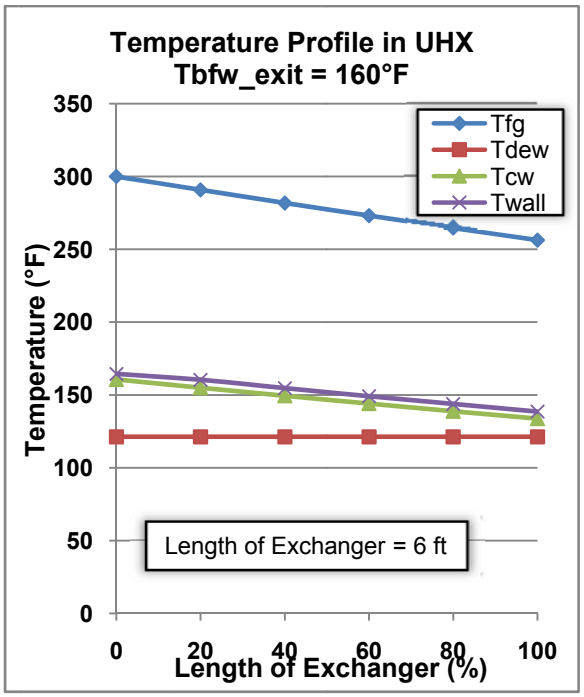

41(e) - Tbfw_Target = 160°F

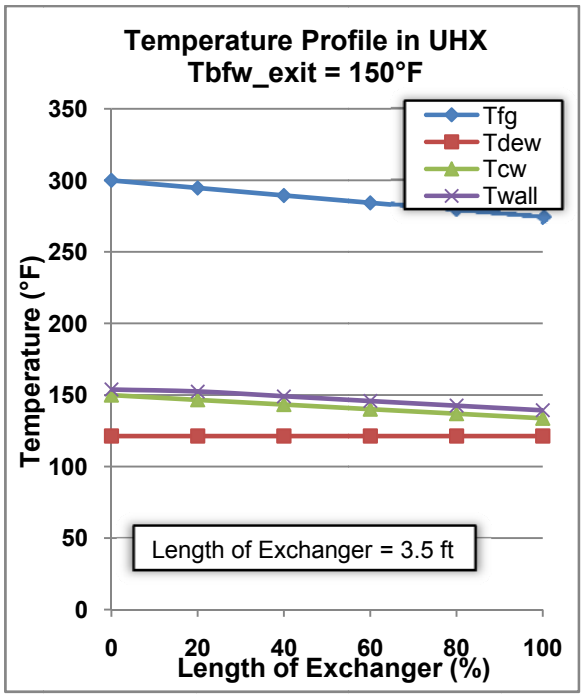

41(f) - Tbfw_Target = 150°F

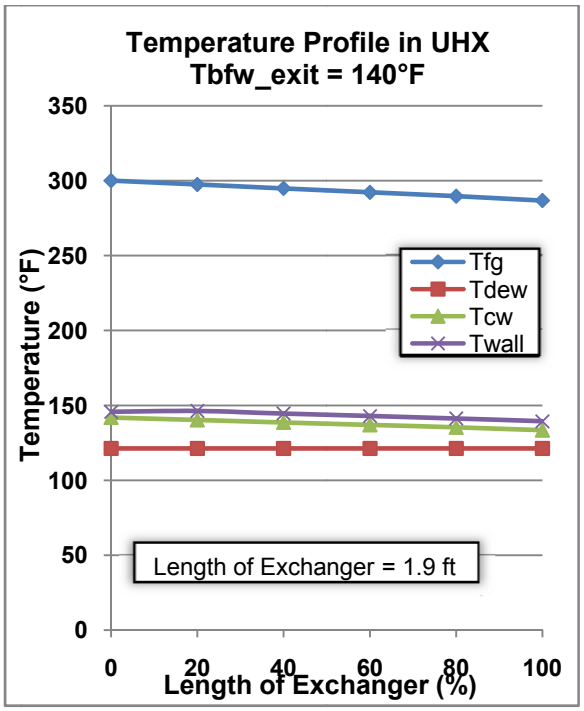

41(g) - Tbfw_Target = 140°F

Figure 41 - Temperature Profiles in UHX of UHX-DHX assembly for various target Temperatures of Boiler Feedwater at the Exit of UHX

Since there is no condensation observed in the UHX as concluded above, the heat exchanger tubes will be required to be made entirely from Nickel alloy 22 material to protect from corrosion which leads to higher fixed costs. Also, it must be noted here that the size of the heat exchanger increases with increase in target temperature of boiler feedwater at the exit of heat exchanger which would result in higher fixed costs and operating costs. So, the total annual cost associated with UHX increases with increase in temperature of boiler feedwater at the exit of UHX as can be seen in Figure (42) below. Figure (42) also shows the condensation efficiency associated with the UHX for various target temperatures of boiler feedwater at the exit of UHX.

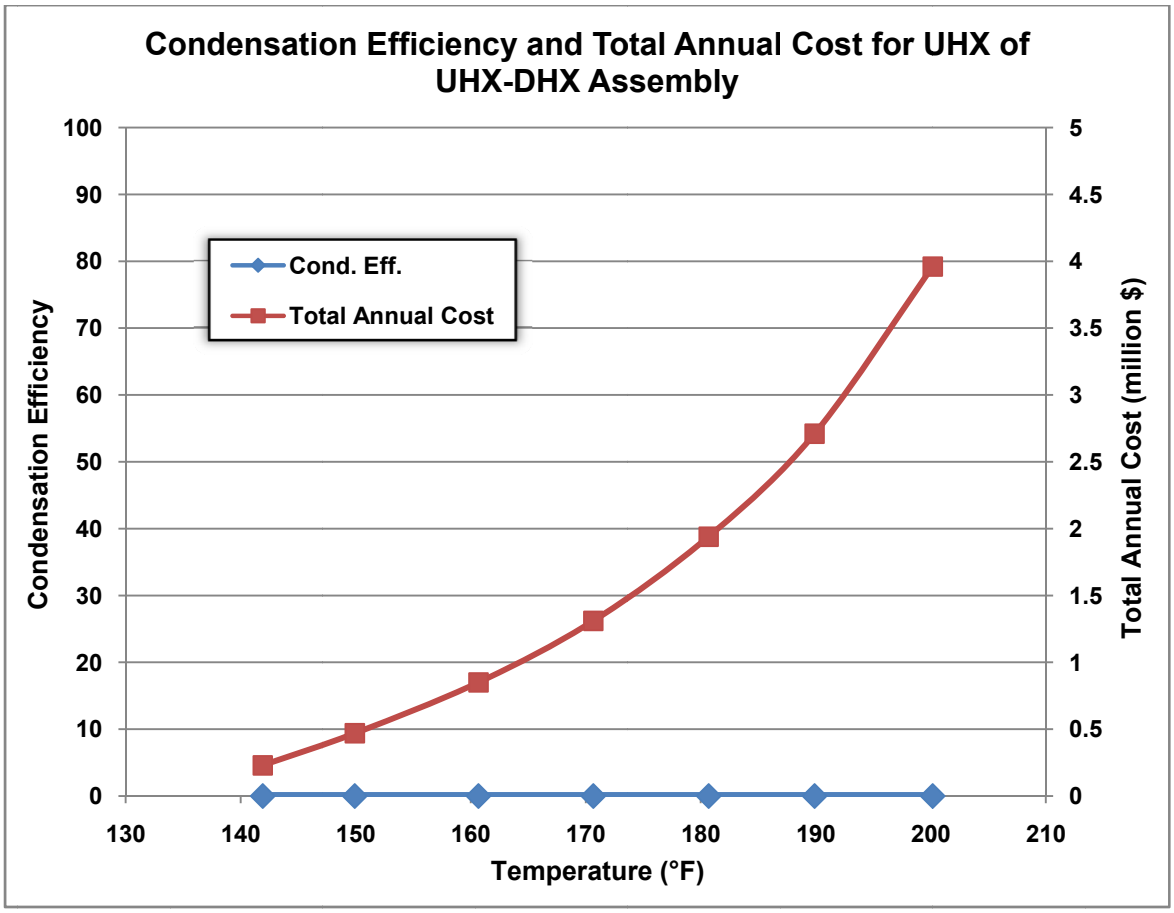

Figure 42 - Condensation Efficiency and Total Annual Cost for UHX of UHX-DHX Assembly for various target boiler feedwater temperatures at the exit of UHX

To obtain the overall performance of the assembly; the total rate of condensation, total power requirements and total annual cost of the assembly were obtained by summing up the individual quantities for UHX and DHX. The results are provided below in Table (35). It must be noted here that the information provided in the Table (35) is for the entire assembly, i.e., the flue gas and boiler feed water temperature are at the inlet as well as exit of the UHX-DHX assembly. Similarly, the overall size of duct, the total heat transfer, total cost, pressure drop etc., are summation of individual results for UHX and DHX.

Also, the case with boiler feedwater target temperature of 134°F is a limiting case as the boiler feedwater gets heated to this temperature at the exit of DHX and thus, UHX will not be required for this case. The limiting case has been included to compare the performance of UHX-DHX assembly with system with only UHX and system with only DHX.

For Comparative study, simulations were also run for a system where only the UHX is used in the flue gas stream, similar to the arrangement discussed in Section 5.1 in this study, and the length of heat exchanger was determined to heat boiler feedwater, entering UHX at 87°F, to target temperatures same as that for UHX-DHX assembly. These cases have been referred to as UHX only for differentiation and the results are available in Table (36). Among these simulations the case with target temperature 134°F was run for UHX i.e, for flue gas conditions upstream of FGD.

Table 35 - Results from Simulations for various Boiler Feedwater Target Temperatures at the Exit of UHX-DHX Assembly

UHX-DHX Assembly									
T_{bfw} Target (°F)		**200**	**190**	**180**	**170**	**160**	**150**	**140**	**134**
Total Length UHX+DHX	ft	38	30	25	21	18	15.5	13.9	12
m° Boiler Feedwater	[10^6 lb/hr]	2.994	2.960	2.930	2.905	2.876	2.848	2.819	2.800
m° Flue Gas for UHX	[10^6 lb/hr]	6.329	6.329	6.329	6.329	6.329	6.329	6.329	6.72
Total Cond. Rate UHX+DHX	[10^3 lb/hr]	124.35	125.70	123.29	122.14	121.01	118.22	120.11	119.19
Total Heat Transfer UHX+DHX	[10^6 BTU/hr]	337.41	306.54	274.90	243.07	212.52	177.86	157.74	132.86
UHX T_{fg} in	(°F)	300	300	300	300	300	300	300	135
DHX T_{fg} out	(°F)	129.06	128.96	129.11	129.17	129.23	129.4	129.27	129.32
DHX T_{bfw} In	(°F)	87	87	87	87	87	87	87	87
UHX T_{bfw} Out	(°F)	200.16	189.89	180.68	170.65	160.67	149.92	141.91	134.13
Boiler Feedwater Δp UHX+DHX	(psi)	346.96	268.79	219.45	180.81	151.97	128.33	113.61	97.06
Flue Gas Δp UHX+DHX	(psi)	0.105	0.083	0.069	0.057	0.048	0.04	0.036	0.031
Total Surface Area UHX+DHX	ft^2	275780.33	216157.35	178892.99	149081.50	126722.89	108090.71	96911.40	85720.06
y_{H2O} at Exit of DHX		0.1489	0.1486	0.1491	0.1493	0.1496	0.1502	0.1498	0.15
Installed Capital Cost UHX+DHX	Million $	41.92	29.88	22.35	16.33	11.81	8.05	5.79	3.53
Annual Fixed Cost UHX+DHX	Million $	3.95	2.81	2.1	1.54	1.11	0.76	0.54	0.33
Total Power Req. UHX+DHX	kW	1193.90	918.13	743.24	607.11	505.52	422.64	370.23	314.33
Annual Operating Cost UHX+DHX	Million $	0.50	0.38	0.31	0.26	0.21	0.18	0.15	0.13
Total Annual Cost UHX+DHX	Million $	4.45	3.20	2.42	1.79	1.32	0.94	0.70	0.46

Table 36 - Results from Simulations for various Boiler Feedwater Target Temperatures at the Exit of System with Only UHX

UHX Only									
Tbfw_Target (°F)		**200**	**190**	**180**	**170**	**160**	**150**	**140**	**134**
Length of UHX alone	ft	43	32	24	18.5	14.5	11	8.5	7
m° Boiler Feedwater	[10^6 lb/hr]	2.990	2.960	2.930	2.905	2.880	2.848	2.819	2.802
m° Flue Gas	[10^6 lb/hr]	6.329	6.329	6.329	6.329	6.329	6.329	6.329	6.329
Cond. Point	% distance from upstream end of UHX	78.99	76.98	74.14	70.94	66.80	61.54	54.90	48.40
Total Cond. Rate	[10^3 lb/hr]	57.76	48.80	43.03	37.99	34.66	29.90	26.54	24.52
Total Heat Transfer	[10^6 BTU/hr]	336.92	303.50	271.51	240.62	212.68	179.90	151.89	132.67
T_{fg} in	(°F)	300	300	300	300	300	300	300	300
T_{fg} out	(°F)	140.54	154.74	169.97	184.95	199.18	215.28	229.4	239.23
T_{bfw} In	(°F)	87.31	87.79	87.25	87.05	86.37	86.77	86.9	86.94
T_{bfw} Out	(°F)	199.8	190.15	179.83	169.93	160.37	149.99	140.83	134.33
Boiler Feedwater Δp	(psi)	399.41	288.34	211.96	160.32	123.28	91.74	69.44	56.45
Flue Gas Δp	(psi)	0.119	0.089	0.068	0.053	0.041	0.032	0.024	0.02
Total Surface Area	ft^2	320485.53	234777.5	175154.52	134163.73	104352.24	78267.19	59635.01	48455.7
y_{H2O}-EXIT		0.1067	0.1088	0.1101	0.1113	0.1121	0.1132	0.1139	0.1144
Installed Capital Cost	Million $	53.9	38.73	28.1	20.83	15.51	10.97	7.72	5.77
Annual Installed Cost	Million $	5.08	3.65	2.65	1.96	1.46	1.03	0.73	0.54
Total Power	kW	1367.83	981.38	716.58	538.59	411.48	304.35	228.82	185.27
Annual Operating Cost	Million $	0.57	0.41	0.30	0.23	0.17	0.13	0.10	0.08
Total Annual Cost	Million $	5.65	4.06	2.95	2.19	1.63	1.16	0.82	0.62

The plots for rate of condensation and total annual cost were developed and compared to the results for the UHX only and DHX only cases. These plots are available in Figure (43) and Figure (44) below:

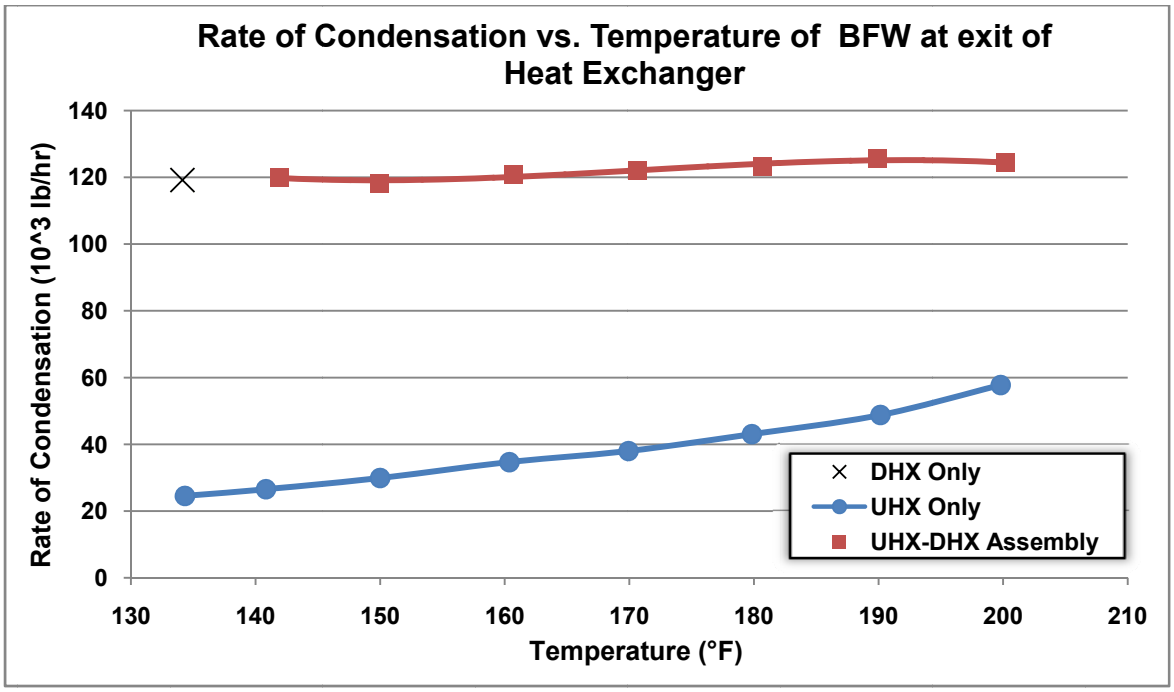

Figure 43 - Rate of Condensation for UHX-DHX assembly compared to UHX only and DHX only cases for different Target Boiler Feedwater Temperatures

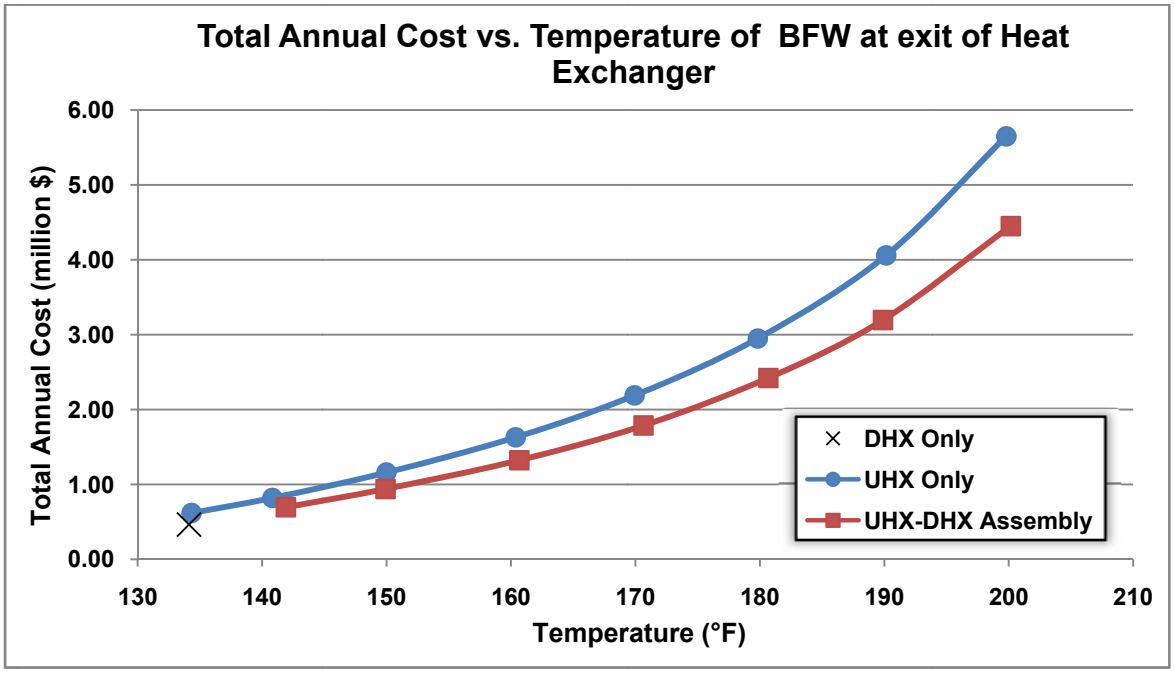

Figure 44 - Total Annual Cost for UHX-DHX assembly compared to UHX only and DHX only cases for different Target Boiler Feedwater Temperatures

From Figure (43), it is clear that the total rate of condensation for the UHX-DHX assembly remains higher than that observed for system with only UHX. It is also noticed that the rate of condensation is comparable to that observed for only DHX case. This can be attributed to the fact that there is no condensation observed in the UHX of the assembly and the variation in the rate of condensation is minimal in DHX for small change in mass flow rate of boiler feedwater as observed in Figure (37). It must be noted here that the flue gas entering DHX is saturated, while for the UHX only case, flue gas has only 12% moisture by mole fraction. The percentage of moisture in flue gas at the exit of the heat exchanger is provided in Table (35) for UHX-DHX assembly and Table (36) for the UHX only case.

It is also observed that the total annual cost for the UHX-DHX assembly is less than that associated with usage of only UHX as indicated in Figure (44). It can be explained by looking at the heat exchanger geometry and material employed. For the UHX-DHX assembly, 12ft of the duct serves as the DHX for which the tubes will be made of stainless steel (SS304) as the flue gas entering DHX is saturated with water. The remaining duct length serves as UHX which is entirely made from Nickel Alloy 22 material, as explained earlier in this section. On the contrary, for the UHX only case, Nickel alloy 22 material is used for tube material up-to the point where condensation begins and SS304 is used thereafter. The point of condensation for UHX only case is also provided in Table (36). It was observed that for any given target temperature of boiler feedwater, the total tube length of nickel alloy 22 material required for UHX only case was more than that for UHX-DHX assembly for the same target temperature of boiler feedwater. This results in lower total installed cost for UHX-DHX assembly as compared to a system using only UHX for a given target exit temperature of boiler feedwater. Further, even though the UHX-DHX assembly tends to have a longer overall duct length compared to system using only UHX to attain the given target exit temperature of boiler feedwater, the annual operating cost which depends only on the overall length of the duct, is overshadowed by the annual installed cost in estimation of total annual cost

To assess the cost benefits associated with UHX-DHX assembly, cost associated with the treatment of condensed water (16), monetary savings from using this condensed water as make

up water in cooling tower (16) and benefits from selling the additional power generated due to improvement in plant heat rate (14), were done by Dr. Levy. The cost benefits calculated for DHX only, UHX only and UHX-DHX assembly are available provided below in Table (37), Table (38) and Table (39), respectively.

Table 37 - Results of Cost Benefit Analysis for system with Only DHX

DHX Only							
Tbfw Target	Annual Income			Annual Expenses			Net Profit
	Power	Water	Total	Heat Exchanger	Water Treatment	Total Annual Cost	
(°F)	$ (million)	$ (million)	$ (million)	$ (million)	$ (million)	$ (million)	$ (million)
134	1.24	0.147	1.387	0.462	0.1014	0.5634	+0.8236

Table 38 - Results of Cost Benefit Analysis for system with Only UHX

UHX Only							
Tbfw Target	Annual Income			Annual Expenses			Net Profit
	Power	Water	Total	Heat Exchanger	Water Treatment	Total Annual Cost	
(°F)	$ (million)	$ (million)	$ (million)	$ (million)	$ (million)	$ (million)	$ (million)
200	4.22	0.0716	4.2916	5.65	0.0598	5.7098	-1.4182
190	3.58	0.0605	3.6405	4.06	0.0541	4.1141	-0.4736
180	3.08	0.0531	3.1331	2.95	0.0444	2.9944	+0.1387
170	2.52	0.0469	2.5669	2.19	0.0397	2.2297	+0.3372
160	2.11	0.0432	2.1532	1.63	0.0363	1.6663	+0.4869
150	1.68	0.0371	1.7171	1.16	0.0312	1.1912	+0.5259
140	1.4	0.0334	1.4334	0.83	0.0273	0.8573	+0.5761

Table 39 - Results of Cost Benefit Analysis for system with UHX-DHX Assembly

UHX-DHX Assembly							
Tbfw Target	Annual Income			Annual Expenses			Net Profit
	Power	Water	Total	Heat Exchanger	Water Treatment	Total Annual Cost	
(°F)	$ (million)	$ (million)	$ (million)	$ (million)	$ (million)	$ (million)	$ (million)
200	4.22	0.147	4.367	4.4485	0.1018	4.5503	-0.1833
190	3.58	0.147	3.727	3.1943	0.1018	3.2961	+0.4309
180	3.08	0.147	3.227	2.4098	0.1018	2.5116	+0.7154
170	2.52	0.147	2.667	1.7958	0.1018	1.8976	+0.7694
160	2.11	0.147	2.257	1.3218	0.1018	1.4236	+0.8334
150	1.68	0.147	1.827	0.9380	0.1018	1.0398	+0.7872
140	1.4	0.147	1.547	0.6942	0.1018	0.7960	+0.7510

Plots were developed for the change in Turbine power and net profit associated with using only DHX or only UHX or UHX-DHX assembly in the system as illustrated in Figure (45) and Figure (46) below:

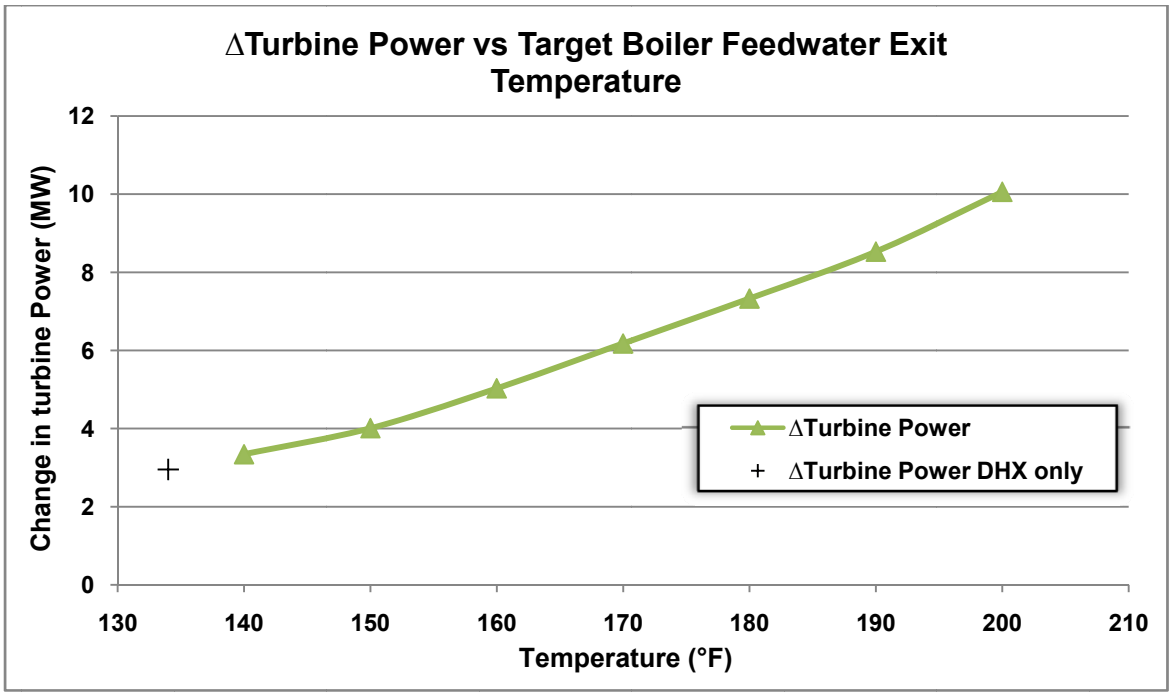

Figure 45 - Change in Turbine Power with Target Boiler Feedwater Exit Temperature

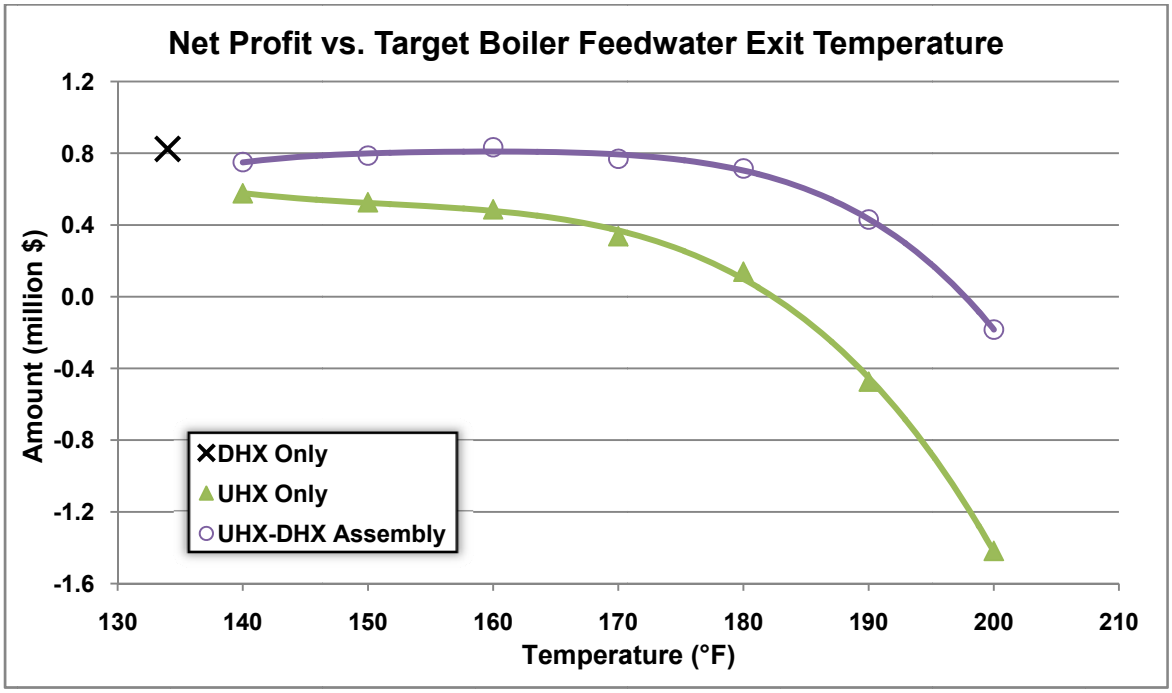

Figure 46 - Net Profit from using UHX-DHX assembly compared to system with Only UHX and Only DHX

In Figure (45), it must be noted that change in net turbine power would be same for both UHX-DHX assembly and UHX Only cases as turbine power is a function of only the temperature of boiler feedwater at the exit of heat exchanger as explained in Section 3 of this report. From Figure (46), it is noted that the usage of UHX-DHX assembly proves beneficial for boiler feedwater temperatures up to ~197°F compared to ~183°F for system with only UHX. Also, it is noted that using UHX-DHX assembly to heat boiler feedwater to a temperature of around 160°F returns maximum benefits which are slightly more than a system employing only DHX.

6. Discussion of Results & Conclusion

A previously validated Matlab code was used to analyze the performance of condensing heat exchangers placed upstream and/or downstream of the wet FGD unit. Five different heat exchanger arrangements were evaluated to identify the heat exchanger design that will return high rate of condensation and rate of heat transfer and also generate revenue if possible.

The use of boiler feedwater as the cooling fluid in condensing heat exchangers offers the benefit of recovering both heat and water from flue gas. The study, done in conjunction with Jonas (16), indicated that the mass flow rate of boiler feedwater available at the inlet of FWH1 depends on the temperature to which it is heated in the condensing heat exchanger. For the specific 600MW power plant analyzed here, the mass flow rate of boiler feedwater would vary between 2.673 million lb/hr for a boiler feedwater temperature of 87°F at the exit of the heat exchanger (of infinitesimally small surface area) to 3.054 million lb/hr for an exit temperature of 220°F.

Both the flue gas and cooling water streams experience pressure drops as they pass through the heat exchanger. Of these two, cooling water experiences higher pressure drops and thus contributes a substantial part of the operating costs. As a result, for a heat exchanger with tubes of 2" NPS diameter and duct length of 20 ft, the total annual cost can vary from $1.43 million to $7.22 million for cooling water to flue gas mass flow rate ratio ranging between 0.75 and 1.5. Increasing the tube diameter to 3.5" NPS brings down the total annual cost to between $0.41 million to $0.71 million for the same range of cooling water to flue gas mass flow rate ratio. Also, it was observed that keeping surface area or length of heat exchanger constant, the change in tube diameter had negligible impact on total heat transfer and condensation efficiency.

The condensing heat exchanger can be placed upstream or downstream of different low pressure FWHs. Depending on the location of the heat exchanger, the temperature of boiler feedwater can be as high as 194°F. It was observed that use of low temperature boiler feedwater before FWH1 resulted in higher rate of heat transfer and condensation efficiency of the heat exchanger. Also, the total installed cost of the heat exchanger was reduced since the point of condensation moved closer to the upstream inlet end of the heat exchanger, thus reducing the requirement of Nickel alloy 22 material for tubes. Taking into account the change in mass flow rate

of boiler feedwater with temperature to which feedwater is heated in the heat exchanger, a cost benefit analysis indicated that increasing the temperature of boiler feedwater to a maximum of ~135°F would return maximum profit.

Keeping the area of cross-section of the heat exchanger constant, the transverse pitch S_t was varied from 4.88" to 6.17" but the longitudinal pitch S_l was kept constant at 2.97". It was observed that the total rate of heat transfer and condensation efficiency increased with decrease in transverse pitch. The decrease in transverse pitch helped accommodate more tubes in the same duct cross-section thus increasing the total surface area of the tubes. It was observed that for the heat exchanger placed downstream of wet FGD, the total annual cost associated with the heat exchangers was dominated by the annual operating cost as expensive Nickel alloy 22 material was not required. Therefore, when the pressure drop for cooling water flowing inside the tubes was reduced with increased number of tubes due to smaller transverse pitch, the annual operating cost was reduced. Thus, the total annual cost also reduced.

Using water spray to precool flue gas to a temperature of 155°F upstream of the wet FGD offered similar rate of heat transfer and condensation efficiency compared to a heat exchanger placed downstream of the wet FGD unit. The total annual cost for this system was also comparable to that observed for heat exchanger placed downstream of wet FGD unit up-to a heat exchanger duct length of 10ft, beyond which the total annual cost started increasing rapidly. For the system using precooled flue gas using water spray, the Nickel 22 alloy material requirements for tube materials increased significantly with increase in duct length, thus, increasing the installed capital cost for the heat exchangers.

The use of coupled heat exchangers provides space flexibility but appears beneficial only at higher mass flow rates of cooling water. The combined fan and pump power required for coupled heat exchanger is only marginally more than that required by a heat exchanger that uses cooling water at higher cooling water to flue gas mass flow rate ratios. Although the rate of condensation remains lower than that for a heat exchanger using cooling water at higher mass flow rate ratios, the rate of heat transfer is higher for coupled heat exchanger assembly. It is also

observed that the use of boiler feedwater directly is more beneficial if the main aim of the system is to recover maximum heat from flue gas.

The use of two cascaded heat exchangers offers the benefits of a heat exchanger both upstream and downstream of the wet FGD unit. From the overall performance evaluation of the cascaded heat exchanger assembly and its comparison with system using only UHX or only DHX, it was observed that if the systems were designed to obtain the same rate of total heat transfer, the cascaded heat exchanger offered higher condensation efficiency comparable to that of the DHX but at lower total annual cost. The system designed to heat boiler feedwater to a temperature of ~160°F was most beneficial. It is also observed that if we raise the temperature of boiler feedwater to a temperature of 160°F, FWH1 can be completely taken off. The additional savings on installed cost associated with FWH1 and the pressure drop that would have been otherwise observed across FWH1 have not been accounted in this study.

7. Assumptions

- All the heat exchangers were assumed to have inline tube arrangement.
- All heat exchanger ducts are assumed to be perfectly insulated and any heat loss to the environment is neglected.
- The cooling water to flue gas mass flow rate ratios are based on Jonas's Aspen Model.
- Unlike the condensing heat exchanger, the calculations for water-to-water heat exchanger are done at average of the inlet and exit temperatures.
- A detailed design analysis of baffle plates for the water-to-water heat exchanger HX2 was not done at this stage. The possibilities to improve HX2 design by modifying baffle arrangement and spacing has not been done at this stage.
- Any flow leakage across the baffle plate weld joints with the heat exchanger shell or along the holes on baffle plates for tube support have been neglected.
- The possibility of fouling on tube surfaces has not been taken into account at this stage.
- Any changes in the price of tube material or manufacturing and installation cost since the study done Hazell have been neglected.
- The cost of heat exchanger tubes is calculated as a function of the total weight of tube material required. Also, the manufacturing and installation cost is assumed to be same for all tube diameters.
- The pump power requirement to remove the condensed water from condensing heat exchanger and transferring it to the treatment plant has not been accounted for.
- The pumping requirements for water spray to precool the flue gas have been neglected at this stage.
- The pump power requirements to circulate cooling water from HX2 to HX1 and then return from HX1 to HX2 have not been taken into account.
- The pump power requirements for transferring boiler feedwater from exit of DHX to the inlet of UHX have been neglected.

- It is assumed that there is no heat loss while cooling water is circulated between HX1 and HX2 or when boiler feedwater is pumped from DHX to UH.

References

1. **Jeong, Dr. Kwangkook.** *Condensation of Water Vapor and Sulfuric Acid in Boiler Flue Gas.* s.l. : Lehigh University, 2008. Ph.D. Dissertation.

2. **Lavigne, Michael A.** *Numerical Simulations of Condensing Heat Exchangers with Oxyfuel Flue Gas.* Bethlehem, PA : Lehigh University, 2010.

3. **Hazell, Daniel.** *Modeling and Optimization of Condensing Heat Exchangers for Cooling Boiler Flue Gas.* Bethlehem, PA : Lehigh University, 2011.

4. *Design of cooler condensers for Mixtures of Vapors with Noncondensing Gases.* **Colburn, A P and Hougen, O A.** s.l. : Industrial and Engineering Chemistry, 1934, Vol. 26.

5. **Zukauskas, A.** Heat Transfer from Tubes in Cross Flow. [book auth.] J P Hartnett, T F Irvine and Eds. Jr. *Advances in Heat Transfer.* New York : Academic Press, 1972.

6. **Gnielinski, V.** s.l. : Int. Chem. Eng., 1976, Vol. 16.

7. **Petukhov, B.S.** [book auth.] J P Hartnett, T F Irvine and Eds. Jr. *Advances in Heat and Mass Transfer Vol. 6.* New York : Academic Press, 1970.

8. *Thermodynamique - Tensions des vapeurs: nouvelle relation entre les tensions et les temperature.* **Antoine, Ch. M.** s.l. : Comptes Rendus des Seances de l'Academie des Sciences, 1888, Vol. 104.

9. **Munson, Bruce R., Young, Donald F. and Okiishi, Theodore H.** *Fundamentals of Fluid Mechanics.* s.l. : John Wiley & Sons, Inc., 1998. ISBN 0-471-35502-X.

10. **Kays, W. M. and London, A. L.** *Compact Heat Exchangers.* s.l. : Krieger Publishing Company, 1998. ISBN: 1-57524-060-2.

11. **Zukauskas, A. and Ulinskas, R.** Bank of plain ans finned tubes. *Heat Exchanger Design Handbook Vol.1-4.* New York : Hemisphere Publishing Corporation, 1983.

12. *Estimating Costs of Shell-and-Tube Heat Exchangers.* **Purohit, G. P.** s.l. : Chemical Engineering, 1983, Vol. 90.

13. *Chemical Process Design and Integration.* **Smith, Robin.** Hoboken : Wiley, 2005.

14. **Jonas, Gordon.** *Using flue Gas cooler to improve Unit Heat Rate.* Bethlehem : Energy Research center Internal Report, 2011.

15. **Kessen, Michael.** *Optimal Design of an Air-Cooled Condenser for Flue Gas from a Power Plant.* Bethlehem, PA : Lehigh University, 2011.

16. **Levy, Edward K., Bilirgen, Harun and DuPont, John.** *Recovery of Water from Boiler Flue Gas using Condensing Heat Exchangers.* s.l. : Department of Energy, 2011.

17. **Jonas, Gordon.** *Thermal Integration of an MEA Post Combustion Carbon Capture System With a Supercritical Coal Fired Power Plant.* Bethlehem : Lehigh University, 2010.

18. **Mukherjee, Rajiv.** *Effectively Design Shell-and-Tube Heat Exchangers.* s.l. : American Institute of Chemical Engineers, 1998.

Appendix A

Table Page.

A.1 Process Conditions for Subcases A - F as obtained from Jonas (14)…….92

A.2 Process Conditions for Subcases 1 - 4 as obtained from Jonas (14)……..93

A.3 Process Conditions for Precooled Flue gas using Water Spray as obtained from Jonas (14) ……..……..……..……..……...94

Figure Page.

A.1 Supercritical Steam Turbine kit diagram used by Jonas (17)…….……..95

Table A. 1 - Process Conditions for Subcases A - F as obtained from Jonas (14)

Process Conditions for Subcases A - F										
Sub-case			H	G	F	E	D	C	B	A
Place Before This FWH		N/A	w/FGD	FWH1	FWH3	FWH2	FWH2	FWH1	FWH1	FWH1
Flue Gas T in	(°F)	N/A	135	303	303	303	303	303	303	303
Net Power	(kW)	591,857	594,539	603,156	596,137	594,175	598,246	593,782	595,605	597,622
Δ Net Power	(kW)	0	2,682	11,300	4,281	2,318	6,389	1,925	3,748	5,765
Unit Heat Rate		9,133	9,092	8,962	9,067	9,097	9,036	9,103	9,076	9,045
Δ Unit Heat Rate	%	0.00	-0.45	-1.87	-0.72	-0.39	-1.07	-0.32	-0.63	-0.96
Efficiency	%	37.36	37.36	37.36	37.36	37.36	37.36	37.36	37.36	37.36
Duty FWH1	(kBtu/hr)	173,265	61,075	0	178,184	178,672	183,173	92,019	15,906	19,292
Duty FWH2	(kBtu/hr)	130,650	131,241	0	131,930	0	0	132,582	131,477	0
Duty FWH3	(kBtu/hr)	120,224	120,224	66,354	33,541	166,866	83,747	120,224	120,224	173,798
Duty FWH5	(kBtu/hr)	215,945	215,945	215,945	215,945	215,945	215,945	215,945	215,945	215,945
Duty FWH6	(kBtu/hr)	228,583	228,583	228,583	228,583	228,583	228,583	228,583	228,583	228,583
Duty FWH7	(kBtu/hr)	368,976	368,976	368,976	368,976	368,976	368,976	368,976	368,976	368,976
Duty Flue Gas Cooler	(kBtu/hr)	0	119,764	371,334	86,682	86,682	167,914	86,682	167,914	248,666
m° Condensation	(lb/hr)	0	108,601	64,568	0	0	0	0	0	0
m° Flue Gas	(lb/hr)	6,309,391	6,309,391	6,309,391	6,309,391	6,309,391	6,309,391	6,309,391	6,309,391	6,309,391
m° BFW	(lb/hr)		2,792,411	3,018,950	3,175,031	3,175,032	3,175,033	2,759,411	2,838,911	2,915,950
$m°_{bfw}$ / $m°_{fg}$			0.443	0.478	0.503	0.503	0.503	0.437	0.450	0.462
BFW T in	(°F)			87.1	193.8	151.9	152.5	87.1	87.1	98.6
BFW T out	(°F)			210	220.9	179.2	205.2	118.5	146.4	177

Table A. 2 - Process Conditions for Subcases 1 - 4 as obtained from Jonas (14)

Process Conditions for Subcases 1 - 4									
Sub-case				4	C	3	B	2	1
Place Before This FWH		N/A	SSR Chg	FWH1	FWH1	FWH1	FWH1	FWH1	FWH1
Flue Gas T in	(°F)	N/A	303	303	303	303	303	303	303
Net Power	(kW)	591,857	591,603	593,097	593,535	594,631	595,392	596,498	597,975
Δ Net Power	(kW)		0	1,494	1,932	3,028	3,790	4,896	6,372
Unit Heat Rate		9,133	9,137	9,114	9,107	9,090	9,079	9,062	9,040
Δ Unit Heat Rate	%		0.00	-0.25	-0.33	-0.51	-0.64	-0.82	-1.07
Efficiency	%	37.36	37.34	37.44	37.46	37.53	37.58	37.65	37.74
Duty FWH1	(kBtu/hr)	173,265	172,847	110,305	91,746	45,807	14,152	0	0
Duty FWH2	(kBtu/hr)	130,650	130,388	130,717	130,814	131,055	131,223	0	0
Duty FWH3	(kBtu/hr)	120,224	119,988	119,988	119,988	119,988	119,988	196,422	167,342
Duty Flue Gas Cooler	(kBtu/hr)	0	0	66,761	86,471	135,518	169,396	224,244	257,084
m° Flue Gas	(lb/hr)	6,309,391	6,309,391	6,309,391	6,309,391	6,309,391	6,309,391	6,309,391	6,309,391
m° BFW	(lb/hr)		2,668,999	2,734,146	2,753,246	2,801,046	2,834,246	2,894,950	2,922,450
$m°_{bfw} / m°_{fg}$			0.423	0.433	0.436	0.444	0.449	0.459	0.463
BFW T in	(°F)		87.1	87.1	87.1	87.1	87.1	87.1	87.1
BFW T out	(°F)		87.1	111.5	118.5	135.5	146.9	164.6	175.1
LMTD	(°F)		215.9543	183.2101	173.5686	149.5469	132.8506	105.3905	88.2051
Cost Benefit	($)	0	0	627,479	811,449	1,271,862	1,591,655	2,056,179	2,676,363

Table A. 3 - Process Conditions for Precooled Flue gas using Water Spray as obtained from Jonas (14)

Process Conditions for Precooled Flue gas using Water Spray									
Flue Gas T in		**87**	**135**	**155**	**165**	**175**	**200**	**250**	**300**
Net Power	(kW)	591,857	594,539	595,524	596,375	596,820	600,257	608,250	620,697
Unit Heat Rate		9,133	9,092	9,077	9,064	9,057	9,005	8,887	8,709
Δ Unit Heat Rate	%	0.00	-0.45	-0.62	-0.76	-0.83	-1.40	-2.70	-4.65
Efficiency	%	37.36	37.53	37.59	37.64	37.67	37.89	38.39	39.18
Duty FWH1	(kBtu/hr)	173,265	61,075	19,508	0	0	0	0	0
Duty FWH2	(kBtu/hr)	130,650	131,241	130,579	120,961	0	0	0	0
Duty FWH3	(kBtu/hr)	120,224	120,224	120,224	120,224	195,678	125,197	0	0
Duty FWH5	(kBtu/hr)	215,945	215,945	215,945	215,945	215,945	215,945	215,945	215,945
Duty FWH6	(kBtu/hr)	228,583	228,583	228,583	228,583	228,583	228,583	228,583	228,583
Duty FWH7	(kBtu/hr)	368,976	368,976	368,976	368,976	368,976	368,976	368,976	368,976
Duty Flue Gas Cooler	(kBtu/hr)	0	119,764	164,123	194,419	225,869	305,105	475,346	663,759
m° Condensation	(lb/hr)	0	108,601	118,342	128,809	140,270	169,314	235,422	307,291
Water Injected	(lb/hr)	0	0	224,728	208,810	192,986	153,924	77,857	4,397
yH2O		17.4%	17.4%	16.4%	16.1%	15.7%	14.9%	13.3%	11.7%
m° Flue Gas	(lb/hr)	6,309,391	6,309,391	6,534,119	6,518,201	6,502,377	6,463,315	6,387,248	6,313,788
m° BFW	(lb/hr)		2,792,411	2,835,411	2,864,946	2,900,950	2,964,950	3,100,985	3,249,985
m°bfw / m°fg			0.443	0.434	0.440	0.446	0.459	0.485	0.515

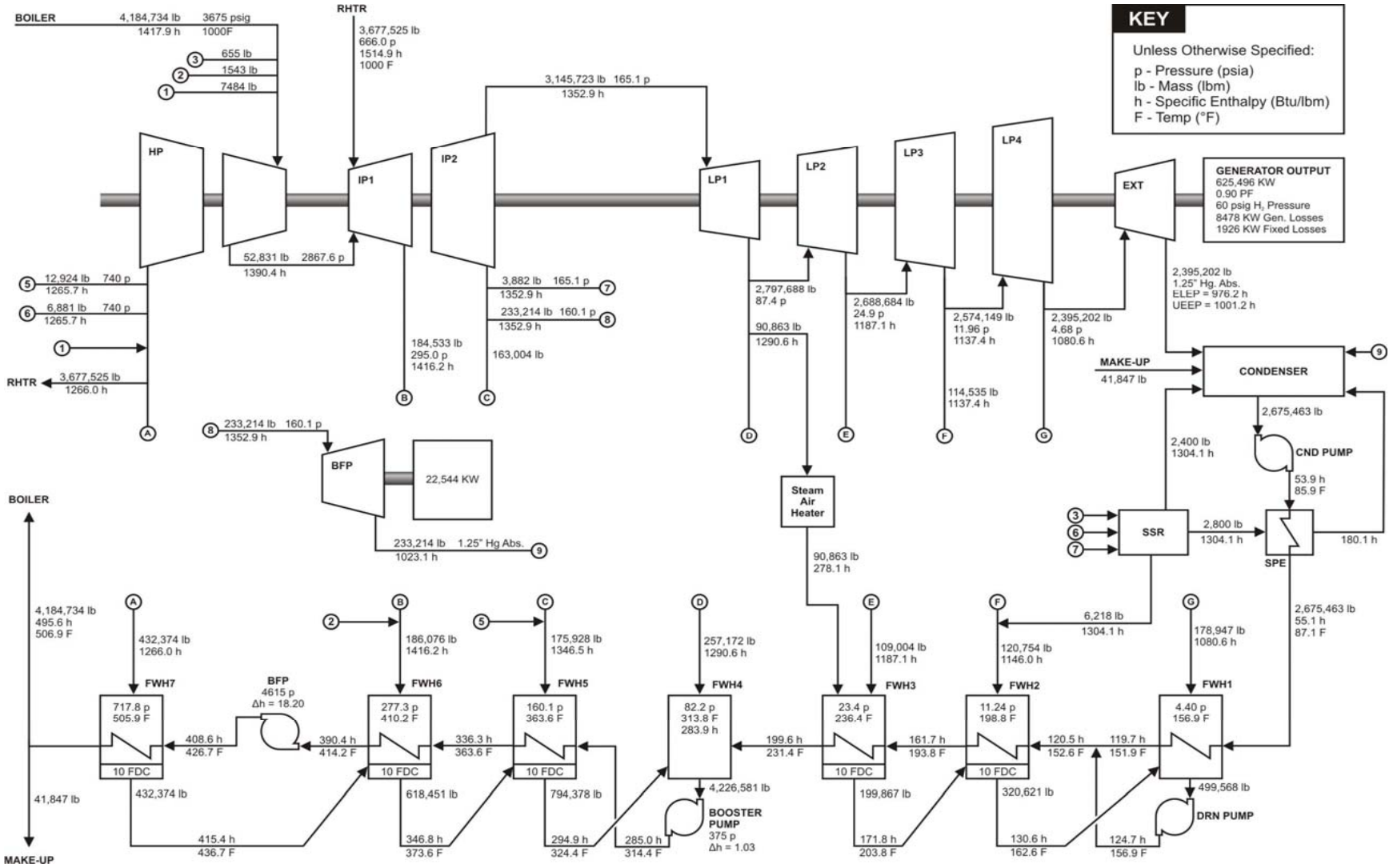

Figure A. 1 - Supercritical Steam Turbine kit diagram used by Jonas (17)

Vita

Nipun Goel was born on July 4th, 1986 in Delhi, India. He received a Bachelor's in Technology in Power Engineering (with Mechanical Specialization) from National Power Training Institute (NR), Delhi, India in 2008. After completing his undergrad, he worked with Bechtel India Private Limited, Haryana, India, for two years where he gained industrial exposure. In the Fall of 2010, he joined Lehigh University to pursue M.S. in Mechanical Engineering.